

**PERFORMANCE AND EMISSION  
CHARACTERISTICS OF A MODIFIED DIRECT  
INJECTION DIESEL ENGINE RUNNING ON  
DIESEL-BIOGAS FUEL**

**MESHACK HAWI OCHIENG'**

**MASTER OF SCIENCE  
(Mechanical Engineering)**

**JOMO KENYATTA UNIVERSITY OF  
AGRICULTURE AND TECHNOLOGY**

**2015**

**Performance and Emission Characteristics of a Modified  
Direct Injection Diesel Engine Running on Diesel-Biogas Fuel**

**Meshack Hawi Ochieng'**

**A thesis submitted in partial fulfilment for the Degree of  
Master of Science in Mechanical Engineering in the Jomo  
Kenyatta University of Agriculture and Technology**

**2015**

## DECLARATION

This thesis is my original work and has not been presented for a degree in any other university.

Signature:..... Date.....

**Meshack Hawi Ochieng'**

This thesis has been submitted for examination with our approval as the university supervisors.

Signature:..... Date.....

**Dr. Robert Kiplimo**

**JKUAT, Kenya**

Signature:..... Date.....

**Dr. (Eng) Hiram M. Ndiritu**

**JKUAT, Kenya**

## DEDICATION

I dedicate this work to my loving dad and mum, Mr. and Mrs. Ochieng'.

## ACKNOWLEDGEMENTS

The author wishes to sincerely appreciate a number of individuals for their vital roles in the realization of this thesis. First and foremost is the Almighty God, the giver and sustainer of life, for giving me the opportunity to do this research. Special appreciation is due to Dr. Robert Kiplimo and Dr. Eng. Hiram Ndiritu, my two very able and highly knowledgeable project supervisors for guiding and supporting me throughout this research. My sincere gratitude also go to Bernard Owiti, Stelamaris Nzove and John Ng'ethe, for their positive criticism which helped to keep me going. I am also heavily indebted to Esther Wangui from the Department of Mechatronics Engineering, JKUAT for her help in formatting my thesis. I also thank the members of staff in the department of Mechanical Engineering and Engineering workshops (JKUAT) for their assistance during the research work. Special gratitude goes to the Engineering workshops manager, Dr. P. Kihato for his invaluable counsel and encouragement during this research and also for granting the permission to use workshop equipment and facilities. During the experimental work, I got a lot of assistance from the staff in different laboratories notably Daniel Kariuki of Thermodynamics laboratory (JKUAT). I am sincerely grateful to you. Finally, I extend my gratitude to my parents for the moral support that they gave me throughout the research period.

# TABLE OF CONTENTS

DECLARATION . . . . .	ii
DEDICATION . . . . .	iii
ACKNOWLEDGEMENTS . . . . .	iv
TABLE OF CONTENTS . . . . .	v
LIST OF TABLES . . . . .	x
LIST OF FIGURES . . . . .	xi
LIST OF APPENDICES . . . . .	xiv
LIST OF ABBREVIATIONS . . . . .	xiv
NOMENCLATURE . . . . .	xvii
ABSTRACT . . . . .	xviii
CHAPTER ONE . . . . .	1
1.0 INTRODUCTION . . . . .	1
1.1 Background . . . . .	1
1.2 Alternative Fuels for IC Engines . . . . .	3
1.3 Problem Statement . . . . .	4
1.4 Objectives . . . . .	5

1.5	Outline of Thesis . . . . .	5
<b>CHAPTER TWO . . . . .</b>		<b>7</b>
<b>2.0</b>	<b>LITERATURE REVIEW . . . . .</b>	<b>7</b>
2.1	Overview . . . . .	7
2.2	Dual Fuel Engines . . . . .	7
2.3	Octane and Cetane Number . . . . .	9
2.4	Use of Biogas in IC Dual Fuel Engines . . . . .	10
2.5	Use of Other Gaseous Fuels in IC (Dual Fuel) Engines . . . . .	14
2.5.1	Hydrogen . . . . .	14
2.5.2	Syngas . . . . .	15
2.6	Use of Liquid Bio-fuels in IC (Dual fuel) Engines . . . . .	17
2.6.1	Ethanol . . . . .	17
2.6.2	Biodiesel . . . . .	18
2.7	Exhaust Gas Recirculation (EGR) . . . . .	19
2.8	Justification of Present Study . . . . .	20
<b>CHAPTER THREE . . . . .</b>		<b>23</b>
<b>3.0</b>	<b>EXPERIMENTAL DESIGN AND METHODOLOGY . . . . .</b>	<b>23</b>
3.1	Introduction . . . . .	23
3.2	Experimental Setup . . . . .	23

3.3	Design and Fabrication of Experimental Set up Components . . . . .	24
3.3.1	The Fuel-Air Mixing Chamber . . . . .	24
3.3.2	The Exhaust Gas Recirculation (EGR) System . . . . .	30
3.3.3	Manual Regulation of Pilot Fuel Quantity . . . . .	31
3.3.4	Independent Fuel Injection System . . . . .	32
3.3.5	Cooling Water Tank for the Engine . . . . .	33
3.3.6	Cooling Water Tank for the Dynamometer . . . . .	34
3.3.7	Starter Motor Mounting Bracket . . . . .	36
3.3.8	Diesel Fuel Metering System . . . . .	37
3.3.9	Biogas Supply and Metering System . . . . .	38
3.3.10	Engine Cooling System . . . . .	40
3.3.11	Engine-Dynamometer Coupling Guard . . . . .	40
3.4	Cleaning of Biogas . . . . .	41
3.4.1	Desulphurization . . . . .	41
3.4.2	Dehydration . . . . .	43
3.5	Exhaust Gas Recirculation . . . . .	44
3.6	Measurement Parameters and Procedures . . . . .	45
3.6.1	Diesel Fuel Consumption . . . . .	46
3.6.2	Biogas Fuel Consumption . . . . .	47
3.6.3	Engine Brake Power . . . . .	49
3.6.4	Brake Specific Fuel Consumption . . . . .	52
3.6.5	Brake Thermal Efficiency . . . . .	53
3.6.6	Emission Measurement . . . . .	54
3.6.7	Temperature Measurement . . . . .	55
3.6.8	Engine Speed Measurement . . . . .	56



3.7	Uncertainty Analysis . . . . .	56
3.7.1	Instrumental Uncertainty . . . . .	57
3.7.2	Experimental Uncertainty . . . . .	58
<b>CHAPTER FOUR . . . . .</b>		<b>61</b>
<b>4.0</b>	<b>RESULTS AND DISCUSSION . . . . .</b>	<b>61</b>
4.1	Introduction . . . . .	61
4.2	Base Line Data for Engine Performance on Single Fuel Mode with Diesel	61
4.2.1	Brake Power . . . . .	61
4.2.2	Brake Specific Fuel Consumption . . . . .	62
4.2.3	Brake Thermal Efficiency . . . . .	63
4.2.4	Emissions . . . . .	64
4.3	Engine Performance on Dual Fuel Mode . . . . .	67
4.3.1	Brake Power . . . . .	67
4.3.2	Brake Specific Fuel Consumption (BSFC) . . . . .	69
4.3.3	Brake Thermal Efficiency . . . . .	70
4.3.4	Exhaust Gas Temperature (EGT) . . . . .	71
4.3.5	Emissions . . . . .	72
4.4	Engine Performance with Exhaust Gas Recirculation on Single Fuel Mode	76
4.4.1	Brake Power . . . . .	76
4.4.2	Brake Specific Fuel Consumption (BSFC) . . . . .	76
4.4.3	Brake Thermal Efficiency . . . . .	77
4.4.4	Emissions . . . . .	78

4.5	Engine Performance on Dual Fuel Mode (Biogas 80%-20% Diesel) with Exhaust Gas Recirculation . . . . .	82
4.5.1	Brake Power . . . . .	82
4.5.2	Brake Specific Fuel Consumption (BSFC) . . . . .	83
4.5.3	Brake Thermal Efficiency . . . . .	85
4.5.4	Exhaust Gas Temperature (EGT) . . . . .	86
4.5.5	Emissions . . . . .	87
<b>CHAPTER FIVE . . . . .</b>		<b>91</b>
<b>5.0 CONCLUSIONS AND RECOMMENDATIONS . . . . .</b>		<b>91</b>
5.1	Conclusions . . . . .	91
5.2	Recommendations . . . . .	93
<b>REFERENCES . . . . .</b>		<b>94</b>
<b>APPENDICES . . . . .</b>		<b>102</b>

## LIST OF TABLES

<b>Table 3.1</b>	Engine Specification and Design Parameters . . . . .	28
<b>Table 3.2</b>	Fuel Properties of Diesel . . . . .	47
<b>Table 3.3</b>	Fuel Properties of Biogas . . . . .	48
<b>Table 3.4</b>	Standard Deviation of Brake Specific Fuel Consumption . . . . .	59

## LIST OF FIGURES

<b>Figure 3.1</b>	Schematic view of the experimental set up . . . . .	24
<b>Figure 3.2</b>	Pictorial view of the experimental set up . . . . .	25
<b>Figure 3.3</b>	Schematic view of the mixing chamber for biogas and air . . . . .	26
<b>Figure 3.4</b>	Pictorial view of the mixing chamber for biogas and air . . . . .	27
<b>Figure 3.5</b>	Pictorial view of the EGR system . . . . .	30
<b>Figure 3.6</b>	Pictorial view of the pilot fuel regulating device with reference to the engine . . . . .	31
<b>Figure 3.7</b>	The independent electronic fuel injection system . . . . .	32
<b>Figure 3.8</b>	Schematic view of the cooling water tank for the engine . . . . .	34
<b>Figure 3.9</b>	Schematic view of the cooling water tank for the hydraulic dy- namometer . . . . .	35
<b>Figure 3.10</b>	Starter motor mounting bracket . . . . .	36
<b>Figure 3.11</b>	Diesel fuel metering system . . . . .	37
<b>Figure 3.12</b>	Biogas supply and metering system . . . . .	39
<b>Figure 3.13</b>	Engine cooling system . . . . .	40
<b>Figure 3.14</b>	Coupling guard . . . . .	41
<b>Figure 3.15</b>	Biogas desulphurizer . . . . .	42
<b>Figure 3.16</b>	Biogas dehydrator . . . . .	43
<b>Figure 3.17</b>	Biogas flow meter . . . . .	48
<b>Figure 3.18</b>	The hydraulic dynamometer . . . . .	49
<b>Figure 3.19</b>	Emission analyzer . . . . .	54
<b>Figure 3.20</b>	Multi-channel digital data logger . . . . .	56
<b>Figure 3.21</b>	Digital tachometer . . . . .	56
<b>Figure 4.1</b>	Variation of brake power with load for single fuel operation . . . . .	62
<b>Figure 4.2</b>	Variation of BSFC with load for single fuel operation . . . . .	63

<b>Figure 4.3</b>	Variation of BTE with load for single fuel operation . . . . .	64
<b>Figure 4.4</b>	Variation of CO emission with load for single fuel operation . . .	65
<b>Figure 4.5</b>	Variation of HC emission with load for single fuel operation . . .	66
<b>Figure 4.6</b>	Variation of CO <sub>2</sub> emission with load for single fuel operation . . .	67
<b>Figure 4.7</b>	Variation of brake power with load for dual fuel mode . . . . .	68
<b>Figure 4.8</b>	Variation of BSFC with load for dual fuel mode . . . . .	69
<b>Figure 4.9</b>	Variation of BTE with load for dual fuel mode . . . . .	70
<b>Figure 4.10</b>	Variation of EGT with load for dual fuel mode . . . . .	71
<b>Figure 4.11</b>	Variation of CO emission with load for dual fuel mode . . . . .	73
<b>Figure 4.12</b>	Variation of HC emission with load for dual fuel mode . . . . .	74
<b>Figure 4.13</b>	Variation of CO <sub>2</sub> emission with load for dual fuel mode . . . . .	75
<b>Figure 4.14</b>	Variation of brake power with load for single fuel operation with EGR . . . . .	77
<b>Figure 4.15</b>	Variation of BSFC with load for single fuel operation with EGR	78
<b>Figure 4.16</b>	Variation of BTE with load for single fuel operation with EGR .	79
<b>Figure 4.17</b>	Variation of CO emission with load for single fuel operation with EGR . . . . .	80
<b>Figure 4.18</b>	Variation of HC emission with load for single fuel operation with EGR . . . . .	81
<b>Figure 4.19</b>	Variation of CO <sub>2</sub> emission with load for single fuel operation with EGR . . . . .	82
<b>Figure 4.20</b>	Variation of brake power with load for dual fuel operation with EGR . . . . .	83
<b>Figure 4.21</b>	Variation of BSFC with load for dual fuel operation with EGR .	84
<b>Figure 4.22</b>	Variation of BTE with engine load for dual fuel operation with EGR . . . . .	85

<b>Figure 4.23</b>	Variation of EGT with engine load for dual fuel operation with EGR . . . . .	86
<b>Figure 4.24</b>	Variation of CO emission with load for dual fuel operation with EGR . . . . .	88
<b>Figure 4.25</b>	Variation of HC emission with load for dual fuel operation with EGR . . . . .	89
<b>Figure 4.26</b>	Variation of CO <sub>2</sub> emission with load for dual fuel operation with EGR . . . . .	90

## LIST OF APPENDICES

<b>Appendix A:</b>	DIESEL ENGINE EXHAUSTS . . . . .	103
<b>Appendix B:</b>	EXHAUST GAS RECIRCULATION . . . . .	104

## ABBREVIATIONS

<b>IC</b>	Internal Combustion
<b>CI</b>	Compression Ignition
<b>SI</b>	Spark Ignition
<b>ICEs</b>	Internal Combustion Engines
<b>DICI</b>	Direct Injection Compression Ignition
<b>HCCI</b>	Homogeneous Charge Compression Ignition
<b>EGR</b>	Exhaust Gas Recirculation
<b>NO<sub>x</sub></b>	Oxides of nitrogen
<b>PM</b>	Particulate Matter
<b>HC</b>	Hydrocarbons
<b>CO</b>	Carbon monoxide
<b>A/F</b>	Air-Fuel
<b>ppm</b>	Parts per million
<b>CA</b>	Crank Angle
<b>BTDC</b>	Before Top Dead Centre
<b>CNG</b>	Compressed Natural Gas
<b>LPG</b>	Liquified Petroleum Gas
<b>BMEP</b>	Brake Mean Effective Pressure
<b>HHV</b>	Higher heating value
<b>LHV</b>	Lower heating value
<b>CV</b>	Calorific value
<b>BTE</b>	Brake Thermal Efficiency
<b>BSFC</b>	Brake Specific Fuel Consumption
<b>LPG</b>	Liquified Petroleum Gas
<b>ON</b>	Octane Number



<b>IMEPg</b>	Gross Indicated Mean Effective Pressure (bar)
<b>T</b>	Torque
<b>L</b>	Litres

## NOMENCLATURE

$\phi$	Diameter
$\rho$	Density
$\dot{w}$	Power
$\dot{m}$	Mass flow rate
$\eta$	Efficiency
$\xi$	Instrumental uncertainty
$\sigma$	Experimental uncertainty
r	Radius
d	Diameter
A	Area
V	Volume
N	Revolutions per minute
P.S	Brake horse power

## Subscripts

m	mass
th	thermal
b	brake
f	fuel
bth	brake thermal
d	diesel
g	fuel gas

## ABSTRACT

The price of fossil fuels is constantly increasing because of the limitations of deposit, supply and increase in demand for petroleum fuels resulting from industrialization. The regulations for emissions from diesel engines have also been strengthened, especially for particulate matter (PM) and oxides of nitrogen ( $\text{NO}_x$ ). There is therefore need to find alternative fuels which will reduce harmful exhaust emissions while maintaining high thermal efficiency. Biogas is one such fuel, which can be adapted for use in internal combustion (IC) engines.

In this research, a Direct Injection Compression Ignition (DICI) engine was modified into a dual fuel engine which uses biogas and diesel, with the focus on reduction of harmful exhaust emissions while maintaining high thermal efficiency. The brake power of the engine was measured using a Fuchino SF-3.5 hydraulic dynamometer and emissions of HC, CO and  $\text{CO}_2$  were measured using an emissions analyzer, Horiba MEXA-544GF. The performance and emission characteristics of the modified engine were compared with those of the conventional diesel engine. The effect of exhaust gas recirculation (EGR) on engine performance and emission was also studied.

The air intake system of the engine was modified to allow mixing of air and biogas before supplying the mixture to the combustion chamber of the engine while the exhaust system was modified to allow measurement of the exhaust emissions. The exhaust system was modified to allow also exhaust gas recirculation (EGR) in order to investigate the effect of EGR on engine performance and emissions. The engine was mounted on a test bench and coupled to the hydraulic dynamometer to allow for performance test by measuring the engine brake power. Exhaust emissions were measured for various operating conditions.

The results obtained from this study showed that a DICI engine can be modified into a dual fuel engine that uses diesel and biogas. Engine performance tests were done for

single fuel (diesel) mode and dual fuel modes consisting of biogas to diesel ratios in the form; 50:50, 70:30 and 80:20. Exhaust emissions of HC, CO and CO<sub>2</sub> were measured for the various operating conditions. The results showed that at maximum substitution of diesel with biogas (Biogas:Diesel in the ratio 80:20) and maximum engine loading, the engine consumes 3.08 kg of biogas per hour. The brake thermal efficiency however, decreased from 31.34% to 20.82% due to the lower calorific value of biogas compared to diesel. The results also showed that EGR improved thermal efficiency by up to 14.5% for single fuel operation and by up to 11.2% for dual fuel operation.

The performance characteristics of the modified engine showed that diesel can be substituted partly with biogas and the engine used for a range of applications. The most appropriate areas of use are stationary applications such as driving of electric power generators, hoisting in construction sites and driving of machines such as water pumps and concrete mixers. This is due to the challenge of compact storage of the gas.

# CHAPTER ONE

## 1.0 INTRODUCTION

### 1.1 Background

Compression ignition (CI) engines are widely used as power source for automobiles due to their high thermal efficiency, excellent fuel economy and low regulated emissions of unburned hydrocarbon (HC), carbon monoxide (CO) and carbon dioxide (CO<sub>2</sub>) compared to those of spark ignition (SI) engines. From an environmental point of view, however, diesel engines generally exhaust a larger amount of particulate matter (PM) and nitrogen oxide (NO<sub>x</sub>) pollutant emissions than those of gasoline engines [1,2].

Air pollution by exhaust emissions from IC engines has become a major concern in most of the countries of the world since it is responsible for causing respiratory diseases and cancers. Poor ambient air quality is a major concern, mostly in urban areas where there are more emissions due to the high number of automobiles. Air pollution is also responsible for serious phenomena such as acid rain and global warming [3]. It is as a result of these adverse effects of the emissions on human life and the environment, that the regulations for emissions from IC engines have been strengthened. This has led to research on alternative fuels for the IC engines, which would reduce harmful exhaust emissions while maintaining high thermal efficiency [4,5].

In addition to challenges of emissions from IC (Internal Combustion) engines due to use of fossil fuels, the price of the fossil fuels is constantly increasing due to increase in demand [6]. All countries are at present heavily dependent on petroleum fuels for transportation and agricultural machinery. The fact that a few nations produce the bulk of petroleum has led to high price fluctuation and uncertainties in supply for the consuming nations. This in turn has led them to look for alternative fuels that

they themselves can produce. Among the alternatives being considered are methanol, ethanol, biodiesel and biogas [7].

Studies have shown that biogas derived from organic wastes is a good alternative to petroleum fuels and can be used in compression ignition (CI) engines, because of its better mixing ability with air and clean burning nature [8]. Biogas is produced by anaerobic digestion of various organic substances such as kitchen wastes, agricultural wastes, municipal solid wastes and cow dung.

Recent studies in Kenya have also shown that water hyacinth can be used as a potential feedstock for biogas production due to its abundance in polluted freshwater lakes such as Lake Victoria [9]. When water hyacinth is used in production of biogas, it will not only bridge the present gaps in energy provision but will also contribute to sustainable management of the plant, which is currently a threat to the lake ecosystem and the communities living around the lake. In Lake Victoria for example, the infestation currently covers 12,000 ha and is affecting the livelihoods of more than 40 million people in Kenya, Tanzania and Uganda [10]. By the end of 1997, research agencies reported a 70% decline in economic activities at the Kenyan port of Kisumu as a result of the water hyacinth choking the port and fish breeding grounds [11,12]. To salvage the situation, there is need to harvest the weed and use it as feedstock for production of biogas for IC engines which can be used in generation of electricity.

Research by Kenya Agricultural Research Institute (KARI) indicates that more than 75% of the Kenyan population live in the rural areas, with agriculture as their main occupation. The main farming systems feature cash crops, food crops, fruits and vegetables, forages, livestock, and tree growing. As a result of this, biogas production and subsequent use in internal combustion engines for generation of electricity for the rural areas is a viable means of fostering national economic growth and development [13,14].

## 1.2 Alternative Fuels for IC Engines

Petrol and diesel are common liquid fuels for internal combustion engines, while methanol, ethanol and biodiesel are alternative liquid fuels [7]. Use of Liquefied Petroleum Gas (LPG) in IC engines is also common, especially in food processing and manufacturing industries while alternative gaseous fuels for IC engines include hydrogen, syngas and biogas [15].

Biogas is a gaseous fuel produced by anaerobic fermentation of organic material, that can be extracted from varied sources like animal wastes, vegetable wastes, wastes from households, wastes from the food and fodder industry and waste from productive livestock husbandry [16]. It is regarded as an alternative clean energy resource for CI engines in view of its environmental friendly nature.

Renewable energy and its conversion to heat and power are key factors for sustainable development in countries with low or no oil fuel reserves. One of the most important renewable fuels is biogas, which is composed mainly of methane (30-70%, by vol.) and carbon dioxide (20-40%, by vol.) and is a promising alternative fuel for internal combustion engines since it is renewable and environmental friendly [17].

Methane exhibits greater resistance to the knock phenomenon due to its higher octane rating and auto-ignition temperature, making it appropriate for engines with high compression ratios. In addition, the carbon content of methane is also relatively low compared to that of conventional diesel fuel, resulting in a significant decrease in pollutant exhaust emissions [17].

Utilizing biogas in engines, when compared to fossil fuels avoids any additional greenhouse gas emission. Due to the organic nature of the components of biogas, burning it in a gas engine for power generation emits the same amount of  $\text{CO}_2$  into the atmosphere as was originally absorbed in the process of photosynthesis in the natural  $\text{CO}_2$

cycle [18].

### **1.3 Problem Statement**

The use of diesel fuel in CI engine releases pollutants such as particulate matter, oxides of nitrogen, carbon monoxide, unburned hydrocarbon and carbon dioxide. The quantity of pollutants released is highly dependent on the oxygen level, combustion temperature and type of fuel. These pollutants have detrimental effects on human health and the environment [3].

Exposure to these emissions may lead to health ailments that reduce labour productivity, thereby leading to a rise in poverty level. In addition, pollutant accumulation results to rise in emission of greenhouse gases causing global warming. These impacts coupled with the challenges of escalating fuel prices due to increase in demand create a need to produce and utilize alternative fuels such as biogas.

The use of biogas in CI engines requires a means of admitting the gas into the engine combustion chamber and a way of regulating the pilot fuel, implying that biogas cannot be used in the diesel engine without modification. These challenges demonstrate that there is a need to develop a dual fuel engine that would utilize biogas as an alternative fuel for DICI engines.

Although there are researches on the combustion and emission characteristics of bio-fuels and petroleum fuels with the dual-fuel concept, it is necessary to investigate also in more detail, the performance characteristics of the biogas-diesel dual-fuel engine. Furthermore, dual fuel engines are not readily available locally hence the need to develop them for the local market since a substantial amount of biogas is currently being produced across the country.



## 1.4 Objectives

The principal objective of this research was to modify a diesel engine to run on biogas and diesel fuels as a dual fuel engine with diesel as the pilot fuel and biogas as the primary fuel and to achieve optimum thermal efficiency with reduced gaseous emissions. To achieve these objectives, the following specific objectives were to be accomplished;

- To design and fabricate an efficient mixing device for biogas and air for the dual fuel engine.
- To evaluate the performance of the modified dual fuel engine and compare with that of the diesel engine.
- To investigate the effect of Exhaust Gas Recirculation on engine performance and exhaust emission.

## 1.5 Outline of Thesis

The thesis is divided into five chapters. The present chapter highlights the existing problem related to increase in price of petroleum fuels coupled with high levels of harmful emissions from CI engine and identifies the need to find alternative fuels for the CI engine. Chapter 2 is a review of existing literature on research that has been undertaken towards use of alternative fuels in IC engines. It presents a critical review on use of biofuels such as biogas and biodiesel in IC engines. The gaps that have been identified in this review have been outlined.

Chapter 3 outlines the experimental set-up and the procedure involved in modification of the diesel engine into a dual fuel engine that uses biogas and diesel fuels. It also presents the parameters measured to establish performance of the modified CI

engine. The parameters include torque, engine speed and fuel consumption. In chapter 4, the results obtained from engine performance tests and emissions analysis from the modified dual fuel engine are presented and discussed. Chapter 5 contains the conclusions deduced from the determined parameters of the dual fuel engine and the recommendations for further work on use of biogas in CI engines.

## CHAPTER TWO

### 2.0 LITERATURE REVIEW

#### 2.1 Overview

The combustion of fossil fuels in IC engines results in pollutant emissions that have adverse effects on the environment and human health. In an attempt to address this challenge, there has been an enormous amount of research in recent years in the area of alternative fuels. In addition, the price of fossil fuels is constantly increasing due to worldwide demand and as a result, bio-fuels have been considered an attractive alternative due to their socio-economic advantages. The focus of most of the research work has been reduction of exhaust emissions while maintaining high performance of the engines. Mitigation efforts have varied influences in controlling the emissions from IC engines while some affect engine performance as well. This chapter presents a review of research work that has been done concerning use of biogas and other alternative fuels in dual fuel engines and the gaps that need to be addressed in further research.

#### 2.2 Dual Fuel Engines

Garnier *et al.* [19] defined a dual fuel engine as an ideal multi-fuel engine that operates effectively on a wide range of fuels including the flexibility of operating as a conventional diesel engine. During dual fuel operation, a carbureted mixture of air and high octane index gaseous fuel is sucked and compressed the same way air is sucked in a conventional CI engine. The compressed mixture of air and fuel-gas does not auto-ignite due to poor ignition quality of the gaseous fuel. Hence, it is ignited by a small liquid fuel injection, known as a pilot fuel, which ignites spontaneously at the end of the compression phase. A dual fuel engine therefore uses a primary and secondary fuel. The primary fuel is

the pilot fuel such as diesel and the secondary fuel may be natural gas (NG), liquified petroleum gas (LPG), hydrogen or biogas [20].

In 2006, J. Stewart *et al.* [21] modified a direct-injection CI engine into a dual fuel engine and fueled it with three different gaseous fuels: Methane, propane, and butane to investigate performance at various gaseous concentrations. They reasoned that a simple central point mixing system is the most inexpensive and straightforward method of admitting a gaseous fuel to the dual fuel engine. A simple venturi type gas mixer was therefore installed at a distance of ten times the gas pipe diameter, upstream of the inlet manifold to ensure complete mixing of air and the fuel was achieved. Engine performance data were obtained under steady state operating conditions at three loads corresponding to quarter, half and three quarters load (relative to 100 percent loading being 18.7 kW). They concluded that propane showed the most promising characteristic as a dual fuel engine fuel, with a reduction of up to 20 percent energy consumption being recorded. This was attributed to the enhanced reactivity of the fuel. Methane which has been the fuel of choice was found to increase the brake specific energy consumption for all cases considered. The study also stated that the engine clearly showed the benefits of reduced CO<sub>2</sub> emission which must be considered if proposed global reductions are to be achieved within the transport sector. Emission of CO<sub>2</sub> was reduced by up to 20 percent. This showed that dual fuel engines can be used to help achieve reduction in exhaust emissions. The study also recommended that better engine performance and further reduction in CO<sub>2</sub> emission could be achieved with the employment of modern fuel injection equipment such as high pressure common-rail and multiple injection strategies.

Research has shown that dual fuel engines already operate under the NO<sub>x</sub> and SO<sub>x</sub> limits set out by the International Maritime Operations Tier 3 regulation, representing an interesting alternative to diesel engines equipped with EGR or exhaust gas after-

treatment [22]. According to a comprehensive simulation study by C. Christen *et al.* [22], a homogeneous mixture of fuel gas and air is crucial in order to achieve low  $\text{NO}_x$  emission as well as reducing the risk of knocking combustion. Continuous admission of fuel gas was found to achieve best mixing results. Too much gas admission led to increased accumulation of rich fuel gas in cylinder crevices which was a main source of unburned hydrocarbons. The starting point of the simulation-based study was an engine model calibrated with measured data obtained from a single cylinder turbocharged dual fuel engine with Miller cycle and fixed camshaft featuring a standard main diesel injection system, a common-rail system for pilot fuel injection and a port injection system for gas admission. This simulation model was extended and modified with two-stage turbocharging system and increased compression ratio. The results also showed that efficiency and power output of dual fuel engines can be substantially improved by introducing two-stage turbocharging and variable valve timing, pilot fuel injection system capable of flexible start of injection setting, optimized but fixed compression ratio and a mechanical structure for a gas engine with brake mean effective pressure of 26 bar and cylinder firing pressure up to 220 bar. This technical information is useful in developing a dual fuel engine from a diesel engine.

### **2.3 Octane and Cetane Number**

Octane number is the fuel property that describes how well a fuel will or will not self-ignite. It is a numerical scale generated by comparing the self-ignition characteristics of the fuel to that of standard fuels in a specific test engine at specific operating conditions. The two standard reference fuels used are isooctane (2, 2, 4 trimethylpentane), which is given the octane number (ON) of 100, and n-heptane, which is given the ON of 0. The higher the octane number of a fuel, the less likely it will self-ignite. Engines with low compression ratios can use fuels with lower octane numbers, but high-compression

engines must use high-octane fuels to avoid self-ignition and knock [23].

In a compression ignition engine, self-ignition of the air-fuel mixture is a necessity. The correct fuel must be chosen which will self-ignite at the precise time in the engine cycle. It is therefore necessary to have knowledge and control of the ignition delay (ID) time of the fuel. The property that quantifies this is called the cetane number (CN). The larger the cetane number, the shorter is the ID and the quicker the fuel will self-ignite in the combustion chamber environment. A low cetane number means the fuel will have a long ID.

Like octane number rating, cetane numbers are established by comparing the test fuel to two standard reference fuels. The fuel component n-cetane (hexadecane),  $C_{16}H_{34}$ , is given the cetane number value of 100, while heptamethylnonane (HMN),  $C_{12}H_{34}$ , is given the value of 15. The cetane number of other fuels is then obtained by comparing the ID of that fuel to the ID of a mixture blend of the two reference fuels as shown in Eq. 2.1 [23].

$$C = N + 0.15H, \quad (2.1)$$

where  $C$  = cetane number of the test fuel,  $N$  = percentage of hexadecane fuel in the mixture of reference fuels,  $H$  = percentage of heptamethylnonane in the mixture.

## 2.4 Use of Biogas in IC Dual Fuel Engines

Dual fuel engines have been a subject of high interest due to their potential to reduce smoke emission with improved performances [24]. They exhibit good thermal efficiency and low smoke level at high power output [25]. The drawback is that this reduction is often accompanied by an increase in emissions of carbon monoxide (CO)

and unburned hydrocarbons [21]. In the last ten years, many studies on the IC engines aimed at increasing engine performance and reduction of exhaust emissions have been carried out by changing operating parameters such as valve timing, injection timing, and atomization rate among others.

Experimentally, I.D. Bedoya *et al.* [26] found out that gasoline pilot port injection with high equivalence ratios above 0.4 in a Homogeneous Charge Compression Ignition (HCCI) engine lowered CO and HC emissions while NO<sub>X</sub> emission was increased. A typical biogas composition of 60% CH<sub>4</sub> and 40% CO<sub>2</sub> in a volumetric basis was simulated by controlling the CH<sub>4</sub> and CO<sub>2</sub> flow rates. It was concluded that HCCI combustion of biogas enables high overall efficiency, and the strategies explored in the research allowed higher power output, and more stabilized combustion. Though the findings of this research are worth appreciating, it is noted that the research used simulated biogas by mixing methane and carbon dioxide in certain ratios. This might not give accurate results since actual biogas has other components such as hydrogen sulphide, nitrogen, hydrogen and oxygen. The use of actual biogas would have given more reliable results for engine performance and emission characteristics.

An experimental investigation was performed by S.H. Yoon *et al.* [17] to study the influence of dual-fuel combustion characteristics on the exhaust emissions and combustion performance in a diesel engine fueled with biogas and biodiesel. Biogas was injected during the intake process by two electronically controlled gas injectors installed in the intake pipe of the engine. The results of this study showed that significantly lower NO<sub>X</sub> emissions were emitted under dual-fuel operation for both cases of pilot fuels compared to single-fuel mode at all engine load conditions. Also, biogas-biodiesel provided superior performance in reductions of soot emissions due to the absence of aromatics, the low sulfur, and oxygen contents for biodiesel. The results of this work clearly show that the use of bio-fuels in IC engines is a sure way of reducing exhaust emissions while

maintaining high thermal efficiency. However, the research did not include a mixing device to ensure a homogeneous biogas-air mixture for better combustion. Better engine performance and lower emissions would be expected if an efficient mixing device was incorporated and EGR was employed.

A performance evaluation of a constant speed IC engine on compressed natural gas (CNG), methane enriched biogas and biogas was done by R. Chandra *et al.* [27]. A venturi type air intake and fuel gas supply system was used to supply the gaseous fuel into the engine. The observed loss in brake power due to conversion of diesel engine into spark ignition engine were 31.8%, 35.6% and 46.3% for compressed natural gas, methane enriched biogas and raw biogas, respectively. The results indicate that the power losses were quite high, with the highest loss recorded for raw biogas. Provision of a mixing chamber in the setup instead of a venturi type air intake could give a more homogenous air-fuel mixture resulting in better combustion and improved engine performance. This is because a mixing chamber provides a longer retention time of air and fuel inside it leading to a homogenous mixture with better combustion ability [28].

In a study by S. Siripornakarachai *et al.* [29], a bus diesel engine was modified to use biogas as fuel for electricity production in a farm. Modifications included addition of biogas carburettor for air-fuel mixing, replacing the fuel injection system with spark ignition system and reduction of compression ratio from the original 16:1 to 8:1 using a cylinder head spacer. The results showed that there was high emission of CO, though the engine power output was 134.20 kW which is satisfactory. Literature suggests that the compression ratio should be between 10:1 and 12:1 for biogas operation [28, 30]. Since the compression ratio was lowered to 8:1, this could have led to incomplete combustion hence increase in CO emission.

In another study by H.S. Sorathia *et al.* [31], the first and second laws of thermodynamics were employed to analyze the quantity and quality of energy in a single-cylinder,



direct injection diesel engine using petroleum diesel oil and biogas as fuel. Balances of energy and exergy rates for the engine were determined and then various performance parameters, energy and exergy efficiencies were calculated for diesel oil and diesel-biogas dual fuel. The maximum brake thermal efficiency for biogas was 27.50% as compared to 28.25% for diesel oil. For the diesel and diesel-biogas dual fuels, calculation results showed that 7.31% and 6.48% of the fuel exergy input was lost in heat transfer from the engine, respectively. The study concluded that diesel-biogas dual fuel mode produced lower energy conversion efficiency; which was offset by large replacement of diesel and induction air by biogas. The study concluded also, that biogas premixed charge dual fueling for the engine produced almost no performance deterioration at all test speeds. The results of this theoretical thermodynamic analysis are impressive and are worth validating through experimental methods.

N.S. Ray *et al.* [32] modified a CI engine into a dual fuel engine and used biogas for partial substitution of diesel to study the effect on performance of the engine. The study indicated good performance of the modified engine in terms of power output as well as reduction of exhaust emissions. There was a reduction in both CO and HC emissions, though the brake engine power decreased slightly with increase in percentage of biogas. This was due to lower energy content of biogas compared to diesel. It was concluded that 50% substitution of diesel with biogas was the optimum ratio for dual fuel operation. The highest ratio tested was Biogas:Diesel in the ratio 50:50. There is therefore need to investigate performance of the engine at higher substitution ratios such as Biogas:Diesel in the ratio 90:10.

## 2.5 Use of Other Gaseous Fuels in IC (Dual Fuel) Engines

### 2.5.1 Hydrogen

Hydrogen can be used in internal combustion (IC) engines with minimal emissions of pollutant gases [33]. A hydrogen-operated engine produces water as its main combustion product. It does not produce significant amounts of carbon monoxide (CO), hydrocarbon (HC) and carbon dioxide (CO<sub>2</sub>). The only undesirable emission is nitric oxide (NO) and nitrogen dioxide (NO<sub>2</sub>), which are oxides of nitrogen (NO<sub>x</sub>).

Gopal *et al.* [34] investigated the performance in a conventional single cylinder four-stroke diesel engine with hydrogen as inducted fuel under a wide range of the engine operation. The results showed that the thermal efficiency obtained was comparable with pure diesel operation and up to half the engine's energy requirement could be derived from hydrogen. However, the onset of knocking was well before stoichiometric combustion. The research showed a smooth and smokeless engine operation from the use of hydrogen. Therefore, the challenge that needs to be addressed is the early onset of knocking and the high cost of hydrogen.

From T. Korakianitis *et al.* [5], increased NO<sub>x</sub> emissions and pre-ignition tendencies during hydrogen and emulsified biodiesel dual fuel operation compared with normal CI engine operation are major constraints on engine power output. One method that has been used to successfully reduce NO<sub>x</sub> emissions is exhaust gas recirculation (EGR). While EGR is very effective in reducing NO<sub>x</sub> emissions (reductions of the order of 50% with a 20% EGR volumetric intake substitution [35]), previous work [36, 37] showed that hydrogen dual-fueling with EGR produces lower thermal efficiencies than hydrogen dual-fueling without EGR. This is primarily due to the dilution effect of EGR, where the oxygen concentration of the intake charge is reduced. It is therefore important to

establish a trade-off between engine performance and emissions when EGR is applied.

According to a review by L. P. Goswami *et al.*, a dual fuel engine has a high efficiency and it remains unchanged using secondary fuel, such as hydrogen, natural gas (NG) and liquified petroleum gas (LPG) [20]. A diesel-hydrogen dual fuel engine can be operated with less fuel than neat diesel operations, resulting in lower smoke level and higher brake thermal efficiency.  $\text{NO}_x$  emission is however high due to the high combustion temperatures for hydrogen. The review also suggested that  $\text{NO}_x$  emission can be reduced through exhaust gas recirculation.

### 2.5.2 Syngas

Syngas is a gaseous fuel composed majorly of hydrogen and carbon monoxide. B.B Sahoo *et al.* [38] modified a diesel engine to run on diesel and syngas as a dual fuel engine. Components such as gas mixer, non-return valve, pressure regulator and gas carburetor were incorporated in the modification. At light loads (20 - 40% of full load) dual fuel operation with gaseous fuel induction showed an inferior engine performance. This is due to the lower combustion rate caused by CO content in the syngas fuel. Again, at these loads, a small pilot quantity led to poor ignition and combustion of lean air-gas mixture. At higher loads beyond 40%, the engine performance improved with increase in load. Emission of  $\text{NO}_x$  was found to be high due to faster combustion rate of  $\text{H}_2$  present in syngas. The study however did not consider modifying the engine for EGR as a means of reducing  $\text{NO}_x$  emissions.

B.B Sahoo *et al.* [38] did an experimental evaluation on the effect of  $\text{H}_2$ :CO ratio in syngas on the performance of a dual fuel diesel engine operation. The CO content of syngas resulted in significant increases of the CO emissions as compared to 100%  $\text{H}_2$  mode due to incomplete combustion of CO in the fuel-gas. Again for syngas that con-

tains CO in its composition, the CO emission levels seemed to be sensitive to the engine load. At low engine loads, the CO emissions were increased significantly. In addition, at high engine loads (beyond 60%), the more pronounced premixed and advanced combustion of syngas fuels resulted in increased cylinder pressure and temperature and hence, tended to increase the  $\text{NO}_x$  concentration. This is due to the increase of the combustion temperature at higher loads as a result of faster combustion rate of  $\text{H}_2$  and CO. From this experiment, it was revealed that use of syngas in IC engines requires a means of reducing emission of  $\text{NO}_x$ .

In the year 2012, C.T. Spaeth [39] did a research on performance characteristics of a diesel fuel piloted syngas compression ignition engine. He converted a single cylinder diesel engine to operate in dual fuel mode through the elimination of the governor system and addition of an in-cylinder pressure transducer and custom intake system to facilitate the mixing of the gaseous fuel and combustion air. He then tested the engine on dual fuel operation using methane and syngas separately, with diesel as the pilot fuel. When operated on methane, the engine attained higher peak in-cylinder pressures along with higher torque, power, and thermal efficiency values for equal equivalence ratios. The results show that greater amounts of syngas had to be used to reach comparable results with methane due to the lower energy content of syngas. The ignition delay was greater for syngas, and the onset of knock occurred earlier with syngas in comparison to methane. The researcher concluded that it is necessary to use greater amounts of syngas to create similar performance values to that of methane due to the low energy content of syngas in comparison to methane. This was due to the fact that at the same equivalence ratio, the brake torque and brake power produced by syngas were less than those for methane, and the energy input was less for methane than for syngas. In addition, syngas operation produced lower thermal efficiencies and higher BSFC values for corresponding equivalence ratios in comparison to methane

operation. The primary benefit of using syngas was that it is a renewable fuel source that is carbon neutral. These results imply that since the major component of biogas is methane, its use in a diesel engine could give results comparable to those of methane.

## **2.6 Use of Liquid Bio-fuels in IC (Dual fuel) Engines**

### **2.6.1 Ethanol**

C. Sayin *et al.* [40] experimentally investigated the influence of injection timing on the exhaust emission of a single cylinder, four stroke, direct injection, naturally aspirated diesel engine using ethanol blended diesel fuel from 0% to 15% with an increment of 5%. The experimental test results showed that  $\text{NO}_x$  and  $\text{CO}_2$  emissions increased as CO and HC emissions decreased with increasing amount of ethanol in the fuel mixture. However, with advanced injection timings ( $30^\circ$  and  $33^\circ$  CA BTDC), HC and CO emissions diminished, while  $\text{NO}_x$  and  $\text{CO}_2$  emissions were boosted for all test conditions. These results showed that there is need to find ways of reducing the  $\text{NO}_x$  emission for engine operation on ethanol.

In 2009, Zhiyou Wen *et al.* did a research on production of ethanol and its use in spark ignition engines [41]. They reported that Brazil, U.S.A and China are the top three ethanol producers in the world. The ethanol production from these three countries accounts for 78 percent of worldwide ethanol production. The research also indicated that ethanol has a higher octane number (ON 113) than regular unleaded gasoline (ON 87) and premium unleaded gasoline (ON 93) and the higher octane number reduces the tendency for an engine to pre-ignite and knock, making it run more smoothly. The findings of this research showed that some engines (vehicle engines) can operate on any blend of up to 85 percent ethanol. Currently, all major automakers (General Motors,

Ford Motor, Daimler Chrysler, Acura/Honda, Audi, BMW, Hyundai, Infiniti/Nissan, Isuzu, Jaguar, Kia, Land Rover, Lexus/Toyota, Mercedes-Benz, Mazda, Mitsubishi, Porsche, Rolls Royce/Bentley, Saab, Saturn, Subaru, Suzuki, Volkswagen, and Volvo) approve the use of gasohol (a mixture of gasoline and ethanol.) up to 10 percent ethanol, under warranty for the vehicles they produce [41]. Ethanol was revealed to be a suitable alternative fuel for SI engines. However, it has a higher volatility than regular gasoline; therefore, its emissions increase slightly in warm weather due to evaporation.

## 2.6.2 Biodiesel

Biodiesel is produced when vegetable oil is reacted with an alcohol in the presence of a catalyst through a process of transesterification [42]. The alcohol replaces the glycerin in the vegetable oil molecule to produce an ester and glycerin. The glycerin is then allowed to settle out. Often the biodiesel is water-washed to extract any remaining glycerin or other impurities. Biodiesel production gives by-products of waste water and glycerin. The favoured alcohol, methanol, is potentially hazardous and care has to be taken with its use. There are numerous variations of biodiesel production and each has its own inherent advantages and disadvantages.

Daming H. *et al.* [42] categorized feed stocks for biodiesel into crops; including soybean and rapeseed among others. Oil trees such as palm oil were also included in their findings. They noted that these types of oils come from vegetables or animal fat, making them biodegradable and nontoxic. Given the fact that feedstock of biodiesel depends greatly on climate and local soil conditions, biodiesel may not be a very reliable fuel considering climatic change and soil degradation. Some of the plants which form the feedstock for biodiesel also take a long time to mature, leaving biogas as a more reliable bio-fuel compared to biodiesel.

## 2.7 Exhaust Gas Recirculation (EGR)

High  $\text{NO}_X$  emission from diesel engines remains a major problem with regard to pollution. In order to reduce emission levels, some external engine features can be applied, such as EGR or after-treatment systems. EGR systems have been used to reduce emissions of nitrogen oxides ( $\text{NO}_X$ ) from diesel engines. Depending on the engine operating conditions, these systems divert 5-30% of an engine exhaust stream back to the combustion chamber [43]. The exhaust gas mainly consists of  $\text{CO}_2$ ,  $\text{N}_2$  and water vapour. When a part of this exhaust gas is re-circulated to the cylinder, it acts as diluent to the combusting mixture. This also reduces the  $\text{O}_2$  concentration in the combustion chamber. The specific heat of the exhaust gas is much higher than fresh air, hence EGR increases the heat capacity (specific heat) of the intake charge, thus decreasing the temperature rise for the same heat release in the combustion chamber [6].  $\text{NO}_X$  formation is a highly temperature-dependent phenomenon and takes place when the temperature in the combustion chamber exceeds 2000 K. Formation of  $\text{NO}_X$  is almost absent at temperatures below 2000 K [6]. Therefore, in order to reduce  $\text{NO}_X$  emissions in the exhaust, it is necessary to keep peak combustion temperatures under control.

Dual-fuel engines at part load inevitably suffer from lower thermal efficiency and higher emission of carbon monoxide and unburned fuel. In a research by Hosseinzadeh *et al.* [44], they used a quasi-two-zone combustion model developed for studying the second-law analysis of a dual-fuel (diesel-gas) engine operating under part-load conditions. They investigated the combustion phenomenon from second-law point of view at part load and using exhaust gas recirculation (EGR) to improve the aforementioned problems. Various availability components were identified and calculated separately with crank position. These included chemical availability, thermo-mechanical availability, work availability, availability transfer through heat and irreversibility. The

results showed that second-law efficiency was increased by using low amounts of radical and thermal cases of EGR. The results also showed that with employment of EGR, the combustion process improved due to enhancement of the oxidation process in lean mixtures. Also, it was noted that the presence of very active radicals and a higher intake charge temperature can promote the combustion process and therefore reduce the chemical availability of unburned fuel in the exhaust gases. The results also indicated that the dual-fuel engine can obtain maximum work availability, minimum destruction availability and minimum chemical availability of unburned fuel when 2% of thermal or combined cases of EGR is introduced to the dual-fuel engine under part load operating conditions. Research therefore shows that EGR can be applied in reducing emission of oxides of nitrogen ( $\text{NO}_x$ ) and improving thermal efficiency.

## **2.8 Justification of Present Study**

From the foregoing review, use of both liquid and gaseous bio-fuels in the IC engine has been the focus of researchers in an attempt to find solutions to the challenges of environmental concerns and depletion of petroleum resources. Researchers have also experimented on the use of various gaseous fuels such as hydrogen, acetylene and compressed natural gas (CNG) in the IC engine as an alternative to the conventional diesel and petrol fuels. However, the high fuel costs and increase in the  $\text{NO}_x$  emissions associated with these fuels still remains a challenge. In addition, some of the gases such as acetylene, despite their remarkable combustion properties require special handling due to very high flammability. Biogas, which is produced by anaerobic fermentation of organic material has been identified as an alternative clean energy resource for the CI engine in view of its environmental friendly nature.



Dual fuel engines have been a subject of high interest due to their potential to reduce smoke emission with improved performances. This can be achieved through proper design of the mixing device for air and the gaseous fuel leading to improved thermal efficiency as well. The challenges involved in the modification of a diesel engine into a dual fuel engine results to; emission of particulates and carbon monoxide and loss of engine power due to inefficient mixing of air and the fuel gas for complete combustion.

From this review, it is evident that sufficient research has not yet been done to determine the optimum performance of a CI engine when run on biogas while keeping the exhaust emissions as low as possible. Some of the research work have also used simulated biogas by mixing methane and carbon dioxide in certain proportions and such may not give accurate results for engine performance on biogas.

Though emission of oxides of nitrogen from dual fuel engine running on biogas is relatively low compared to that for pure diesel mode, Exhaust Gas Recirculation (EGR) can be applied as a means of further reduction of  $\text{NO}_x$  emission. This has not been considered by most of the researchers. In addition, it is also important to investigate the effect of EGR on engine performance parameters such as brake power, brake specific fuel consumption and brake thermal efficiency.

Use of biogas as an alternative fuel for automobiles still remains a challenge due to the problem of compact storage. However, as researchers seek to address this challenge, application can be made to stationary IC engines such as in power generation, hoisting in construction sites and for pumps where biogas can be produced and used at the point of production.

The fact that there are no locally available engines that run on biogas and diesel as dual fuel engines provided a platform to modify a CI engine into a dual fuel engine that uses biogas and diesel; since Kenya has the capacity to produce biogas in large

quantities for running IC engines. The procedure adopted for the modification of the engine and thereafter its performance measurements, are presented in the next chapter.

## **CHAPTER THREE**

### **3.0 EXPERIMENTAL DESIGN AND METHODOLOGY**

#### **3.1 Introduction**

In this chapter, the modification of a Direct Injection Compression Ignition (DICI) engine into a dual fuel engine for diesel and biogas is presented. The engine was modified to use biogas, with the focus of maintaining high thermal efficiency while reducing harmful exhaust emissions. The procedure used in the design and fabrication of various components as well as the set up of the experiment showing the engine and its auxiliary components are shown. Thereafter, the setup to measure the parameters necessary to evaluate the engine specific fuel consumption, brake thermal efficiency and emission characteristics is presented.

#### **3.2 Experimental Setup**

Schematic and pictorial views of the experimental set up are shown in Figs. 3.1 and 3.2 respectively. The experimental setup consisted of the engine, the dynamometer, fuel supply and metering systems, engine and dynamometer water systems and measuring devices. Some of the components were designed and fabricated while others were modified to suit various applications. The following section presents the design and fabrication of the various components.

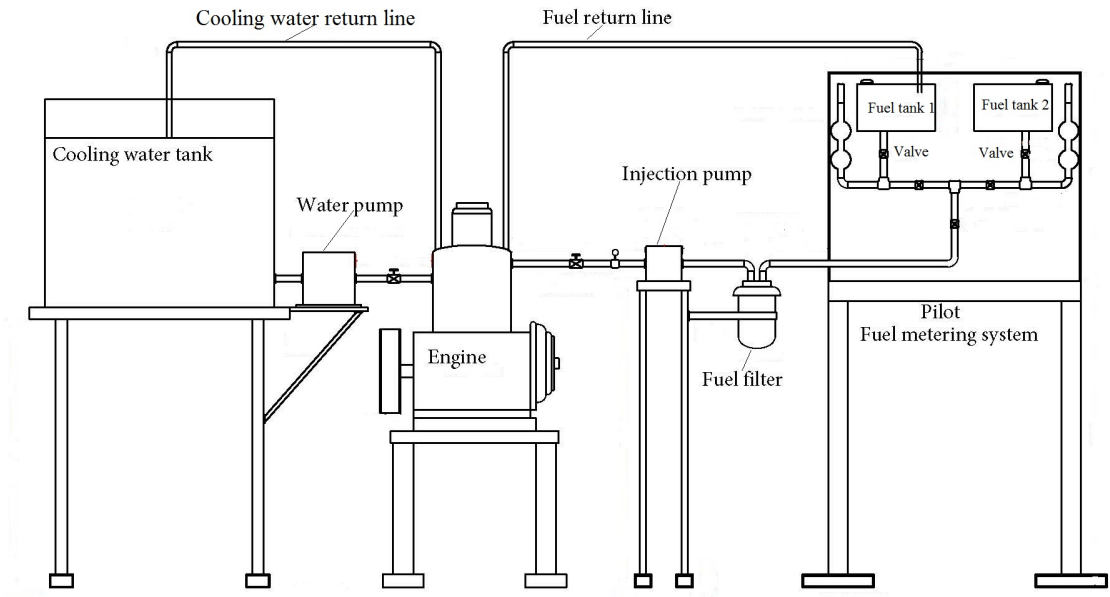


Figure 3.1: Schematic view of the experimental set up

### 3.3 Design and Fabrication of Experimental Set up Components

#### 3.3.1 The Fuel-Air Mixing Chamber

Schematic and pictorial views of the mixing chamber are shown in Figs. 3.3 and 3.4 respectively. The mixing chamber was designed and fabricated from mild steel pipes due to ease of fabrication and low cost of the material. The mixing chamber consisted of a short flow pipe of circular cross-section, with an inlet for air and for biogas each and an outlet for the mixture. The air inlet to the chamber and the outlet for the air-fuel mixture were designed to be tangential to the main body so as to cause swirling of air during operation and facilitate better mixing of air and fuel gas. The gas inlet was made from a copper tube closed at one end and with three holes drilled on its side. The gas tube was axially connected to the chamber so that biogas exited radially as it mixed with the swirling air. This design created turbulence in the flow of air and fuel

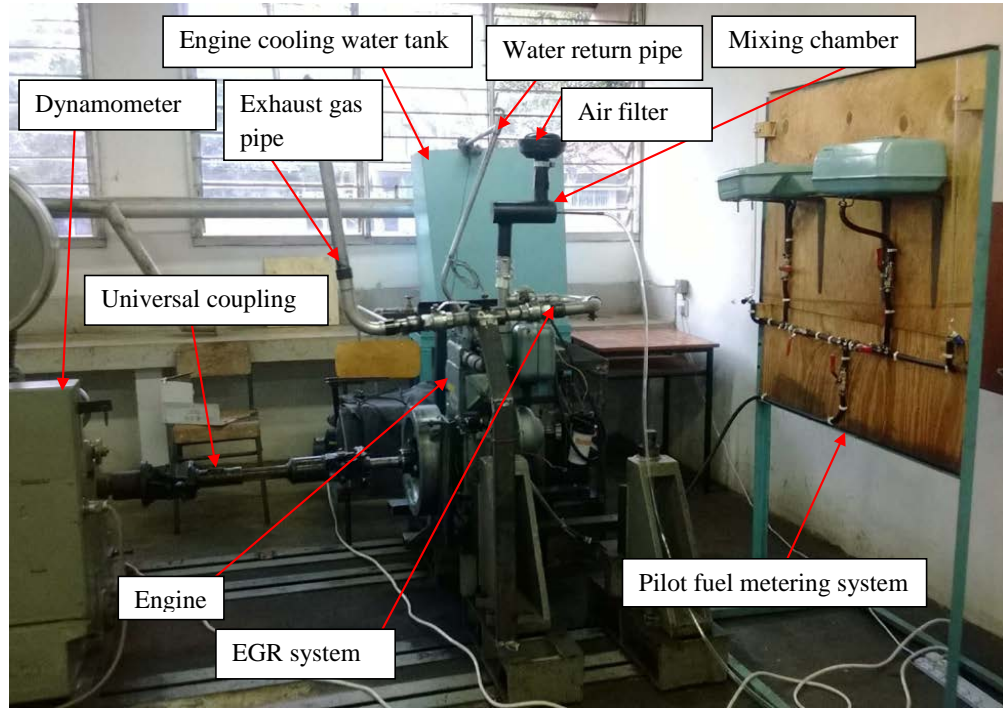


Figure 3.2: Pictorial view of the experimental set up

within the chamber resulting in homogeneous mixing of biogas and air before charging into the engine.

Design of the mixing chamber was based on engine capacity i.e cubic volume of engine, volume of the air filter, diameter of the air intake manifold, rated power of engine, biogas density, calorific value and biogas supply pressure. The parameters that guided the design of the mixing chamber are summarized in Table 3.1. Design equations (Eqs. 3.2 - 3.7) were adapted from a handbook by K. von Mitzlaff [28].

### Volume of the Mixing Chamber

The mixing chamber was made from a cylindrical mild steel pipe of diameter 100 mm and thickness 3 mm and therefore the formula for volume of a cylinder (Eq. (3.1) ) was used in finding the length. The volume of the mixing chamber was guided by the cubic capacity of the engine and volume of the air filter. The larger volume between the two

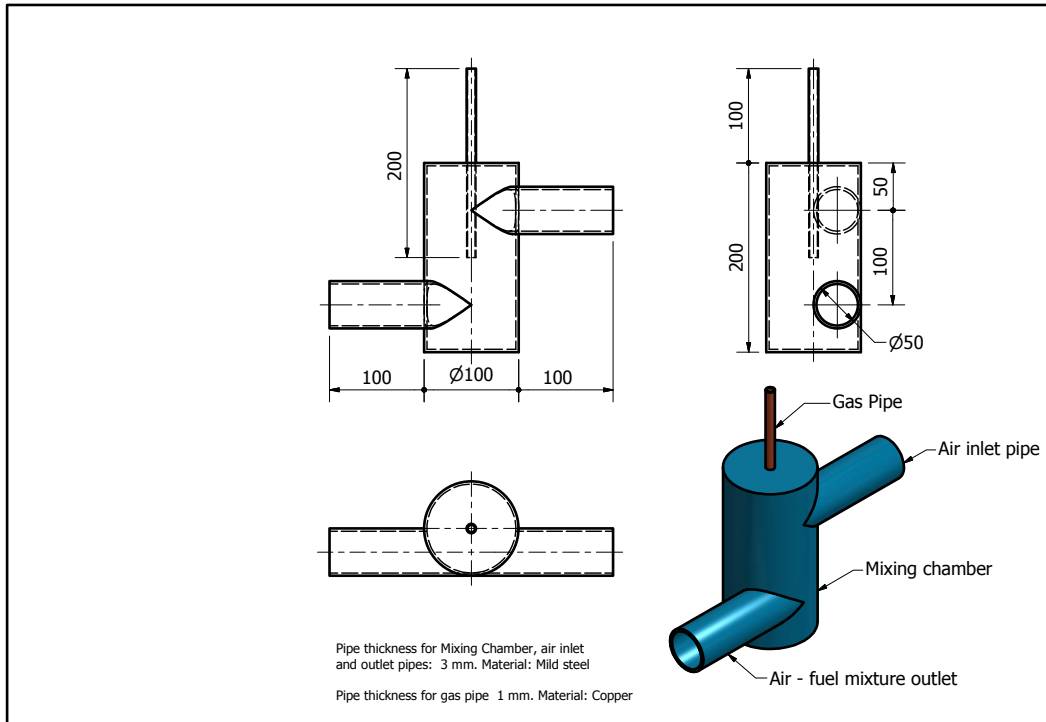


Figure 3.3: Schematic view of the mixing chamber for biogas and air

(i.e  $V = 1528 \text{ cm}^3$ ) was taken as the volume of the chamber; this is the recommended design procedure so as to ensure sufficient air is delivered to the engine [28].

$$V = \pi \frac{d^2}{4} l, \quad (3.1)$$

where  $V = 1528 \text{ cm}^3 =$  volume of the chamber,  $d = 100 \text{ mm} =$  diameter of the chamber, and  $l =$  length of the chamber. The design length of the chamber was found to be 200 mm.

### Connection to Engine and Air Filter

Air inlet to the mixing chamber and the outlet for air-fuel mixture were made from a mild steel pipe of diameter 50 mm and thickness 3 mm. This is from the recommended diameter of half the chamber body diameter [28]; this creates the required swirling



Figure 3.4: Pictorial view of the mixing chamber for biogas and air

motion of air and air-fuel mixture inside the mixing chamber. This diameter also matches the air filter connection (50 mm) and the engine intake manifold diameter (50 mm) and therefore facilitates smooth flow of air and air-fuel mixture respectively, as recommended. The connection of the chamber to the engine intake manifold and air filter was secured by use of worm drive clamps for circular pipes.

### **Sizing of the Gas Pipe**

The gas pipe dimension is mainly dependent on fuel energy required by the engine at maximum rated power and speed i.e 7.5 kW and 1500 rpm respectively and the volumetric calorific value of biogas i.e 23,302 kJ/m<sup>3</sup>. The procedure involved first evaluating the volumetric air intake,  $V_{air}$  (4-stroke engine) using Eq. (3.2).

$$V_{air} = \frac{V_h n}{2 \times 60 \times 1000} \eta_{vol}, \quad (3.2)$$

Table 3.1: Engine Specification and Design Parameters

	Parameter	Value
1	Number of cylinders	1
2	Number of strokes	4
3	Injection pressure (bar)	200
4	Injection timing ( $^{\circ}$ btdc)	23
5	Combustion system	Direct injection
6	Cubic volume of engine (cc)	950
7	Volume of the air filter (cm <sup>3</sup> )	1528
8	Rated power of engine (kW)	7.5
9	Rated speed of engine (rpm)	1500
10	Compression ratio	16.5:1
11	Fuel consumption (g/kWh )	251
12	Inner diameter of the air intake manifold (mm)	50
13	Density of biogas (kg/m <sup>3</sup> )	1.22
14	Volumetric calorific value of biogas (kJ/m <sup>3</sup> )	23,302
15	Volumetric efficiency of engine, $\eta_{vol}$ (%)	85
16	Percentage substitution of diesel by biogas (%)	80

where  $V_{air}$  = volumetric air intake in m<sup>3</sup>/s,  $\eta_{vol}$  = volumetric efficiency,  $V_h$  = engine cubic capacity in m<sup>3</sup> and n = engine speed in rpm.

The intake velocity,  $c_i$  was then evaluated from Eq. (3.3).

$$c_i = \frac{4V}{\pi d^2}, \quad (3.3)$$

where  $c_i$  = intake velocity in m/s,  $V$  = volumetric air intake in m<sup>3</sup>/s,  $d$  = manifold connection diameter or air inlet diameter = 50 mm.

Volume flow of biogas (fuel consumption,  $f_c$ ) at rated power was evaluated using Eq. (3.4).

$$f_c = \frac{sfcP}{3600}, \quad (3.4)$$

where  $f_c$  = biogas fuel consumption in m<sup>3</sup>/s,  $sfc$  = 0.8 m<sup>3</sup>/kWh = engine specific fuel



(gas) consumption in [28],  $P = 7.5 \text{ kW} = \text{rated power of engine}$ .

Assuming that maximum substitution of diesel with biogas would be 80% i.e percentage of biogas in total fuel (for dual fuel operation), based on literature, Eq. (3.5) was used to calculate the fuel consumption.

$$f_{c_d} = 0.8f_c, \quad (3.5)$$

where  $f_{c_d}$  = biogas fuel consumption in dual fuel operation ( $\text{m}^3/\text{s}$ ).

The cross-sectional area,  $A_g$  and diameter,  $d_g$  of nozzle were then calculated from Eqs. (3.6) and (3.7) respectively.

$$A_g = \frac{f_{c_d}}{c_g}, \quad (3.6)$$

where  $A_g$  = cross-sectional area of nozzle,  $f_{c_d}$  = biogas fuel consumption in dual fuel operation ( $\text{m}^3/\text{s}$ ),  $c_g$  = velocity at gas nozzle in  $\text{m}/\text{s}$ .

$$d_g = \sqrt{\frac{4 \cdot A_g}{\pi}}, \quad (3.7)$$

where  $d_g$  = diameter of nozzle in  $\text{m}$  and  $A_g$  = cross-sectional area of nozzle in  $\text{m}^2$ .

The design procedure gave a nozzle diameter of  $d_g = 9 \text{ mm}$ , for operation under the conditions specified. However, a 10% safety factor was included as an allowance; should the engine be operated at a higher rate of power and speed [28].

### 3.3.2 The Exhaust Gas Recirculation (EGR) System

A pictorial view of the EGR system is shown in Fig. 3.5.

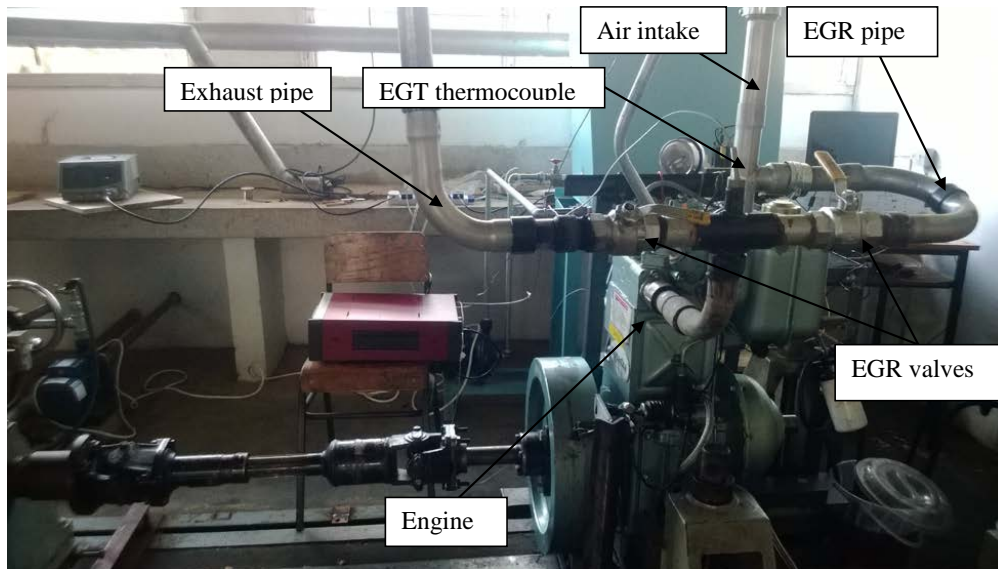


Figure 3.5: Pictorial view of the EGR system

The exhaust system was modified to allow testing and analysis of exhaust emissions as well as recirculating part of the exhaust gases to allow investigation on the effect of EGR on performance of the engine. The EGR system was designed and made from stainless steel alloy pipe of internal diameter 50 mm and thickness 2 mm. The system consisted of a pipe connection between the exhaust pipe and air inlet to the engine, and two stainless steel butterfly (gate) valves to regulate the quantity of recirculated exhaust gas from 0 to 30%. The pipes were connected by overlap joints fastened by bolt drive clamps to make the joints firm and leak proof. The main exhaust gas pipe was extended out of the engine room so as to direct exhaust gases out into the atmosphere. The extended pipe was supported at intermediate lengths using vertical steel supports fabricated from rectangular mild steel tubes of dimensions 100 mm by 50 mm by 3 mm to reduce vibrations as exhaust gases exited. The supports gave it stability to prevent failure from vibration and weight.

### 3.3.3 Manual Regulation of Pilot Fuel Quantity

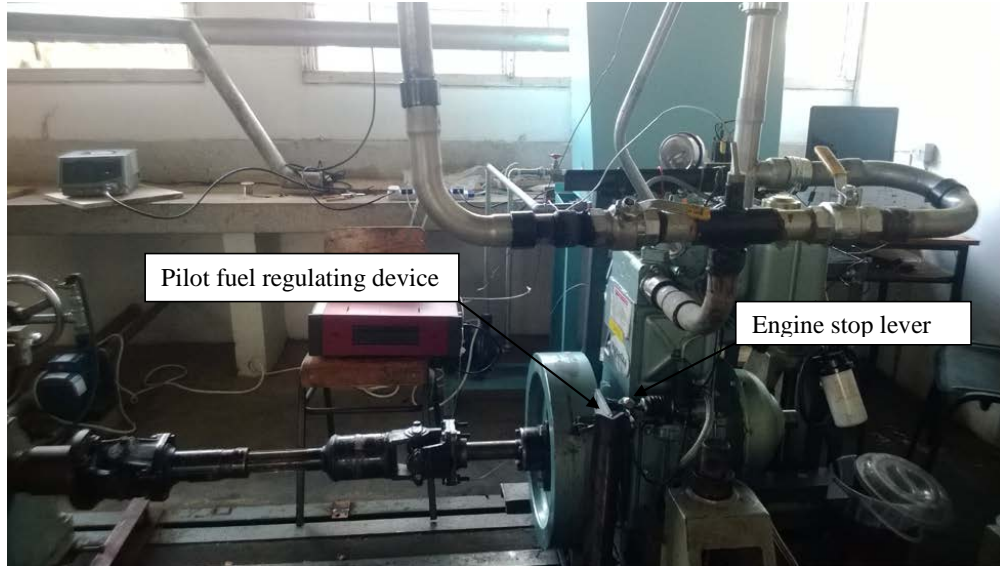


Figure 3.6: Pictorial view of the pilot fuel regulating device with reference to the engine

A pictorial view of the pilot fuel regulating device is shown in Fig. 3.6. The modification was done at the engine stop lever to allow for regulation of the amount of diesel fuel injected into the combustion chamber per cycle. This was to allow reduction of the diesel fuel injection quantity during dual fuel operation since diesel was to be used in small quantity as pilot fuel to ignite biogas. The pilot fuel regulating device was fabricated from V-section mild steel angle line of dimensions 50 mm by 50 mm by 5 mm, mild steel plate of 50 mm by 40 mm by 5 mm and M24 bolt and nut. A hole of diameter 30 mm was drilled in the plate which was then welded onto a 400 mm long section of the angle line at 55 mm from one end. The nut was then welded in the hole to allow fastening or loosening of the bolt in regulating the pilot fuel quantity by adjusting the position of the stop lever. The angle line was welded onto the engine support frame with the position of the nut close to and directly in line with the engine stop lever. Fastening the bolt in the nut would push the engine stop lever, constricting the fuel pump outlet and hence reducing the amount of fuel supplied to the injector. The

fuel regulating mechanism was calibrated to ensure that it delivers precise quantities of pilot fuel to the engine. This was done by cranking the engine with the manual fuel injector hanging out of the engine cylinder while collecting the injected fuel in an airtight bottle. The injected fuel was collected for twenty engine cycles, weighed on an electronic mass balance and the average calculated for one engine cycle. This was done for all the modes of engine operation and calibration marks put on the regulating bolt as a guide during engine operation.

### 3.3.4 Independent Fuel Injection System

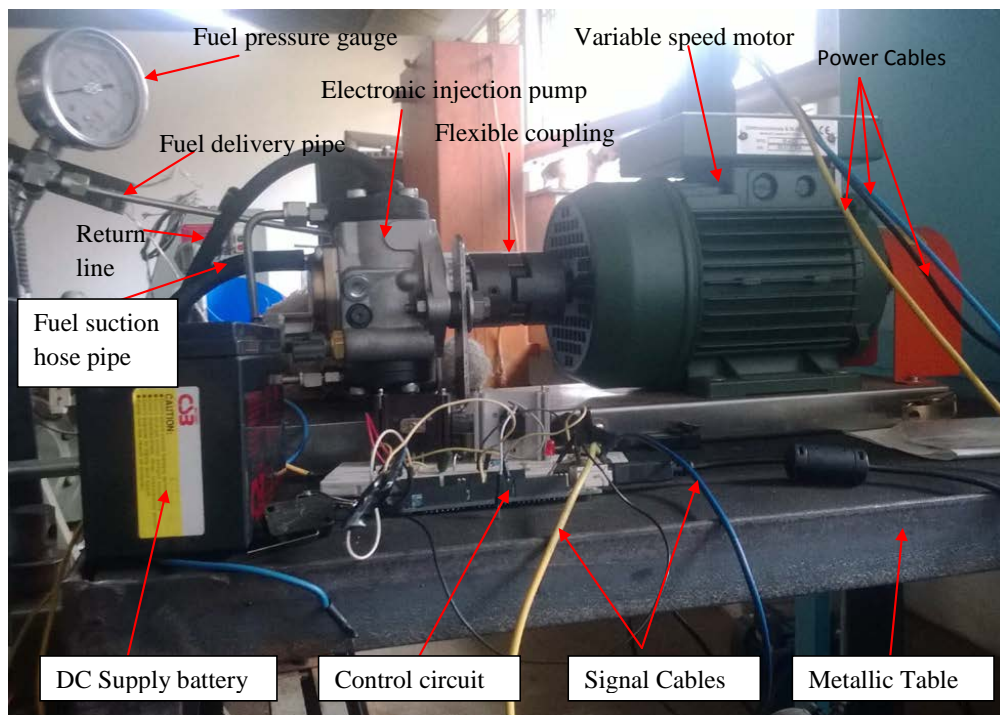


Figure 3.7: The independent electronic fuel injection system

A pictorial view of the electronic injection system is shown in Fig. 3.7. The system modification involved isolation of the mechanical in-built injection pump in the engine and installation of an external electronic injection pump driven by a variable speed motor and controlled by a signal from a sensor mounted at the engine flywheel. This was

done to allow varying of the diesel injection pressure while studying the effect on engine performance and emission characteristics. The injection pressure of the electronic injection pump, unlike that of the inbuilt manual pump of the engine could be varied through the variable speed motor. The system was controlled by arduino controller connected to a computer for programming of the controller and data acquisition. The independent fuel injection system was also calibrated to ensure that it delivers precise quantities of pilot fuel to the engine. This was done by cranking the engine with the manual fuel injector hanging out of the engine cylinder while collecting the injected fuel in an airtight bottle. The injected fuel was collected for twenty engine cycles, weighed on an electronic mass balance and the average calculated for one engine cycle. The mass of fuel injected in one cycle during manual operation was used to calibrate the electronic injection system by programming the controller to keep the injector nozzle open for a specified period of time to allow the right quantity of fuel for a given cycle.

### **3.3.5 Cooling Water Tank for the Engine**

A schematic view of the cooling water tank is shown in Fig. 3.8. The engine used in this research was a water-cooled type that required a recommended volume of 0.4 m<sup>3</sup> of cooling water to maintain the engine temperature at an optimum of about 80°C during operation (From the engine manual). The cooling water was to be circulated by a centrifugal pump from the tank through the engine and back to the tank. A rectangular water tank of the recommended capacity of 0.4 m<sup>3</sup> was fabricated from mild steel sheets of thickness 1.5 mm. The sheets were measured, marked and cut into five pieces; two pieces measuring 1000 mm by 800 mm, two measuring 1000 mm by 600 mm and one piece measuring 800 mm by 600 mm. A hole of diameter 15 mm was drilled at the center of the piece measuring 800 mm by 600 mm as a provision for connecting tank drain pipe. Another hole of diameter 15 mm was also drilled in one

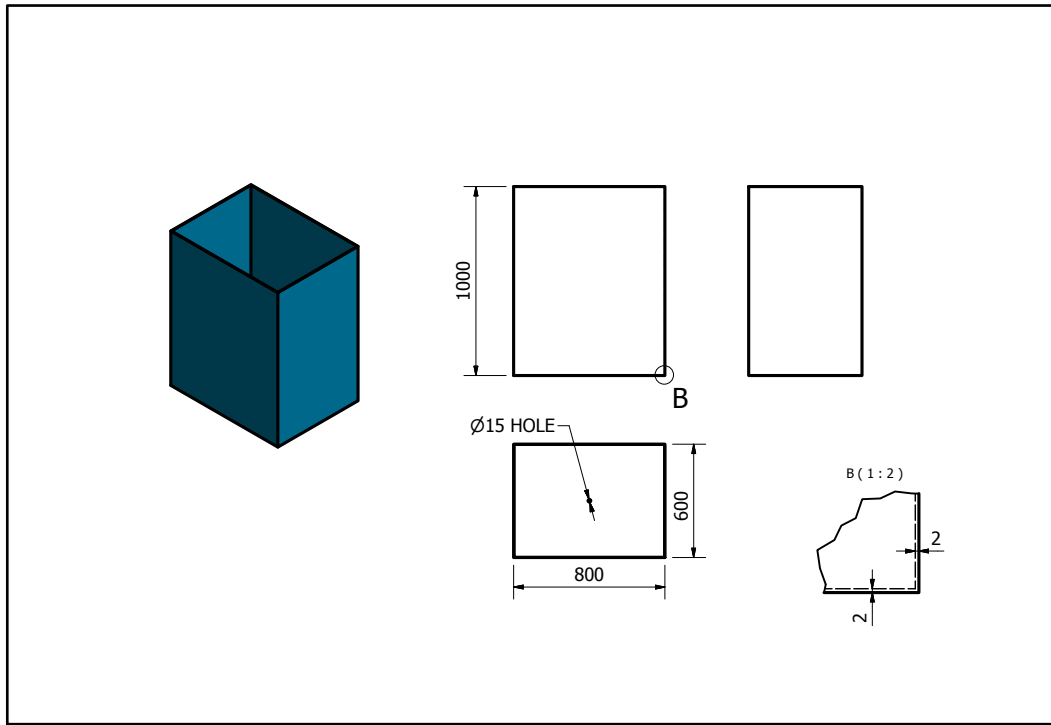


Figure 3.8: Schematic view of the cooling water tank for the engine

of the two pieces measuring 1000 mm by 600 mm, at 100 mm from one end (along the length) and midway the shorter side, as a provision for connecting tank outlet pipe. The pieces were set at right angles to one another and arc welded to make a rectangular water tank of dimensions 800 mm by 600 mm by 1000 mm with a volume of  $0.48 \text{ m}^3$ . The tank was spray-painted to protect it from corrosion and to improve the aesthetics. It was fabricated from mild steel sheets because of its low cost, ease to arc weld and good strength.

### 3.3.6 Cooling Water Tank for the Dynamometer

A schematic view of the dynamometer water tank is shown in Fig. 3.9. The SF-3.5 hydraulic dynamometer that was used in this research to measure the engine brake

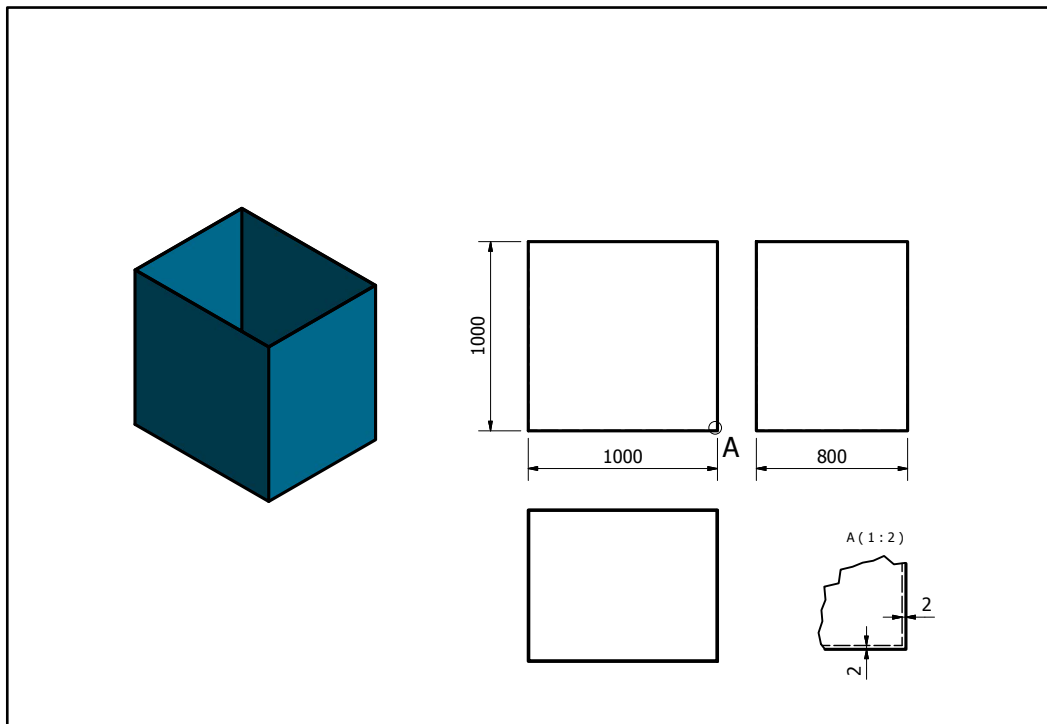


Figure 3.9: Schematic view of the cooling water tank for the hydraulic dynamometer power required a water supply of about 18 liters per horse power per hour, which was to be kept at outlet temperature of  $50^{\circ}\text{C}$  to  $70^{\circ}\text{C}$  during test. The recommended capacity of the tank holding the cooling water was  $0.75\text{ m}^3$  as indicated in the dynamometer manual. A rectangular tank was fabricated from mild steel sheets of thickness 1.5 mm. The sheets were first marked and cut into five pieces; two pieces measuring 1000 mm by 1000 mm and three pieces measuring 1000 mm by 800 mm. The pieces were then set at right angles to one another and arc welded to make a rectangular water tank of dimensions 1000 mm by 800 mm by 1000 mm, with a capacity of  $0.8\text{ m}^3$ . It was spray painted to provide protection from corrosion and to improve the aesthetics. The tank was fabricated from mild steel sheets because of low cost of the material, ease to arc weld and good strength.

### 3.3.7 Starter Motor Mounting Bracket

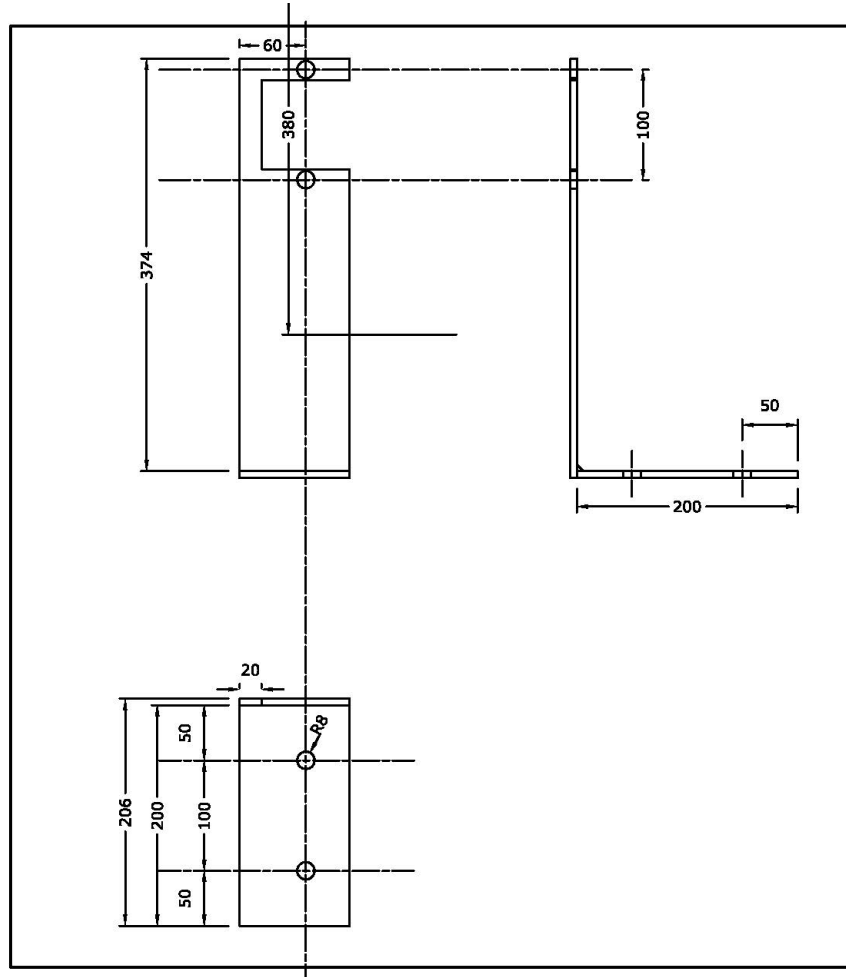


Figure 3.10: Starter motor mounting bracket

A schematic view of the mounting bracket designed and fabricated for holding the engine starter motor, is shown in Fig. 3.10. The engine available for this research was a manually started engine that is started by use of a cranking lever, inserted onto a shaft at the rear side of the engine and then turned by hand till the engine attains a speed of about 200 rpm at which it picks up. In order to make the starting easier, a modification was done to the engine to allow cranking through a starter motor by fixing the motor at the rear end of the engine. A mounting bracket for the starter motor was designed and fabricated from mild steel plate, 100 mm wide by 10 mm thick. The



motor was fastened on the mounting bracket via two M12 bolts and nuts; the bracket was in turn fastened onto the engine support frame by use of two M12 bolts. A spur gear of pitch circle diameter 150 mm was also designed, machined, and fixed onto the rear end shaft to act as the driven gear for starting the engine. The driver gear (of the starter) and the driven gear (on engine shaft) were then aligned for accurate meshing of the two during engine start.

### 3.3.8 Diesel Fuel Metering System

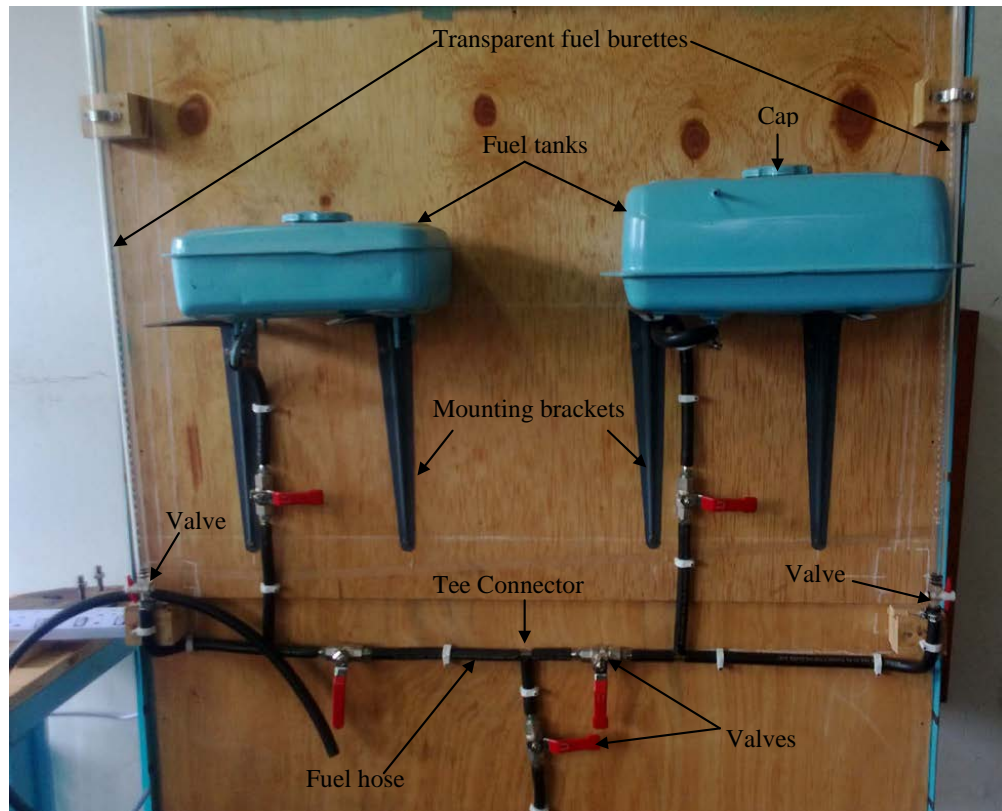


Figure 3.11: Diesel fuel metering system

A pictorial view of the fuel metering system is shown in Fig. 3.11. In order to determine the performance of the engine in terms of BSFC and BTE, the amount of fuel consumed by the engine per unit time had to be measured and recorded to be used

in analysis. This was made possible through design and fabrication of a fuel metering system consisting of two fuel tanks of 5 liter capacity each, two 50 ml capacity burettes, flexible rubber fuel tubes (internal diameter, 6 mm) and three shut-off taps (Chrome, internal diameter 1/4 inch). The fuel metering system was designed with two tanks as a provision for using blends of two different liquid fuels such as diesel and biodiesel in future research experiments. In this research however, the second tank was used as a back-up fuel reservoir.

The components were mounted on a block-board measuring 1000 mm by 1000 mm by 25.4 mm, fixed in a vertical frame made from mild steel angle bars of dimensions 40 mm by 40 mm by 3 mm. Each of the two fuel tanks was supported with two steel wall brackets fixed onto the board via steel screws. The frame was made from mild steel because of the strength and low cost of the material and was painted to improve the aesthetics.

### **3.3.9 Biogas Supply and Metering System**

A pictorial view of the biogas supply and metering system is shown in Fig. 3.12. Biogas was used to run the modified diesel engine in dual fuel mode and was supplied to the engine from a flexible gas bag, through a flow meter to measure the amount of gas consumed by the engine. The system consisted of a flexible (collapsible) gas bag of 3 m<sup>3</sup> capacity, flexible clear tube (internal diameter 8 mm), biogas pressure pump, flow meter, pressure meters (gauges), desulphurizer, dehydrator and flow switch. The gas was produced from water hyacinth in a digester at the Institute of Energy and Environmental Technology (IEET) in JKUAT. It was cleaned by passing it through the desulphurizer to eliminate hydrogen sulphide gas and then through the dehydrator to eliminate moisture, then packaged in the gas bag and transported to the engine

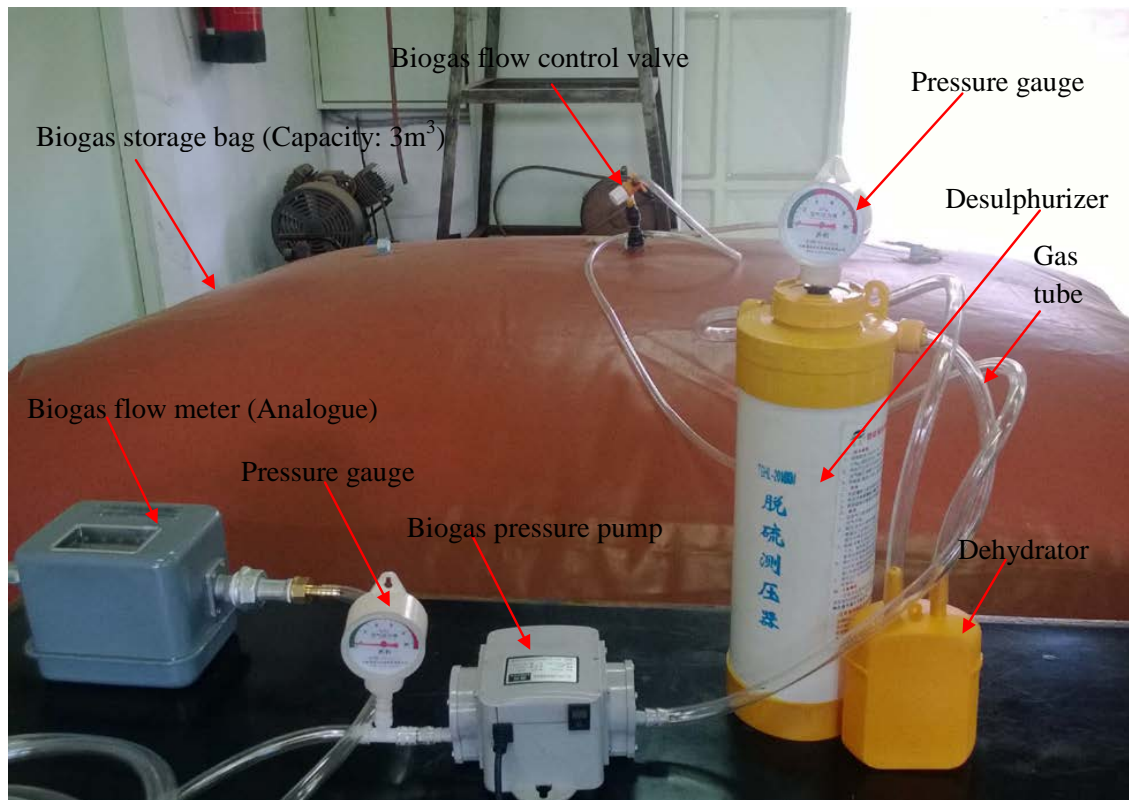


Figure 3.12: Biogas supply and metering system

room (laboratory) where experiments were done. At 50% substitution of diesel with biogas, the gas flowed into the engine by natural aspiration while at higher substitution levels of 70% and 80%, the flow of biogas into the engine was accelerated by use of the biogas pressure pump. This was done in order to boost the low supply pressure and meet the high demand for fuel by the engine. The pressure pump was a simple transfer pump of maximum pressure rating 10 kPa, for transfer of biogas to the engine. The flow switch (shut-off valve) was used to regulate the gas flow by turning it to quarter, half, three quarter or fully open positions and for closing the gas supply when not in use.

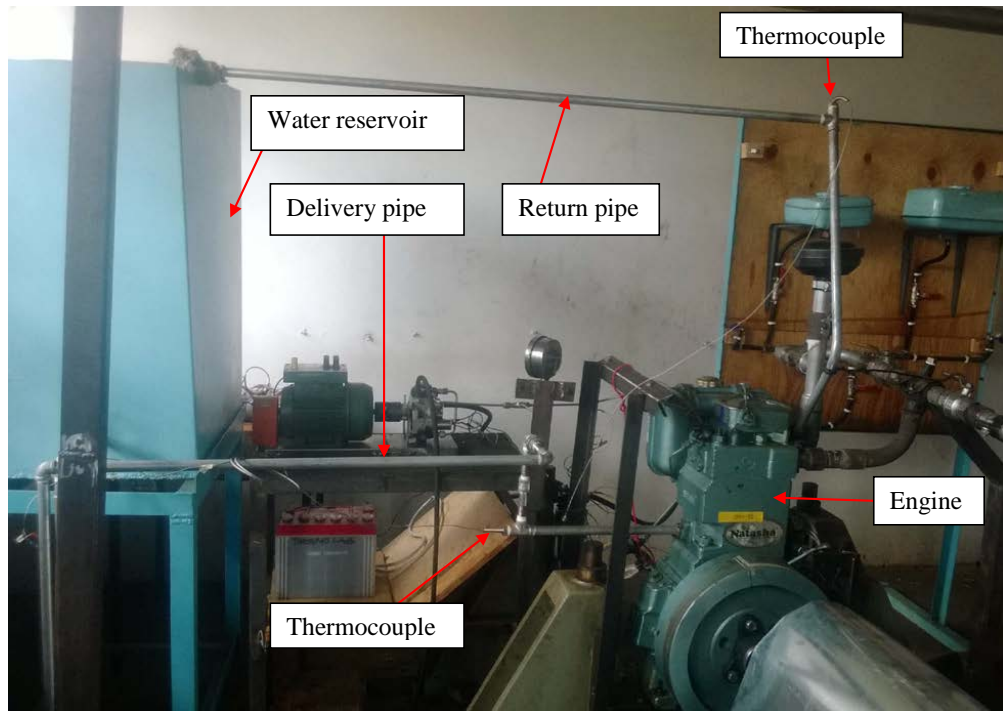


Figure 3.13: Engine cooling system

### 3.3.10 Engine Cooling System

Figure 3.13 shows a pictorial view of the engine cooling system. It consisted of a reservoir tank, a centrifugal pump for recirculating the coolant water, half inch diameter water pipes and thermocouples to measure the coolant water temperature at inlet and outlet of the engine. Cooling water was recirculated through the engine during operation in order to keep the engine temperature below  $80^{\circ}\text{C}$ , as recommended by the manufacturer.

### 3.3.11 Engine-Dynamometer Coupling Guard

A pictorial view of the engine-dynamometer coupling guard is shown in Fig. 3.14. The protective guard for the engine-dynamometer coupling was designed and fabricated from galvanized iron (GI) sheet of thickness 1.5 mm. The sheet metal was cut into

a piece of length 2200 mm and width 1200 mm. Four holes of diameter 14 mm were drilled on the sheet, one at each of the four corners, 50 mm from the edges. All the edges were folded at 20 mm from the edge as a safety precaution and the sheet rolled into a parabolic shape, after which it was securely fixed over the coupling using M12 bolts and nuts.



Figure 3.14: Coupling guard

### 3.4 Cleaning of Biogas

Biogas contains traces of hydrogen sulphide gas and moisture which are detrimental to the engine since they cause corrosion of engine parts [45,46]. It was therefore treated to eliminate the two components, before supplying it to the engine.

#### 3.4.1 Desulphurization

Hydrogen sulfide is the chemical compound with the formula  $H_2S$ . It is a colorless, corrosive, very poisonous, flammable gas with the characteristic foul odor of rotten

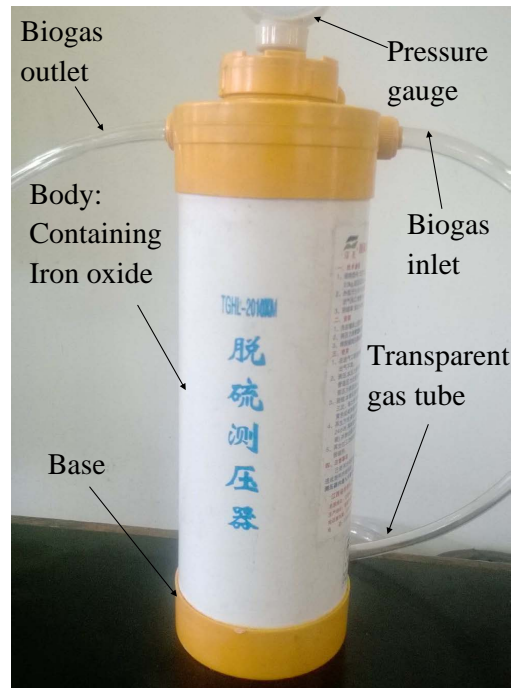
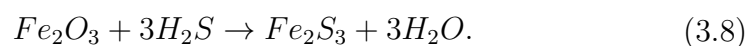
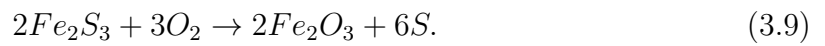


Figure 3.15: Biogas desulphurizer

eggs [47]. It results mostly from the bacterial breakdown of organic matter in the absence of oxygen; a process commonly known as anaerobic digestion, which is the main process in biogas formation [48]. Due to its corrosive nature,  $H_2S$  had to be removed before biogas could be used in the engine. It was removed by passing biogas through the desulphurizer shown in Fig. 3.15 during packaging from the digester and during use. The biogas desulphurizer consisted of a cylindrical plastic container-main body (of volume 2.5 liters, measuring 350 mm height by diameter 110 mm ), gas inlet and outlet openings on the upper part of the body (for diameter 10 mm soft pipe or diameter 16 mm hard pipe), a pressure gauge for pressures between 0 and 16 kPa and 2.0 kg of desulfurizing agent (Iron oxide,  $Fe_2O_3$ ). Hydrogen sulphide gas was removed through chemical mechanism as it reacted with iron oxide ( $Fe_2O_3$ ) to form iron sulfide ( $Fe_2S_3$ ) as shown in Eq. (3.8) [49].



The iron oxide was regenerated with oxygen according to the reaction in Eq. (3.9) by exposing it to the atmosphere to react with the atmospheric oxygen [49].



### 3.4.2 Dehydration

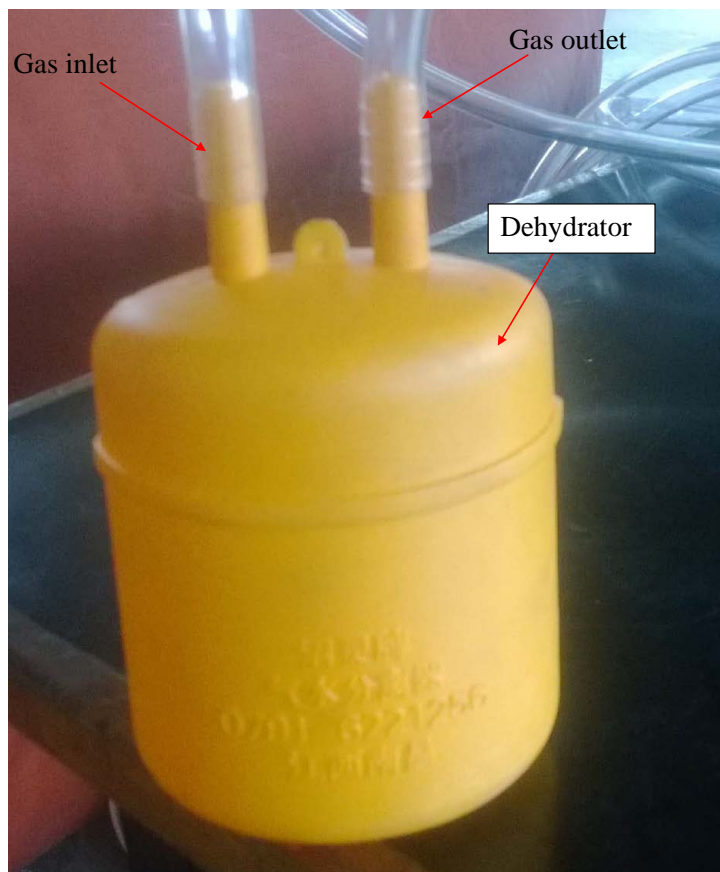


Figure 3.16: Biogas dehydrator

During packaging of biogas, it was passed through the dehydrator shown in Fig. 3.16 to eliminate the moisture present in it and further dehydration was done during experiments to eliminate any moisture which would have remained in the gas during packaging [49]. The dehydrator introduces an expansion point in the gas flow system,

where moisture in the biogas condenses and is collected as the fuel gas flows through it.

### 3.5 Exhaust Gas Recirculation

Exhaust Gas Recirculation (EGR) is a technique used to reduce  $\text{NO}_x$  emission in which part of the exhaust gas is recirculated and taken back to the combustion chamber along with the intake air [50, 51]. It acts as a diluent to the combustion mixture and reduces oxygen concentration while increasing specific heat of incoming charge. This ultimately reduces peak combustion temperature under which  $\text{NO}_x$  is generated. EGR has also the advantage of resupplying of unburned hydrocarbons, giving them an opportunity to re-burn [52, 53].

The percentage of exhaust gas recirculation is defined as volume of the EGR to total intake charge into the cylinder, given by Eq. (3.10) [43, 51].

$$\%EGR = \frac{100V_{EGR}}{V_{TOTAL}}, \quad (3.10)$$

where  $\%EGR$  = Percentage of exhaust gas recirculation,  $V_{EGR}$  = Volume of recirculated gas,  $V_{TOTAL}$  = Total volume of intake charge to the cylinder.

The EGR system used in this research is shown in Fig. 3.5. The investigation of the effect of EGR on engine performance was started by running the engine at a rated speed of 1500 rpm till the warm-up period was reached. The engine was then loaded in terms of 0%, 25%, 50%, 75% and 100% corresponding to the loading conditions of no load, quarter load, half load, three quarter load and full load respectively. At each load, the engine was run with different EGR conditions. The exhaust gases were tapped from the exhaust pipe and directed to the air inlet through the EGR system,



consisting of two control valves and a graduated flat metal plate to indicate the degree of valve opening.

After attaining the steady state condition, observations were made for various parameters such as exhaust gas temperature, fuel consumption, torque and actual engine speed which were then recorded at various loads. Exhaust emissions of CO, CO<sub>2</sub> and HC were recorded simultaneously by the exhaust gas analyzer. For dual fuel operation, the effect of maximum diesel substitution (Biogas 80%-20% Diesel) and EGR on engine performance and emissions were evaluated at an engine speed of 1500 rpm. At each load the experiment was conducted by varying EGR rates such as 0%, 10%, 20% and 30%.

The first stage of the experiment was performed with the pure diesel at different loads from no-load to full load with different EGR rates of 0%, 10%, 20% and 30% respectively at constant speed. The reason why higher EGR rates (beyond 30%) were not considered in this study is the reduction in BTE and an increase in CO, HC and smoke emissions with higher EGR rates [54]. The second stage of the experiment was conducted under dual fuel operation and the same procedure repeated. The optimum percentage EGR for NO<sub>x</sub> emission was based on the EGR rate which yielded the highest BTE and lowest BSFC. The optimum percentage EGR was determined also by the EGR rate which led to the least rise in CO and HC emissions.

### **3.6 Measurement Parameters and Procedures**

The performance of the engine was determined by utilizing diesel in single fuel mode and biogas as primary fuel and diesel as pilot fuel in dual fuel mode, then evaluating the brake specific fuel consumption and brake thermal efficiency at each of the operating conditions. For this to be done, it was necessary that the quantity of fuel consumed by

the engine and the resulting brake power at each condition be known. In this section the method used in determining the rate of fuel consumption and the engine brake power is presented. Subsequently, the procedure for measurement of exhaust emissions is presented.

### 3.6.1 Diesel Fuel Consumption

The rate of diesel fuel consumption in each test was measured using the set up shown in Fig. 3.11. This was done by noting the time taken to consume 20 ml of the fuel then dividing the mass by the time. The mass flow rate was then obtained by multiplying the volume flow rate by the density of the fuel (Eq. 3.11). The fuel tank was filled before the start of every experiment, while keeping the tank outlet valve closed. At the start of the experiment, the fuel tank outlet valve was opened to allow fuel into the burette and to fill the fuel line. The fuel tank outlet valve was closed and the engine allowed to run on fuel from the metering burette while noting the time taken to consume 20 ml of fuel. The procedure was repeated to obtain five sets of data for every loading condition, from no load to full load. The recorded data for volume of fuel consumed and the time taken was used to calculate the fuel flow rate into the engine, using Eq. (3.11).

$$\dot{m}_f = \frac{V\rho}{t}, \quad (3.11)$$

where  $\dot{m}_f$  = rate of fuel flow into the engine in kg/s,  $V$  = volume of fuel consumed in  $\text{m}^3$ ,  $\rho$  = density of diesel in  $\text{kg}/\text{m}^3$  and  $t$  = time taken to consume the measured volume of the fuel in seconds. Properties of diesel are as shown in Table 3.2.

### Diesel Substitution

Table 3.2: Fuel Properties of Diesel

S/No.	Quantity	Value
1	Density (kg/m <sup>3</sup> )	837
2	LHV (kJ/kg)	42,000
3	Cetane Index	52
4	Flash point (°C)	76
5	Auto Ignition Temperature (°C)	230-280
6	Stoichiometric A/F Ratio	14.7
7	Chemical Formula	C <sub>10.8</sub> H <sub>18.7</sub>
8	Carbon (%)	84-87
9	Hydrogen (%)	13-16

The percent diesel substitution in dual fuel operation was calculated by subtracting diesel consumption by the engine on dual fuel mode from diesel consumption by the engine on single fuel mode (diesel alone) and then dividing the difference by diesel consumption by the engine on single fuel mode as shown in Eq. (3.12).

$$ds = \frac{100(D_d - D_{dg})}{D_d}, \quad (3.12)$$

where  $ds$  = diesel substitution, per cent,  $D_d$  = diesel consumption by the engine on single fuel mode, in kg/h,  $D_{dg}$  = diesel consumption by the engine on dual fuel mode, in kg/h.

### 3.6.2 Biogas Fuel Consumption

During dual fuel operation, the procedure for metering the amount of diesel consumed was maintained as described in the previous section while the quantity of biogas consumed was measured using the flowmeter in Fig. 3.17. The mass flow rate was then computed from the known density of the fuel (1.22 kg/m<sup>3</sup>). Other properties of biogas are as shown in Table 3.3. The flow meter had an accuracy of 0.001 m<sup>3</sup> and a range of 0 to 10000 m<sup>3</sup>. For every test, the initial and final meter reading was recorded as

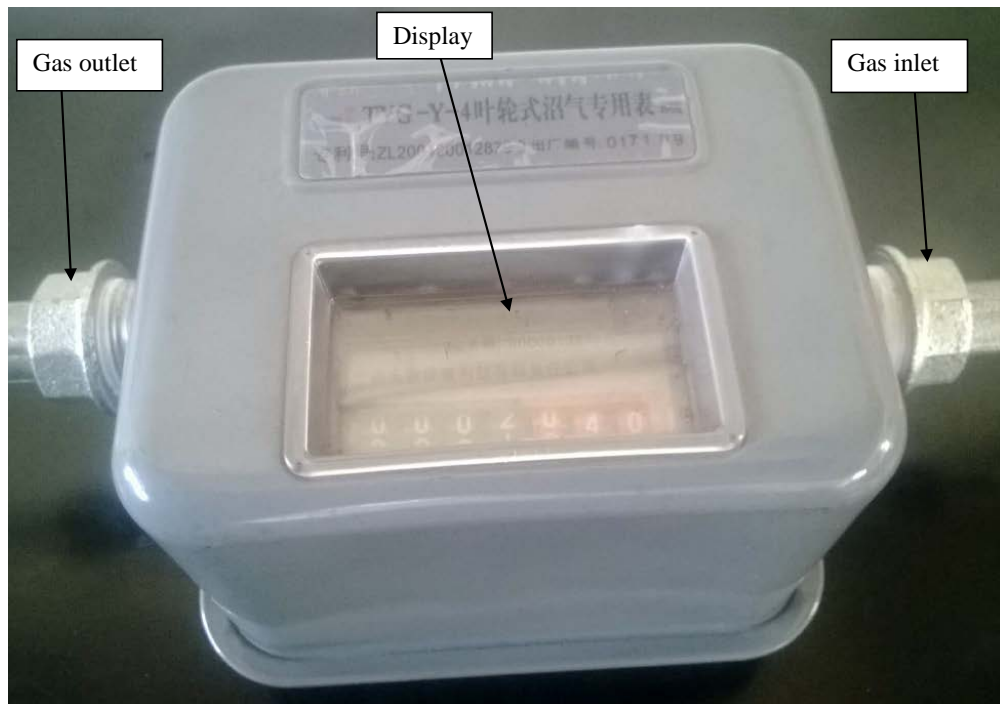


Figure 3.17: Biogas flow meter

well as time taken to consume the gas. The volume of gas consumed by the engine was calculated by subtracting the initial from the final gas reading. Mass flow rate was calculated using volume of gas consumed, density of the gas and the time taken.

Table 3.3: Fuel Properties of Biogas

S/No.	Quantity	Value
1	Methane (%)	49 - 53
2	Carbon dioxide (%)	21 - 29
3	Nitrogen (%)	17 - 19
4	Density (kg/m <sup>3</sup> )	1.22
5	LHV (kJ/kg)	19,100
6	Octane number	130
7	Auto-ignition temperature (°C)	632-813



Figure 3.18: The hydraulic dynamometer

### 3.6.3 Engine Brake Power

Engine brake power is the power output of the drive shaft of an engine i.e the power actually delivered by the engine. A Fuchino SF-3.5 hydraulic dynamometer shown in Fig. 3.18 was used to measure engine brake power at various operating conditions during the test. The dynamometer had a range of measurement of 0 to 150 kgf and an accuracy of 0.5 kgf and was used to load the engine from zero to full load, while noting the reading on the weight dial. For each load value, five sets of data were taken, averaged and the brake horse power obtained from the calculation formula given by Eq. 3.13.

$$P.S = \frac{WN}{1000}, \quad (3.13)$$

where  $P.S$  = brake horse power,  $W$  = torque indication in kg,  $N$  = revolution per minute.

### **Procedure for Measurement of Brake Power**

The dynamometer was calibrated before the start of experiments by use of calibration weights provided, to ensure that the weight dial pointer reading recorded was right. The engine (prime mover) was set on the test bed and connected to the dynamometer (brake) through a universal coupling. The engine and brake were both properly examined to confirm that all bolts and nuts were properly fastened to avoid any danger in the work environment (to the operator or the machine). The drain valve was closed, the inlet valve opened about one turn and the outlet valve regulated to keep the feed water pressure (supplied by a centrifugal pump at 18 liters per horse power per hour) between 1 and 2 kg/cm<sup>2</sup>. The sluice gate was set to fully closed position and the weight balance checked for zero point reading. The fuel tanks were filled with diesel and the connection of burette checked for proper operation without any leakage. For single fuel mode, the engine was started, ensuring the brake casing water pressure did not to exceed 3.0 kg/cm<sup>2</sup>. At this state, the torque (weight dial pointer reading) was recorded as well as the engine speed (using analogue tachometer on the control panel of the brake and a portable digital tachometer-RS 445-9557 laser type). The time taken to consume 20 ml of diesel fuel was recorded for five sets of data and the mean value calculated. The sluice gate was opened slowly to increase absorption power (loading) up to quarter load mark and the readings recorded for torque, speed and time. Readings were taken for five sets of data and then averaged. The procedure was followed for conditions of half load, three quarter load and full load by opening the sluice gate to

increase loading. The weight dial pointer reading recorded for each loading condition was converted to brake horse power using Eq. (3.13).

For dual fuel operation, both diesel and biogas were supplied to the engine from the diesel fuel supply and metering system and biogas supply and metering system respectively. Biogas was supplied to the engine through the mixing device connected to the engine along the air intake. The engine was started on 100% diesel with the biogas supply closed. At the start of test, the pilot fuel regulating device was used to slowly reduce the amount of pilot fuel (diesel) by fastening the fuel adjustment bolt. At bolt advance of quarter the thread length, biogas supply to the engine was started by opening biogas flow control valve quarter way. The brake sluice gate was set to fully closed position and the weight balance checked for zero point reading. Water supply to brake was switched on and the engine started. The engine was started, taking note of the brake casing water pressure not to exceed  $3.0 \text{ kg/cm}^2$ . The torque (weight dial pointer reading) was recorded as well as engine speed.

The time taken to consume 20 ml of diesel fuel was recorded for five sets of data and the mean value calculated. For subsequent tests, the amount of diesel supplied to the engine was reduced further by turning the fuel adjustment bolt while at the same time increasing the amount of biogas supplied to the engine by opening the biogas flow control valve to half open, three quarter open and fully open positions. The engine loading was done in a similar manner as for the single fuel mode. In addition to the data recorded for the operation under single fuel mode, the volume of biogas consumed during the time when 20 ml of diesel was consumed was also recorded. The mass of biogas consumed was evaluated from the volume of biogas consumed and its density, from which mass flow rate was then calculated.

At the end of test, the engine was stopped, the supply pump for dynamometer cooling water was also stopped and the moving parts of the brake checked for looseness. The

sluice gate and cooling water inlet valve were closed, the cooling water outlet valve was fully open and the drain valve also opened to keep the inside of the casing dry.

### 3.6.4 Brake Specific Fuel Consumption

Specific fuel consumption is the ratio of rate of fuel flow into the engine to the engine power as given by Eq. (3.14).

$$sfc = \frac{\dot{m}_f}{\dot{W}}, \quad (3.14)$$

where  $sfc$  = specific fuel consumption,  $\dot{m}_f$  = rate of fuel flow into engine and  $\dot{W}$  = engine power.

Brake power gives the brake specific fuel consumption (Eq. 3.15).

$$bsfc = \frac{\dot{m}_f}{\dot{W}_b}, \quad (3.15)$$

where  $bsfc$  = brake specific fuel consumption,  $\dot{m}_f$  = rate of fuel flow into the engine and  $\dot{W}_b$  = brake engine power.

The mass of gas consumed was determined by multiplication of the volumetric gas consumption by its density. In the set up, the volumetric gas consumption for biogas was measured by using a gas flow meter and then calculated for mass of gas consumption using density of biogas (1.22 kg/m<sup>3</sup>). The time taken by the engine to consume a fixed volume was measured using a stopwatch.



### 3.6.5 Brake Thermal Efficiency

Thermal efficiency is the ratio of engine output power to the power supplied by the fuel (Eq. (3.16)).

$$\eta_{th} = \frac{\dot{W}}{\dot{m}_f CV}, \quad (3.16)$$

where  $\eta_{th}$  = thermal efficiency,  $\dot{W}$  = engine power,  $\dot{m}_f$  = rate of fuel flow into engine and  $CV$  = calorific value of fuel.

Brake power gives the brake thermal efficiency (Eq. 3.17).

$$\eta_{bth} = \frac{\dot{W}_b}{\dot{m}_f CV}, \quad (3.17)$$

where  $\eta_{bth}$  = brake thermal efficiency,  $\dot{W}_b$  = brake power,  $\dot{m}_f$  = rate of fuel flow into engine and  $CV$  = calorific value of fuel.

#### Brake thermal efficiency of engine on dual fuel mode

The formula used for calculating the brake thermal efficiency of engine on dual fuel mode is given by Eq. (3.18) [38, 55]:

$$\eta_{bth} = \frac{\dot{W}_b}{\dot{m}_{fd} CV_d + \dot{m}_{fg} CV_g}, \quad (3.18)$$

where  $\eta_{bth}$  = brake thermal efficiency,  $\dot{W}_b$  = brake power,  $\dot{m}_{fd}$  = rate of flow of diesel fuel into engine,  $\dot{m}_{fg}$  = rate of flow of biogas fuel into engine,  $CV_d$  = calorific value of diesel fuel and  $CV_g$  = calorific value of biogas fuel,  $\dot{m}_{fd} CV_d$  = power input from diesel (pilot fuel) and  $\dot{m}_{fg} CV_g$  = power input from biogas.

### 3.6.6 Emission Measurement

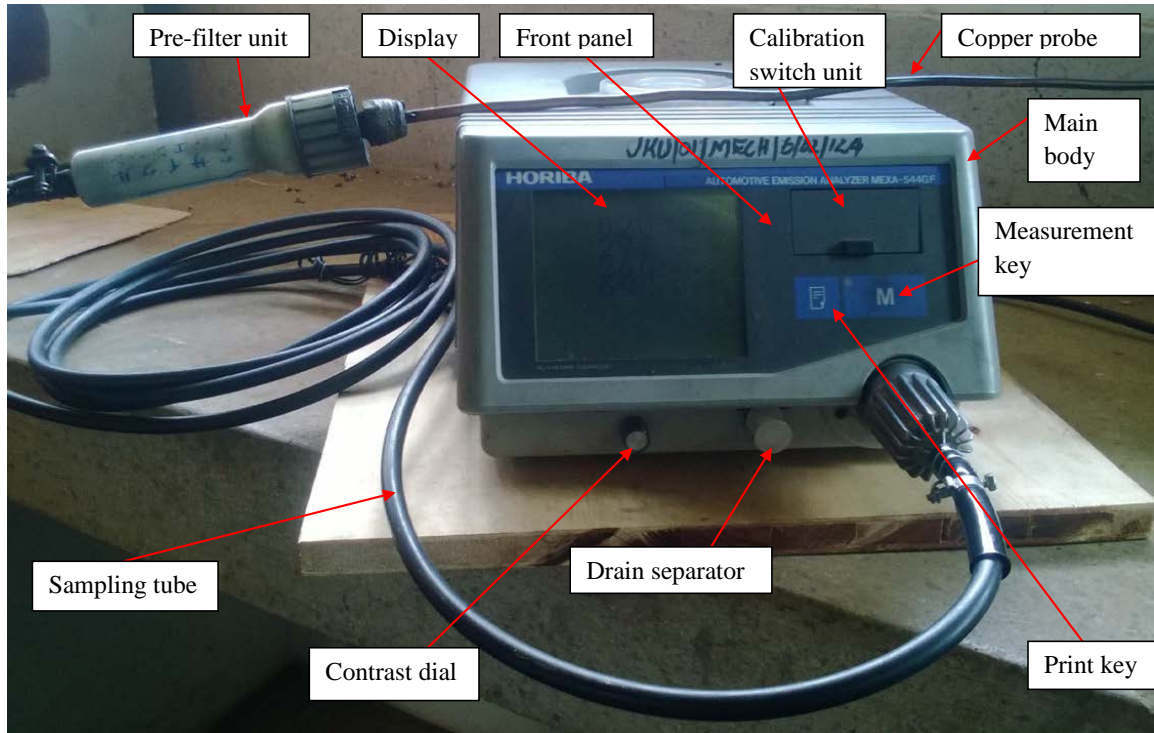


Figure 3.19: Emission analyzer

An automotive emission analyzer, Horiba: MEXA-544GF with an accuracy of 0.01 %vol CO, 01 ppm HC, 0.01 %vol CO<sub>2</sub> and a range of 0 to 10,000 ppm of HC, 0 to 100%volume CO and 0 to 100%volume CO<sub>2</sub>, shown in Fig. 3.19 was used for monitoring exhaust emissions of HC, CO and CO<sub>2</sub>. It consisted of the main body (having a front panel and display, calibration switch unit, standard gas inlet, power switch, dust filter, strainer, drain separator, contrast dial, carrying grip and sample gas inlet), a sampling tube, a pre-filter unit and a copper probe for sampling of gas.

#### Procedure for Emission Measurement

Before the start of the test, the drain separator, sampling tube and pre-filter unit were connected and fastened firmly using hose clips and one end of the drain separator

inserted into the slot of sample gas inlet. Clean filter elements were mounted in the pre-filter unit, dust filter and strainer and the device connected to power supply. The power switch was turned on to allow warming up. After warming up was completed (about 10 minutes), the analyzer was automatically transferred to stand-by mode, ready for measurement. At the start of the test, the measurement key was pressed and the zero calibration and optical sensitivity adjustment automatically done. Upon completion of operations, the analyzer went into measuring mode and the probe inserted into the exhaust port of the engine to start the measurement. Readings of HC, CO and CO<sub>2</sub> on the display were recorded for each operating condition of the engine. Upon completion of measurement, the analyzer was left in measuring mode for approximately 30 minutes to suck clean air to clean the sample gas path before the power was turned off. At the beginning of every test, the analyzer was allowed to suck clean air until the emission display read zero.

### **3.6.7 Temperature Measurement**

The temperature of the engine cooling water at entry and exit to the engine were measured using k-type thermocouple sensors with a measurement range of 0 to 1500<sup>o</sup>C. The exhaust gas temperature (EGT) was also measured using the k-type thermocouple sensor, for all test conditions. The thermocouple sensors were connected to a multi-channel digital data logger model TDS-530 shown in Fig. 3.20. The equipment had an accuracy of  $\pm 5\%$  and it converts the thermocouple signal into a temperature reading of degrees Celsius, which can be read on the display.



Figure 3.20: Multi-channel digital data logger

### 3.6.8 Engine Speed Measurement

The engine speed was measured at all operating conditions, using a portable digital tachometer-RS 445-9557 laser type with an accuracy of  $\pm 5\%$  and is shown in Fig. 3.21.



Figure 3.21: Digital tachometer

## 3.7 Uncertainty Analysis

Uncertainty is the magnitude of error that is estimated to have been made in determination of results [56]. In an experiment, direct measurement of quantities like speed, time, volume and mass are made. The instruments used to make these measurements vary in quality as does the expertise of the researchers using them. Furthermore, pa-

rameters that are out of the control of the researcher may cause undesired variations in the quantities that are being measured. These measured values are used in calculations to obtain experimental results that are usually compared with the predictions of theory or with the results of other experiments [56, 57].

In this research the performance of the modified engine was based on measured data that utilized a number of equipment and measuring devices such as dynamometer, fuel flow meter, tachometer and stop watch. The overall uncertainty was obtained from a repeated number of five measurements and a brief analysis is presented with the equations used in evaluating both the instrumental and experimental uncertainties.

### **3.7.1 Instrumental Uncertainty**

Different instruments were used for collection of data for the respective parameters determined. These devices had rated accuracies that independently contributed to the overall measurements. In this work it was possible to establish the uncertainty on dependent variables based on contributions from independent measurements. This was done through a technique proposed by Robinson and Bevington for estimation of such uncertainties [56].

The performance of the engine involved determination of time to consume a predetermined volume of diesel fuel, the engine speed at a given load and the volume of biogas consumed by the engine. The measured quantities were used to calculate the brake power, brake specific fuel consumption, brake thermal efficiency and percent diesel substitution. The brake thermal efficiency has a connection with brake power, fuel consumed, heating value of fuel and time taken as related by Eq. (3.17). The uncertainty was evaluated using Eq. 3.19.

$$\xi = \sqrt{\left(\frac{\partial BTE}{\partial t}\xi_t\right)^2 + \left(\frac{\partial BTE}{\partial f}\xi_f\right)^2 + \left(\frac{\partial BTE}{\partial s}\xi_s\right)^2 + \left(\frac{\partial BTE}{\partial v}\xi_v\right)^2}, \quad (3.19)$$

where  $\xi_t$ ,  $\xi_f$ ,  $\xi_s$  and  $\xi_v$  were the uncertainties from the respective measuring instruments (stop watch, dynamometer, tachometer and fuel burette, respectively). Eq. (3.19) was rewritten as a percentage to give Eq. (3.20).

$$\frac{\xi}{BTE} = 100 \times \sqrt{(\beta_t)^2 + (\beta_f)^2 + (\beta_s)^2 + (\beta_v)^2}, \quad (3.20)$$

where  $\beta_t = \frac{\xi_t}{t}$ ,  $\beta_f = \frac{\xi_f}{f}$ ,  $\beta_s = \frac{\xi_s}{s}$ , and  $\beta_v = \frac{\xi_v}{v}$  respectively.

From Eq. (3.20), the uncertainty for BTE was determined as 3.31%.

### 3.7.2 Experimental Uncertainty

The data collected repeatedly under a specified condition showed a spread about the mean. The deviations of these data from the mean were evaluated for a sample to determine the experimental uncertainty. The standard deviation is the most used technique as proposed by Robinson and Bevington [56], given by Eq. (3.21). The coefficient of variation (COV) can also be used to measure the variability of the obtained data relative to its mean as given by Eq. (3.23).

$$\sigma = \sqrt{\frac{1}{N-1} \sum_{i=1}^N (BSFC_i - \overline{BSFC})^2}, \quad (3.21)$$

where N was the number of repeated measurements, BSFC was the brake specific fuel consumption and  $\overline{BSFC}$  was the average brake specific fuel consumption given by Eq. (3.22).

$$\overline{BSFC} = \frac{1}{N} \sum_{i=1}^N BSFC_i. \quad (3.22)$$

$$COV = \frac{\sigma}{\bar{x}}, \quad (3.23)$$

where  $\sigma$  is the standard deviation and  $\bar{x}$  is the mean of the obtained data.

The standard deviation was expressed as a percentage to give Eq. (3.24).

$$\sigma = 100 \times \frac{\sqrt{\frac{1}{N-1} \sum_{i=1}^N (BSFC_i - \overline{BSFC})^2}}{\overline{BSFC}}. \quad (3.24)$$

The brake specific fuel consumption was used as one of the parameters to evaluate experimental uncertainties. The significance of the experimental uncertainties was to establish the ability of the modified engine to produce uniform results for any specific engine operating condition. Five readings were taken repeatedly as the engine operated from no load to full load and were used in evaluation of the experimental uncertainties. The results in Table 3.4 indicate the reproducibility of the data. The uncertainty was less than 4.0% and the deviation corresponds with the range of accuracy of instrumental uncertainties.

Table 3.4: Standard Deviation of Brake Specific Fuel Consumption

Engine Loading Condition	Average BSFC (g/kWh)	Standard deviation (%)
No load	267.6	2.5
Quarter load	267.2	2.7
Half load	266.8	3.0
Three quarter load	266.3	3.3
Full load	268.1	2.7

The instrumental and experimental uncertainties show that the data obtained over a repeated set of experiments depicted the performance of the engine under test.

The collected data for engine brake power, fuel consumption, emissions and exhaust gas temperature of the engine are presented and discussed in the chapter that follows.



## **CHAPTER FOUR**

### **4.0 RESULTS AND DISCUSSION**

#### **4.1 Introduction**

In this chapter, the test results on performance and emission characteristics of the dual fuel engine, modified from DICI engine are presented. The determined parameters are presented and discussed to compare variation of performance and emission characteristics of the dual fuel engine with a diesel engine. The effect of EGR on exhaust gas temperature (EGT) and engine performance is also presented.

#### **4.2 Base Line Data for Engine Performance on Single Fuel Mode with Diesel**

The engine was first run on single fuel mode with diesel to collect data for comparison with dual fuel operation and the data obtained was analyzed to show engine performance and emission characteristics on single fuel mode. This section presents the results on performance characteristics of brake power, brake specific fuel consumption and brake thermal efficiency as well as emissions of carbon monoxide, carbon dioxide and unburned hydrocarbons.

##### **4.2.1 Brake Power**

Figure 4.1 shows the variation in engine power output at different engine loads for single fuel operation of the engine. It indicates that with increase in engine load, the

brake power increases linearly from quarter load to full load with maximum power output recorded at full load being 59% more than at quarter load. The increase in brake power is attributed to the increase in fuel consumption rate of the engine with increase in load [58].

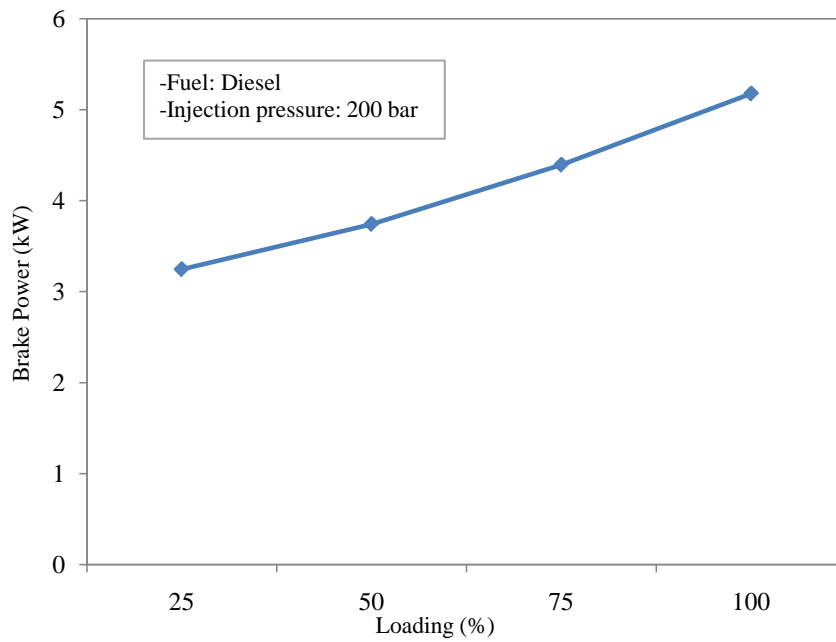


Figure 4.1: Variation of brake power with load for single fuel operation

### 4.2.2 Brake Specific Fuel Consumption

Specific fuel consumption is the fuel flow rate per unit power output. It shows how efficient the engine is in utilizing the fuel supplied to it. When calculated with reference to brake power it is referred to as brake specific fuel consumption. From Fig. 4.2, it was found that an increase in engine load by 75% causes a corresponding decrease of 29% in BSFC. This was attributed to the increase in rate of combustion of fuel in the combustion chamber with rise in thermal load on engine. Similar results were obtained by Pattanaik *et al.* [58]. High rate of combustion of fuel implies the engine uses less fuel

in delivering more brake power. This showed that it was more economical to operate the engine at high loads than at low loads.

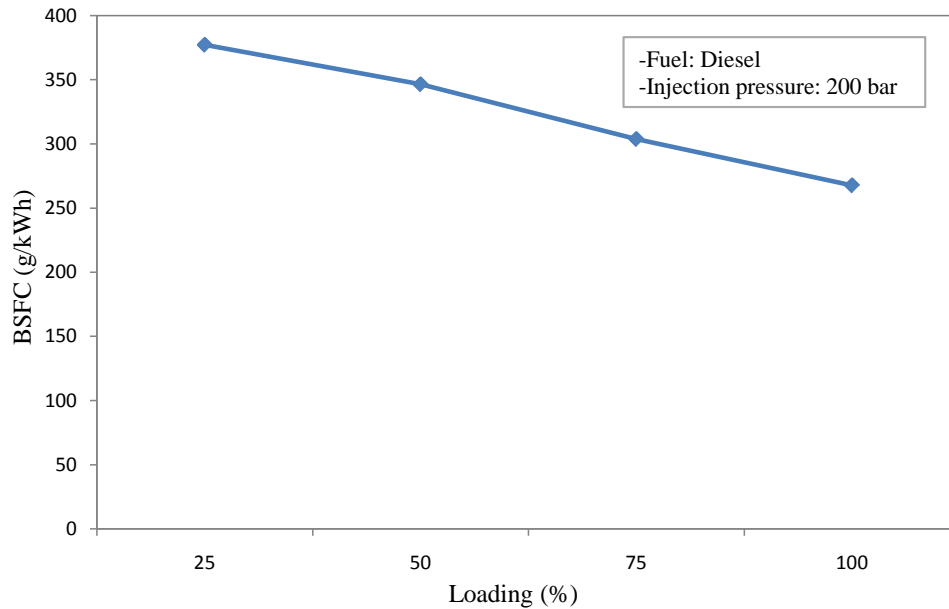


Figure 4.2: Variation of BSFC with load for single fuel operation

### 4.2.3 Brake Thermal Efficiency

Brake thermal efficiency is the ratio of engine output power (brake power) to power supplied by the fuel (fuel power). From Fig. 4.3, the brake thermal efficiency increased linearly with rise in engine load resulting in a 29% difference in BTE between quarter and full load. This is attributed to the fact that the rate of combustion of fuel increased with rise in combustion temperatures from no load to full load [58].

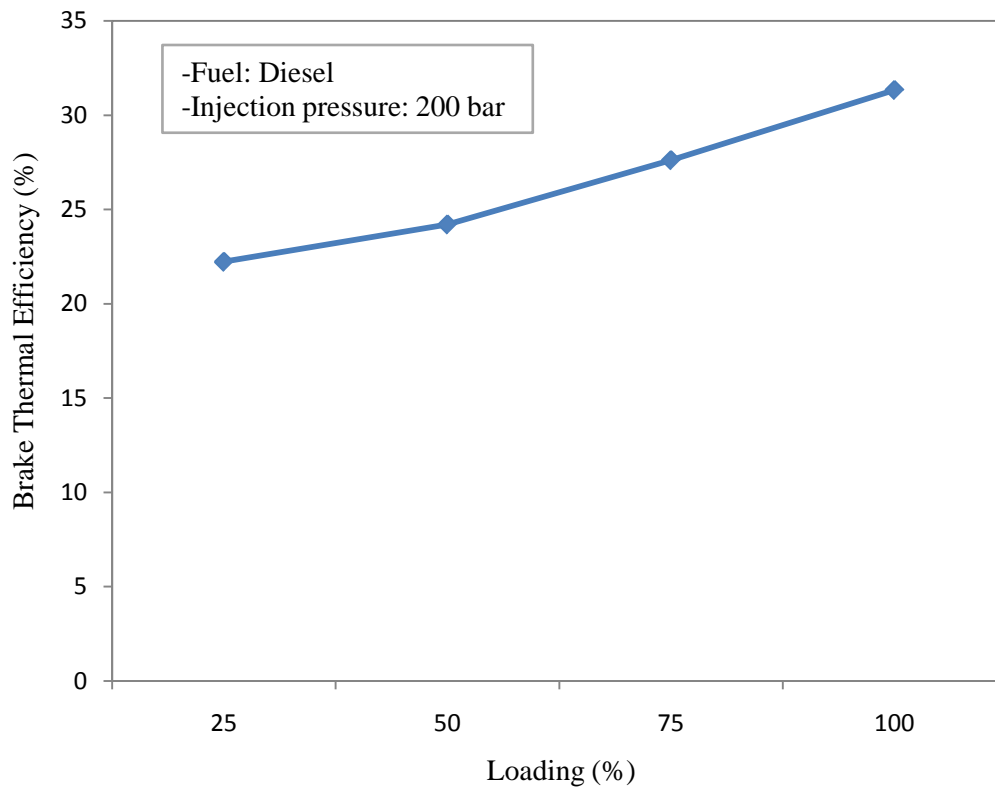


Figure 4.3: Variation of BTE with load for single fuel operation

#### 4.2.4 Emissions

##### (a) Variation of Carbon monoxide Emission with Load

Carbon monoxide, a colorless, odorless, poisonous gas is normally generated in an engine when it is operated with a fuel-rich equivalence ratio. When there is not enough oxygen to convert all carbon to  $\text{CO}_2$ , some fuel does not get burned and some carbon ends up as CO. As shown in Fig. 4.4, the maximum rise in emission of carbon monoxide due to increase in engine load was 11%. The increase in CO emission with load was attributed to the incomplete combustion caused by shorter combustion duration and less homogeneous mixture at high engine load. This increase was therefore more drastic at higher engine loads, beyond 50%.

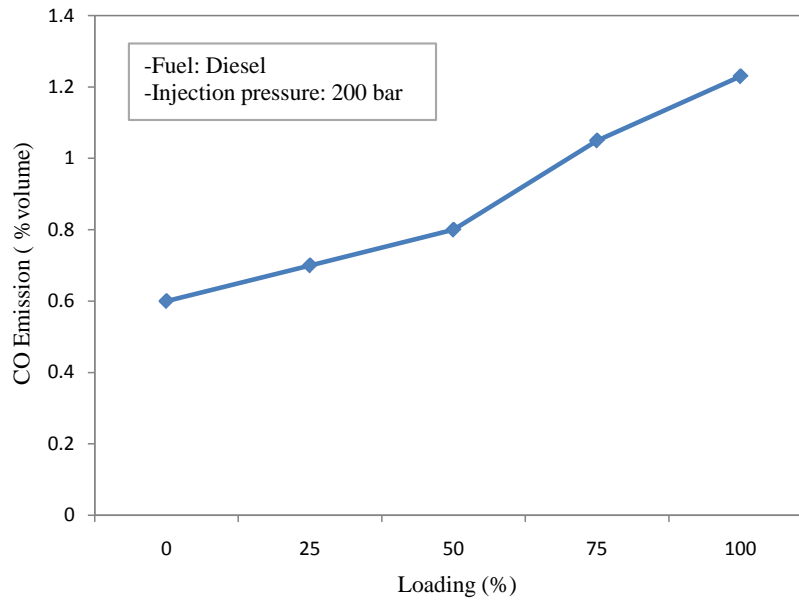


Figure 4.4: Variation of CO emission with load for single fuel operation

### (b) Variation of Unburned hydrocarbon Emission with Load

Unburned hydrocarbon (HC) is one of the regulated emissions, consisting of unburned fuel components and partially reacted components produced from the engine during operation. When hydrocarbon emissions get into the atmosphere, they act as irritants and odorants while some are carcinogenic. HC components also react with atmospheric gases to form photochemical smog. Emission of unburned hydrocarbon increased with engine load by up to 40%, as shown in Fig. 4.5. The increase in HC emission with load was attributed to incomplete combustion caused by shorter combustion duration and less homogeneous mixture at high engine load. This is due to the fact that during engine loading the engine speed was reduced when brake torque was increased. This low speed led to lower aerodynamic turbulence and the degree of homogeneity was reduced, so emissions of HC increased. The increase in HC emission was however gradual at high engine loads beyond 50% due to the effect of high thermal loading on the engine

which slightly improves combustion at high loads.

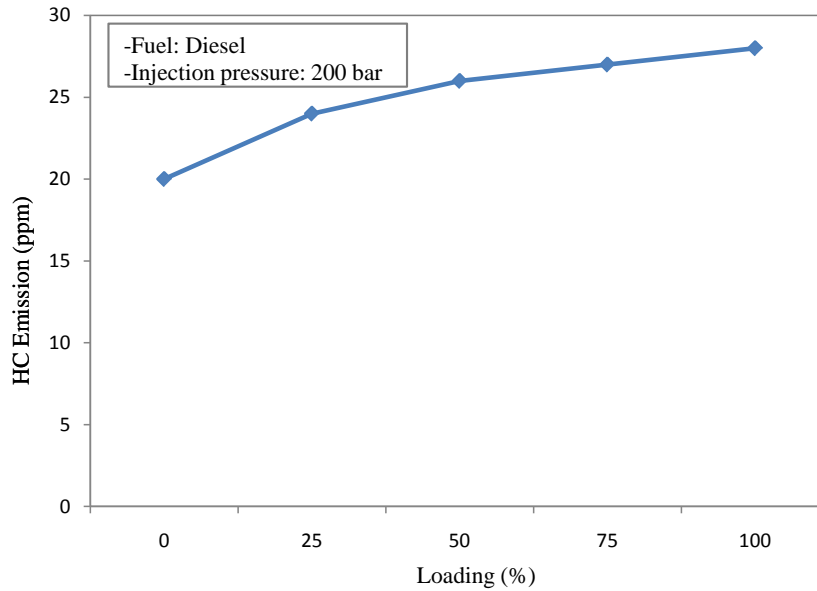


Figure 4.5: Variation of HC emission with load for single fuel operation

### (c) Variation of Carbon dioxide Emission with Load

Carbon dioxide is a product of fuel combustion during engine operation. Emission of carbon dioxide was found to increase linearly with load as shown in the Figure 4.6. A rise in CO<sub>2</sub> emission of more than 3 times was recorded, resulting from increase in load from no load to full load. When engine load was increased, the amount of fuel consumed by the engine went up so as to provide sufficient power to overcome the load. This resulted in increase in CO<sub>2</sub> emission since it is a product of fuel oxidation [58]. The drastic rise in CO<sub>2</sub> emission from 50% loading was attributed to oxidation of more HC at high loads as depicted by Fig. 4.5, resulting in more CO<sub>2</sub> in the exhaust.

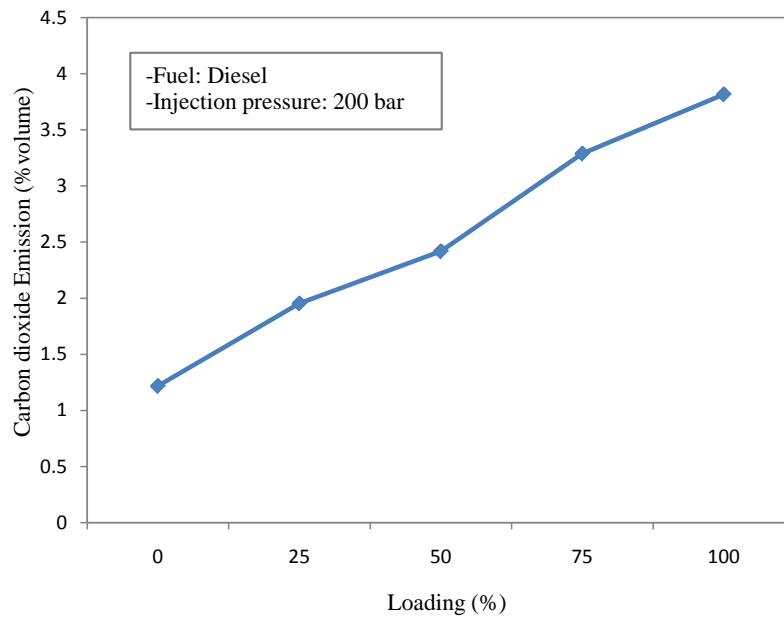


Figure 4.6: Variation of CO<sub>2</sub> emission with load for single fuel operation

### 4.3 Engine Performance on Dual Fuel Mode

Experiments were performed on the engine using biogas and diesel in dual fuel mode to measure four performance parameters namely brake power, brake specific fuel consumption, brake thermal efficiency and exhaust gas temperature, and emission parameters such as carbon monoxide, carbon dioxide and unburned hydrocarbon at different load conditions. The results of engine performance and emission characteristics in dual fuel operation are presented here below.

#### 4.3.1 Brake Power

Figure 4.7 shows the variation in engine power output at different engine loads for single and dual fuel modes of the engine. The power output of the engine was higher during single fuel operation for all test conditions. This was attributed to the fact that the lower heating value of diesel is higher than that of biogas by at least 50%.

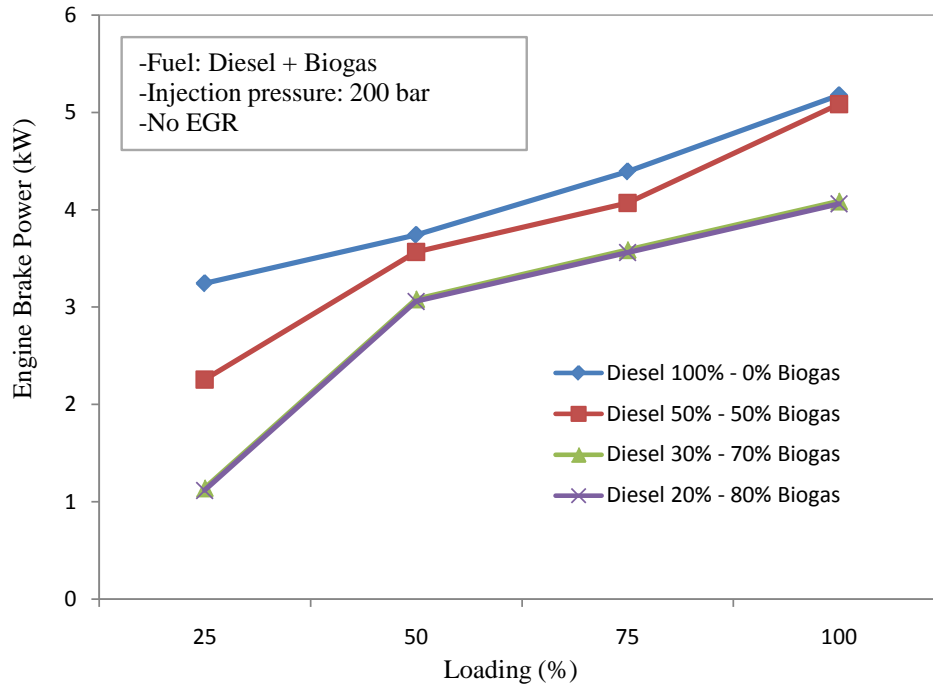


Figure 4.7: Variation of brake power with load for dual fuel mode

The maximum drop in brake power was 65% and was recorded at quarter load, for maximum diesel substitution with biogas. The drop in brake power at full load was upto 21%, implying that dual fuel engines have poorer performance at low loads as revealed by Hosseinzadeh *et al.* [44]. It was concluded that dual fuel engines have lower performance than diesel engines but the output improves at higher loads due to increase in combustion rate resulting from high thermal load [58]. The figure indicates that with engine loading, the brake power increased linearly for single fuel mode and more steeply from quarter to half load for dual fuel operation. This further confirms that the performance of the dual fuel engine increased remarkably at high loads. The rise in brake power with loading was attributed to the higher fuel consumption rate of the engine to overcome the load.



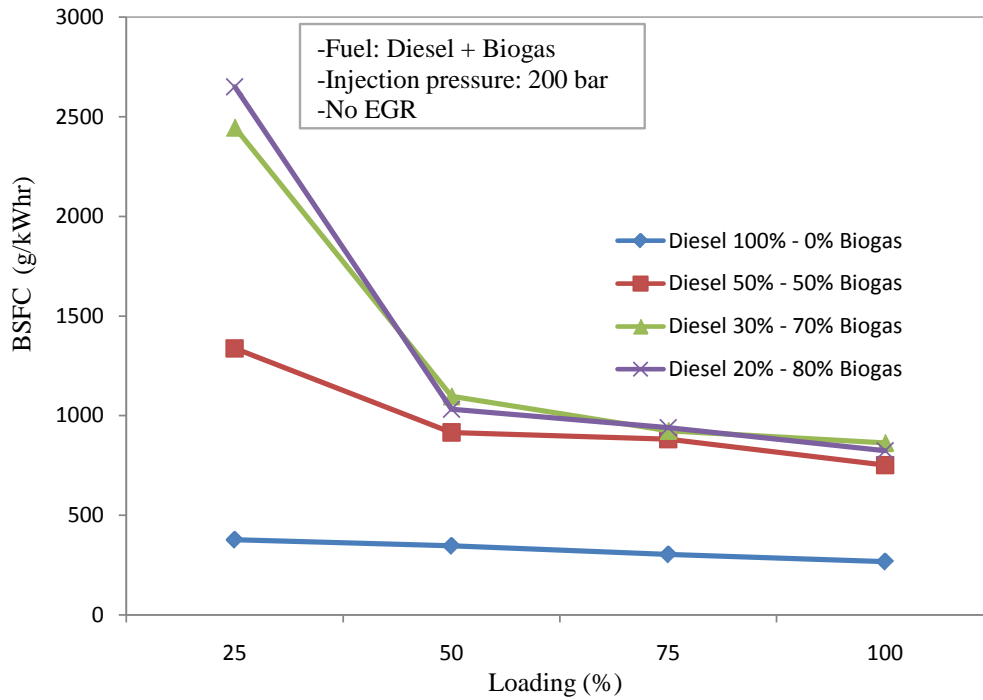


Figure 4.8: Variation of BSFC with load for dual fuel mode

### 4.3.2 Brake Specific Fuel Consumption (BSFC)

Figure 4.8 shows variation of BSFC with engine load. The BSFC for dual fuel operation is computed from the sum of biogas and diesel fuel consumed. The figure shows that BSFC decreased with increase in load for all values of biogas flow rate. In addition, the BSFC was higher during dual fuel operation, for all test conditions. This is attributed to the low calorific value of biogas which requires that a greater amount of biogas be consumed in order to deliver equivalent power as diesel. Similar results were obtained by N.S. Ray *et al.* in an experimental investigation on performance characteristics of a CI engine using biogas and diesel in dual fuel mode [32]. At low engine load condition of 25%, the BSFC for dual fuel combustion was much higher than for single-fuel combustion while it improved significantly as from 50% loading. The best performance of the dual fuel engine was recorded at full load, where the

BSFC was upto 208% as compared to 227% at quarter load. This was attributed to the higher rate of combustion of gaseous fuel at high load due to higher combustion temperatures. In related research work, N.S. Ray *et al.* [32] and Pattanaik *et al.* [58] obtained similar results. It was concluded that at higher loads above 50%, the brake specific fuel consumption is low mainly due to the higher temperatures reached in the combustion chamber. However, brake specific fuel consumption is higher at low loads due to low combustion temperatures. It was therefore concluded that thermal loading has considerable influence at higher loads and tends to a higher reduction in BSFC.

### 4.3.3 Brake Thermal Efficiency

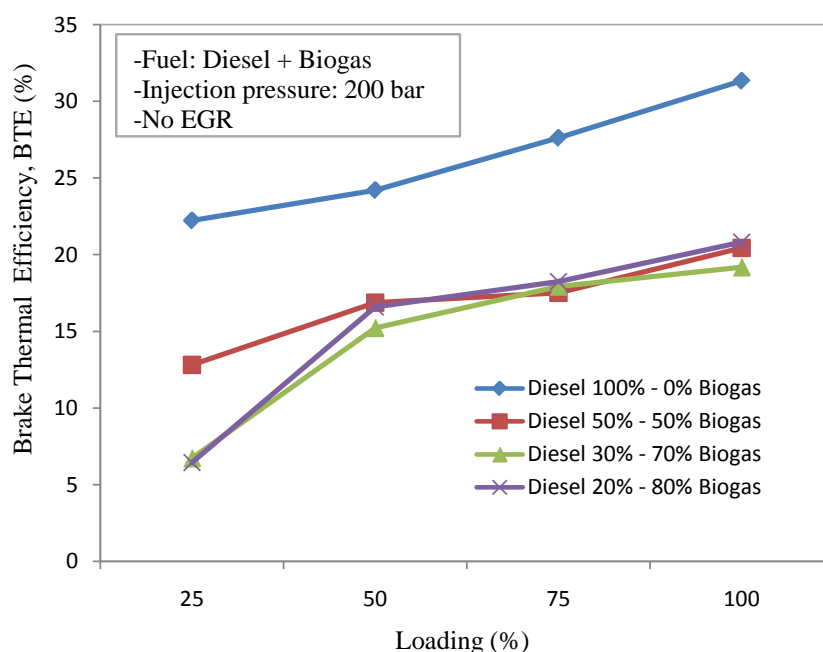


Figure 4.9: Variation of BTE with load for dual fuel mode

The comparison of BTE for diesel and dual fuel operation is shown in Fig. 4.9. It was found that diesel gave better BTE at all loads as compared to biogas-diesel dual fuel. The maximum difference in BTE obtained was 69% and it has been reported

that the lower thermal efficiency of the dual-fuel combustion is because of the effect of biogas residuals and low combustion temperatures during the combustion process [58]. The brake thermal efficiency reduced with increase in proportion of biogas and the reduction was more at loads below 50% where the fuel blend of biogas:diesel being 80:20 recorded an average drop of 55%. The same trend was observed for the other fuel ratios. The highest reduction in BTE was recorded at low loads, showing poor performance of the engine in partial loading due to the lower combustion rate of biogas at low load [32, 58].

#### 4.3.4 Exhaust Gas Temperature (EGT)

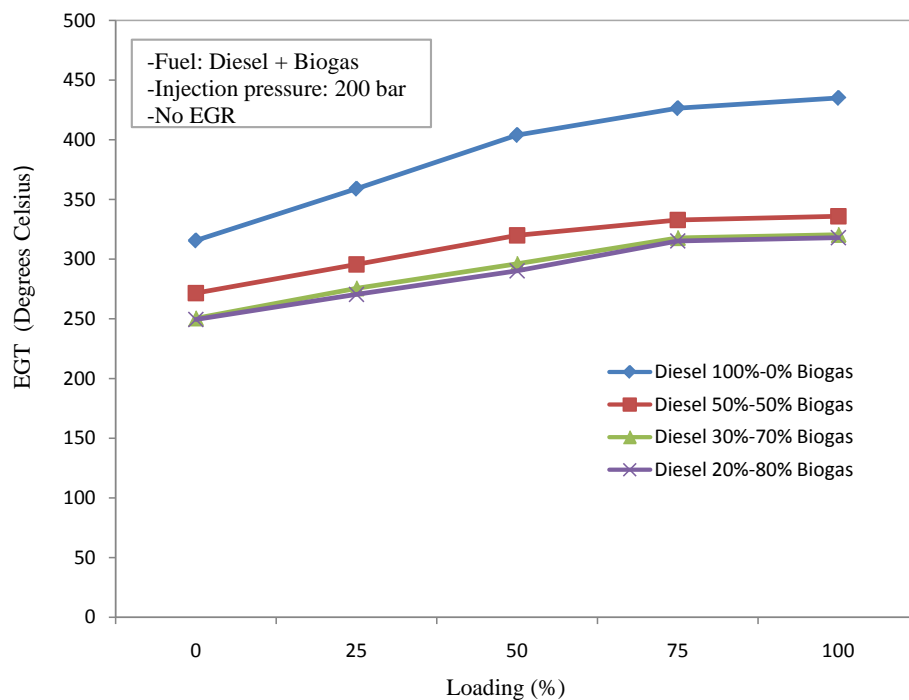


Figure 4.10: Variation of EGT with load for dual fuel mode

Research has shown that  $\text{NO}_x$  formation in diesel engines is a highly temperature-dependent phenomenon and takes place when the temperature in the combustion chamber exceeds 2000 K [6]. Therefore, in order to reduce  $\text{NO}_x$  emissions in the exhaust,

it is necessary to keep peak combustion temperatures under control. An easier way to predict the trend in variation of peak combustion temperatures and therefore the variation in  $\text{NO}_x$  emission is through measuring the exhaust gas temperature [58]. The exhaust gas temperature was therefore measured in this research to help investigate what could be the effect of dual fuel operation on emission of  $\text{NO}_x$ , since there was no emission analyzer for measuring this emission.

Figure 4.10 shows the variation of the exhaust gas temperature with engine load for all the fuel modes. The exhaust temperature measurements were conducted using a thermocouple mounted at a connection on the exhaust manifold. The exhaust gas temperature increased linearly with engine load and this was attributed to the rise in total energy input and higher fuel consumption rate. However, the exhaust gas temperatures were found to be slightly lower for dual-fuel combustion compared to single-fuel modes and these differences increased at higher engine loads. Exhaust gas temperature decreased by up to 21% at quarter load and by up to 27% at full load. The low exhaust gas temperature can be explained by the decreased charge temperature with induction of biogas in the engine which acts as a heat sink due to the carbon dioxide component. It could also be due to the fact that the flame propagation speed of the pilot fuel in intake charge is reduced and then the fuel in the combustion chamber was not burnt completely and therefore the combustion pressure and temperature are reduced [58].

### **4.3.5 Emissions**

#### **(a) Variation of Carbon monoxide Emission with Load**

Figure 4.11 shows the CO emissions at various engine loads. From the figure, the concentration of CO emissions for dual fuel operation were lower than those of diesel

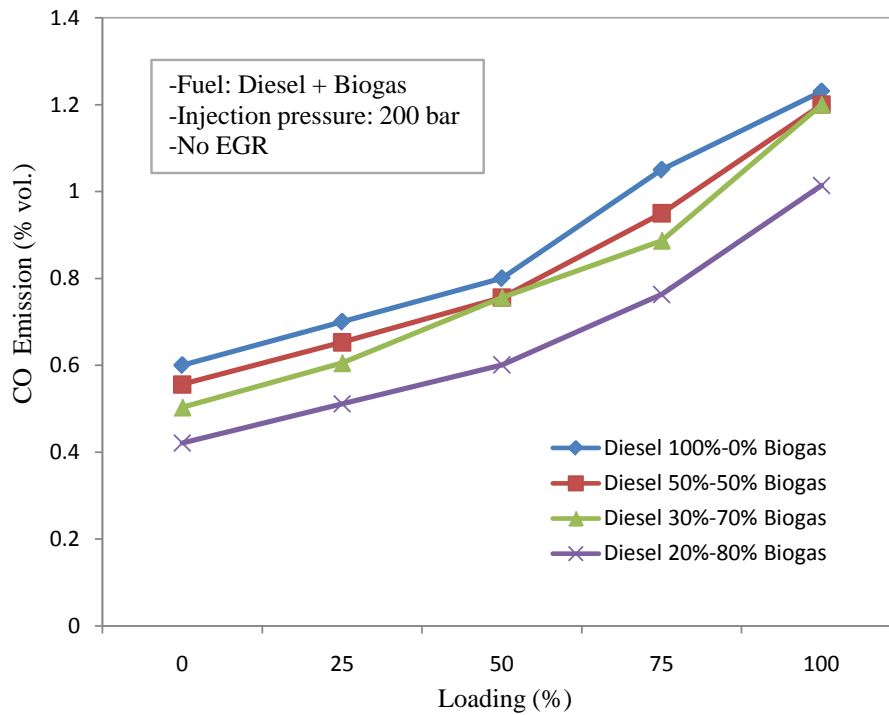


Figure 4.11: Variation of CO emission with load for dual fuel mode

fuel operation for all test conditions. In addition, CO concentration decreased with increase in biogas supply. Reduction in emission of CO by more than 24% was recorded at part loads below 50% while reduction in CO levels at loads above 50% was by more than 26%, for various diesel substitution levels. The greater reduction at high loads was attributed to better combustion rate at high loads due to the high thermal load on the engine. Research findings by N.S. Ray *et al.* on performance characteristics of CI engine using biogas and diesel in dual fuel mode also revealed a decrease in CO emission with increase in percentage of biogas in the fuel. It was concluded that diesel has higher carbon in composition as compared to biogas leading to formation of more CO emission in diesel operation [32].

(b) Variation of Unburned hydrocarbon Emission with Load

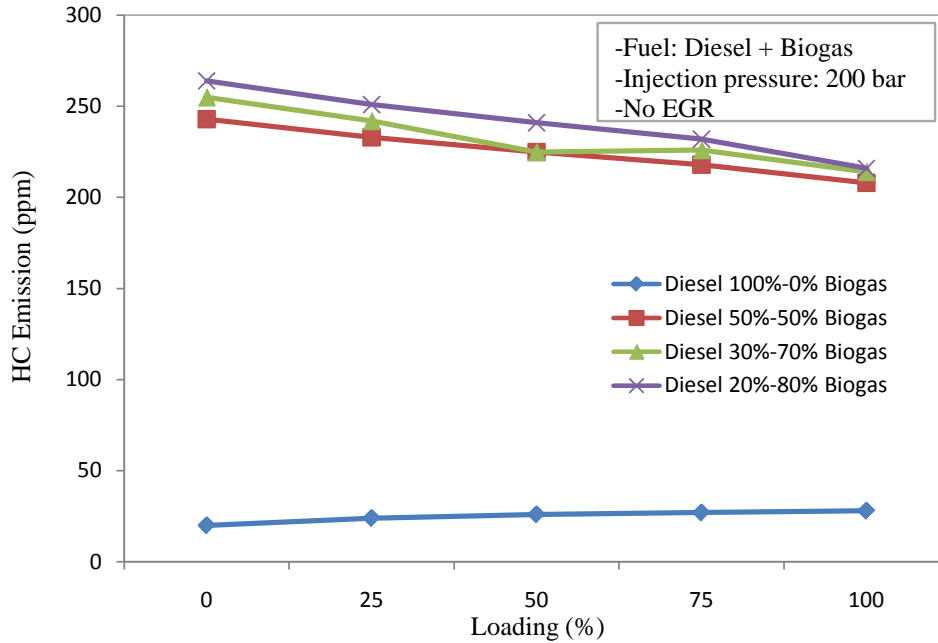


Figure 4.12: Variation of HC emission with load for dual fuel mode

Figure 4.12 shows the HC emissions at different engine loads under different combustion modes. The HC emissions for diesel in single fuel combustion were much lower than those of dual fuel combustion using biogas and diesel for all test conditions. The highest emission of hydrocarbon for dual fuel operation was at no load where emissions recorded were up to 12 times above that of diesel mode. At full load the emissions were relatively low compared to no load condition, though the rise was still as high as 6 times above diesel emission. HC emission was significantly high in dual fuel mode as compared to diesel mode due to the displacement of combustion air by biogas during dual fuel operation. With the induction of biogas into the engine, the  $\text{CO}_2$  content in the mixture increases at the expense of fresh air which in turn reduces the air-fuel ratio and combustion temperature. This leads to incomplete combustion of the fuel hence increase in emission of unburnt hydrocarbons. The HC emissions were found to decrease with load in dual fuel mode, while the converse was found to be the case

for single fuel mode. This was attributed to the fact that at part loads the dual fueled operation suffers from higher unburnt hydrocarbon emissions due to overall lean mixture and incomplete combustion because of small quantity of pilot fuel. There is also low thermal load on the engine at low load, hence low combustion rate of the gaseous fuel. With increase in engine load, the thermal load on the engine increases leading to improved combustion rate of the gaseous fuel [58, 59].

**(c) Variation of Carbon dioxide Emission with Load**

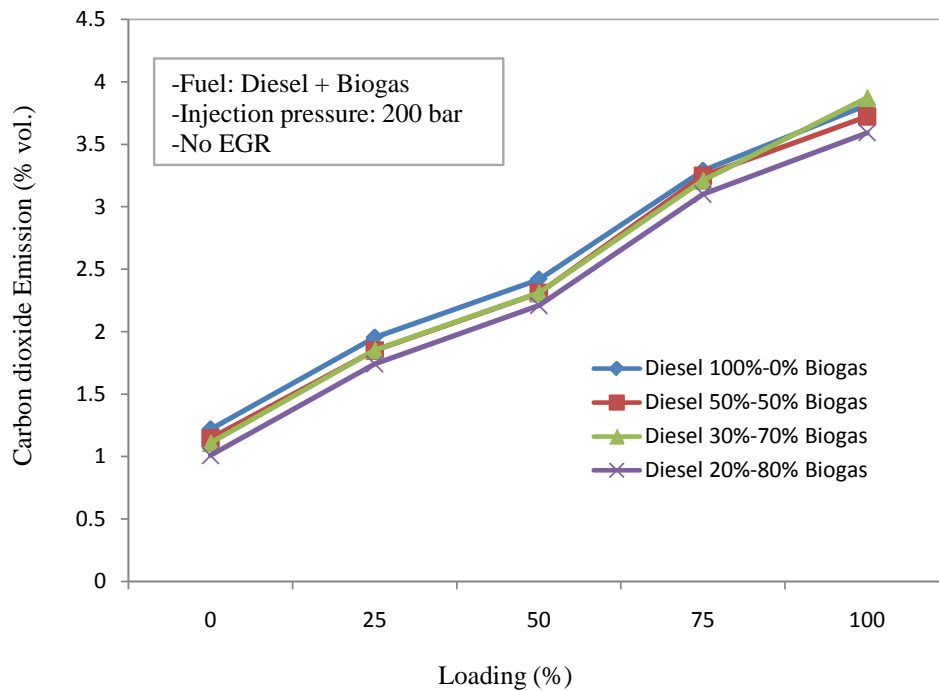


Figure 4.13: Variation of CO<sub>2</sub> emission with load for dual fuel mode

Figure 4.13 shows the concentrations of CO<sub>2</sub> emissions at different engine loads for single and dual-fuel combustion modes. In this figure, the highest CO<sub>2</sub> emissions were produced by single-fuel combustion, where as biogas-diesel dual fuel combustion produced lower CO<sub>2</sub> emissions. Emission of carbon dioxide decreased with increase in biogas supply to the engine due to substitution of some of the air with biogas. This

led to incomplete oxidation of fuel and therefore decrease in  $\text{CO}_2$  which is a product of complete fuel combustion. Carbon dioxide emission decreased by an average of 8% following operation of the engine in dual fuel mode.

#### **4.4 Engine Performance with Exhaust Gas Recirculation on Single Fuel Mode**

The effect of exhaust gas recirculation (EGR) is to reduce oxides of Nitrogen ( $\text{NO}_X$ ) emissions by reducing the combustion temperatures, since  $\text{NO}_X$  formation is a temperature dependent phenomenon in diesel engines [54]. When EGR is applied, it is also important that its effect on the overall performance of the engine be investigated. In this work therefore, experimental investigations were carried out on the single cylinder four stroke naturally aspirated direct injection water cooled diesel engine with exhaust gas recirculation. The effect of EGR on brake power, brake thermal efficiency (BTE), brake specific fuel consumption (BSFC), exhaust gas temperature (EGT) and exhaust emissions was studied. The results are as shown in Figs. 4.14 - 4.19.

##### **4.4.1 Brake Power**

Figure 4.14 shows a linear increase in power output of the engine with increase in load, from no load to full load for all conditions of EGR. The trend also reveals that EGR has virtually no effect on brake power on single fuel mode.

##### **4.4.2 Brake Specific Fuel Consumption (BSFC)**

Figure 4.15 shows variation of BSFC with load under EGR. BSFC decreased with both load and EGR rate for all operating modes. The reduction in BSFC was by an average



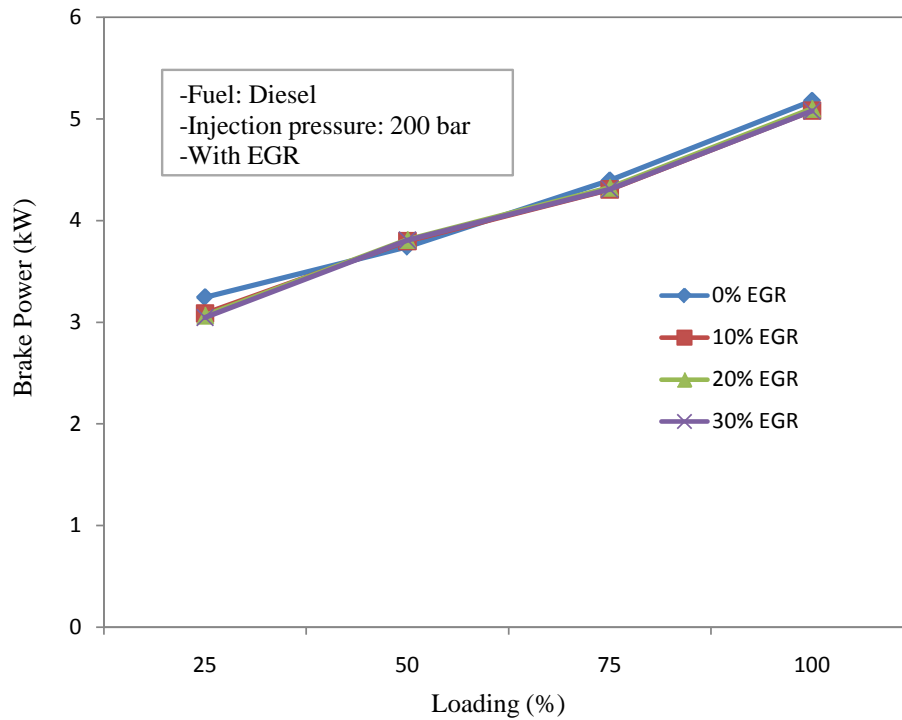


Figure 4.14: Variation of brake power with load for single fuel operation with EGR

of 16% for all loading conditions, with the highest reduction of 25% being recorded at 50% loading. The decrease in BSFC with EGR was attributed to increase in intake charge temperature which enhanced the rate of combustion of the fuel, hence improving BSFC. The decrease in BSFC with engine load may also be attributed to improvement in combustion rate of the fuel, following increase in thermal load on the engine.

#### 4.4.3 Brake Thermal Efficiency

From Fig. 4.16, the brake thermal efficiency increased with engine load for all operating modes. The BTE increased also with the amount of exhaust gas recirculated. The BTE increased at low loads below 50% due to EGR, by an average of 24% while at high loads an average of 15% rise was recorded. This increase in BTE with EGR was attributed to re-burning of HC that enters the combustion chamber with the recirculation of

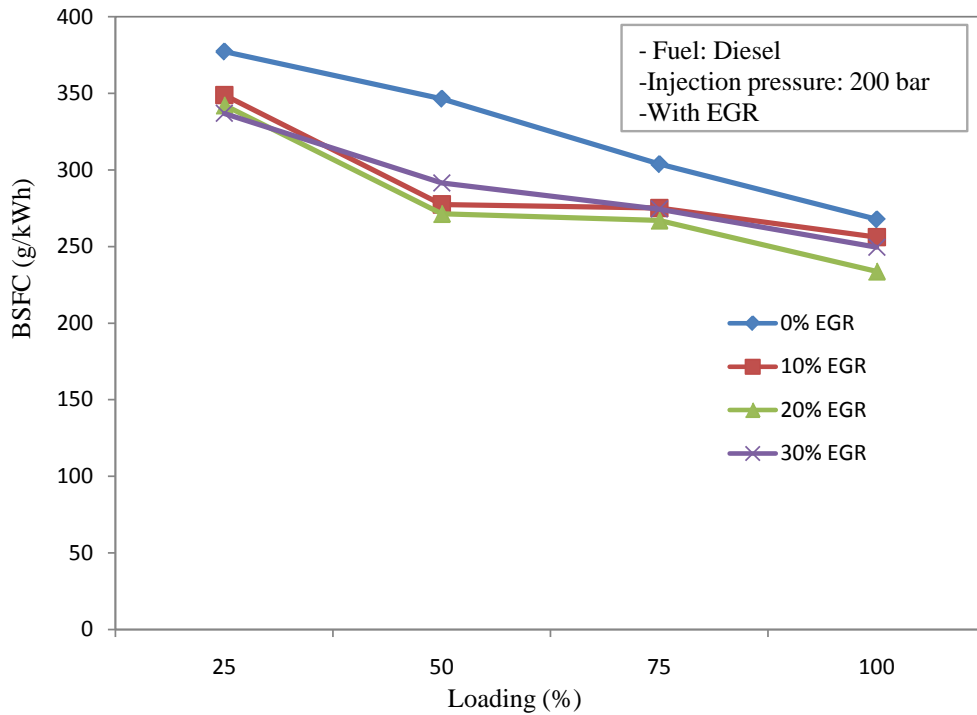


Figure 4.15: Variation of BSFC with load for single fuel operation with EGR

exhaust gases and the increase in intake charge temperature which enhances the rate of combustion of the fuel [44, 54]. Recirculation of too much exhaust gases, beyond 30% however, displaced much of the necessary air for combustion, causing significant decrease in brake thermal efficiency.

#### 4.4.4 Emissions

This section presents results on emission of CO, HC and CO<sub>2</sub> for diesel operation with exhaust gas recirculation.

##### (a) Variation of CO emission with Load

When a hydrocarbon burns in oxygen, it yields carbon dioxide and water vapor, as well as a limited number of products. Regardless of the substance being burned, the state of complete combustion is almost impossible to achieve due to two major reasons; (1)

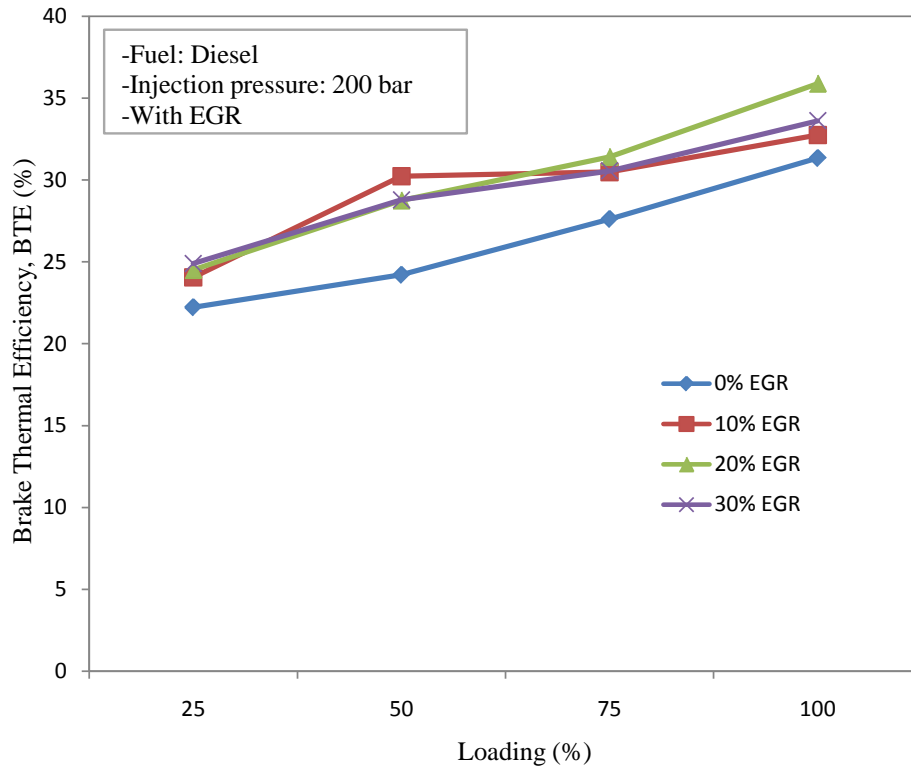


Figure 4.16: Variation of BTE with load for single fuel operation with EGR

it is quite difficult to create enough turbulence to facilitate sufficient fuel and oxidizer mixing and (2) the mixing time is usually very short which may not warrant complete and sufficient mixing of fuel and oxidizer. This is the reason CO is normally emitted in the engine exhaust instead of CO<sub>2</sub>.

Figure 4.17 shows the variation of CO emissions with EGR at various engine loads. CO emission increased with increasing load and percent EGR for all loading conditions. Maximum percent difference in CO emission was at 30% EGR and it varied from 33 to 40% with change in load. This was attributed to deficiency of oxygen with increase in percent EGR. CO is the intermediate species formed before CO<sub>2</sub> in a hydrocarbon combustion and the complete conversion of CO to CO<sub>2</sub> depends on oxygen availability. In exhaust gas recirculation, a considerable amount of CO remains unconverted due to low temperatures and inadequate O<sub>2</sub> resulting from displacement of air by recirculated

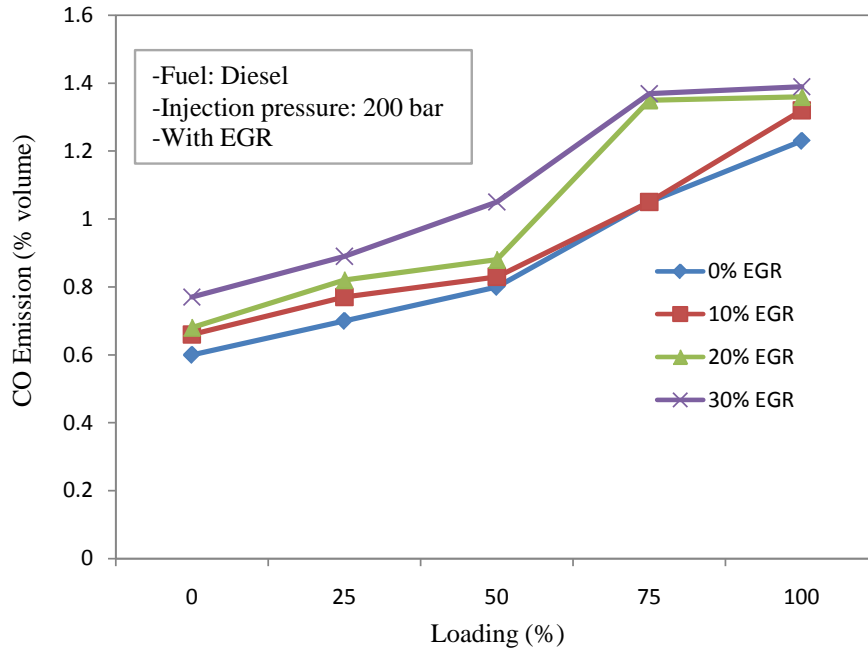


Figure 4.17: Variation of CO emission with load for single fuel operation with EGR

gases and this leads to increase in CO emission.

### (b) Variation of Unburned hydrocarbon Emission with Load

Figure 4.18 shows the effect of EGR on HC emission at various engine loads. HC emission increased with engine load and percent EGR for all loading conditions. Maximum EGR rate of 30% resulted in the highest difference in HC emission of average 24%. The increase in HC emission with EGR was attributed to the  $\text{CO}_2$  content of the induced mixture instead of fresh-air, which led to incomplete oxidation of the fuel in the combustion chamber. Incomplete combustion occurs when there is insufficient oxygen to allow a hydrocarbon fuel to react completely with oxygen to produce carbon dioxide and water. It also happens when the combustion is quenched by a heat sink or due to insufficient time to burn. Recirculated exhaust gas acts as a heat sink due to the  $\text{CO}_2$  content which absorbs heat generated during fuel combustion. It was concluded that EGR leads to increase in HC emission like it does to CO emission, implying that

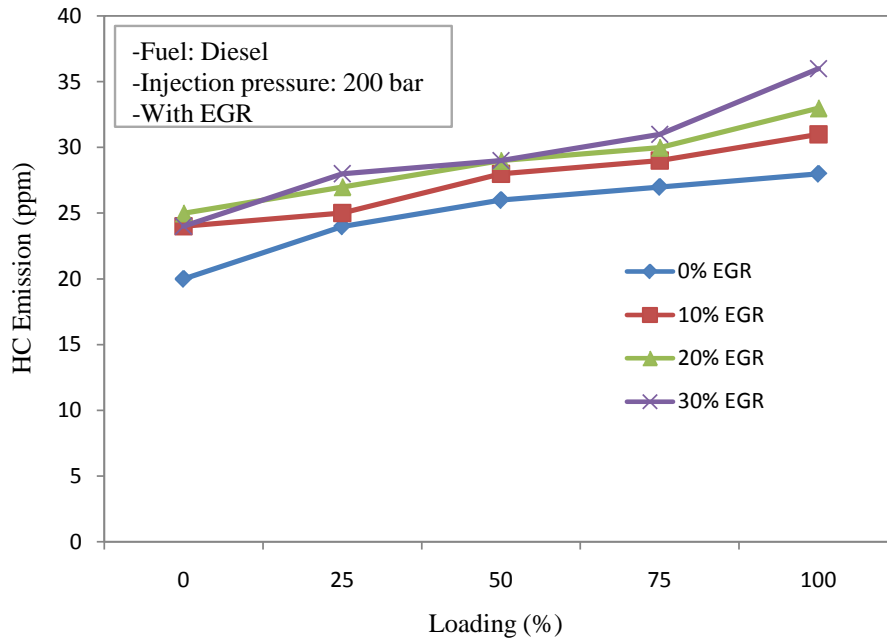


Figure 4.18: Variation of HC emission with load for single fuel operation with EGR

if EGR is applied as a means of reducing  $\text{NO}_x$  emission, the effect on other emissions must be considered and a tradeoff reached.

### (c) Variation of Carbon dioxide Emission with Load

Carbon dioxide is one of the by-products of a combustion process along side water vapour. All other factors constant, the higher the volume of  $\text{CO}_2$  generated, the higher the efficiency of a combustion process. It is therefore an indicator of how complete a combustion process can be achieved. From Fig. 4.19, emission of carbon dioxide increased with engine load for all rates of EGR while the same decreased slightly with EGR. The difference in  $\text{CO}_2$  emission at no load was up to 19% while that at full load was up to 18%. This decrease was attributed to substitution of some of the fresh air with exhaust gas leading to incomplete fuel oxidation and reduction in  $\text{CO}_2$  which is a product of complete fuel combustion. This further showed that EGR has a limitation in relation to combustion of the fuel.

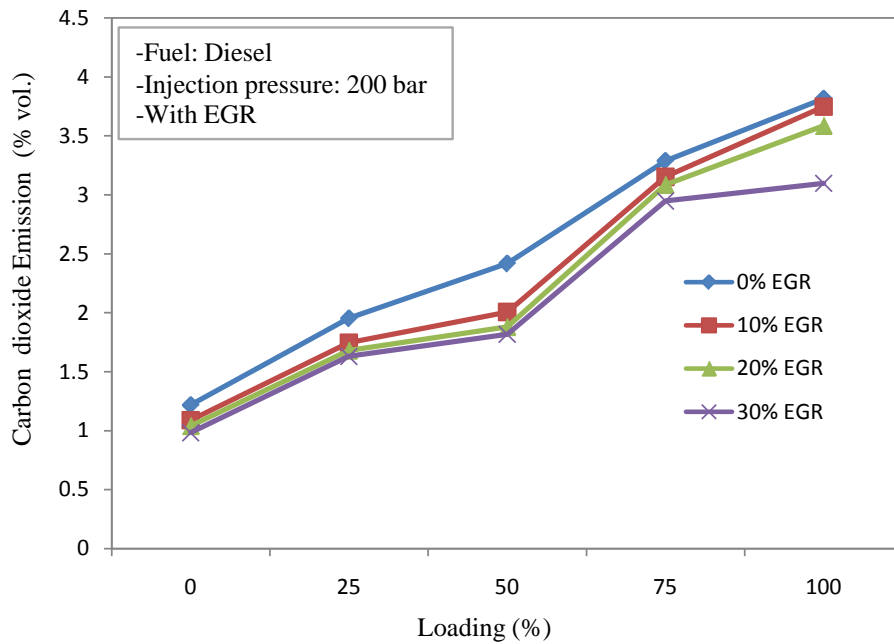


Figure 4.19: Variation of CO<sub>2</sub> emission with load for single fuel operation with EGR

## 4.5 Engine Performance on Dual Fuel Mode (Biogas 80%-20% Diesel) with Exhaust Gas Recirculation

### 4.5.1 Brake Power

The effect of load on brake power of the dual fuel engine at different EGR ratios is shown in Fig. 4.20. The trend revealed that EGR had no significant effect on the power output of the engine and the maximum drop in brake power recorded for all the loading conditions was only 0.33%. This was attributed to the fact that the recirculated gases heated the combustion mixture and improved the combustion rate of the fuel. This countered the power loss due to displacement of some of the air by recirculated gases, leading to marginal difference in power output for various EGR rates. The trend also revealed very low brake power at quarter load but the same increased remarkably with load up to 50% loading. The rapid increase in brake power was attributed to the steeper

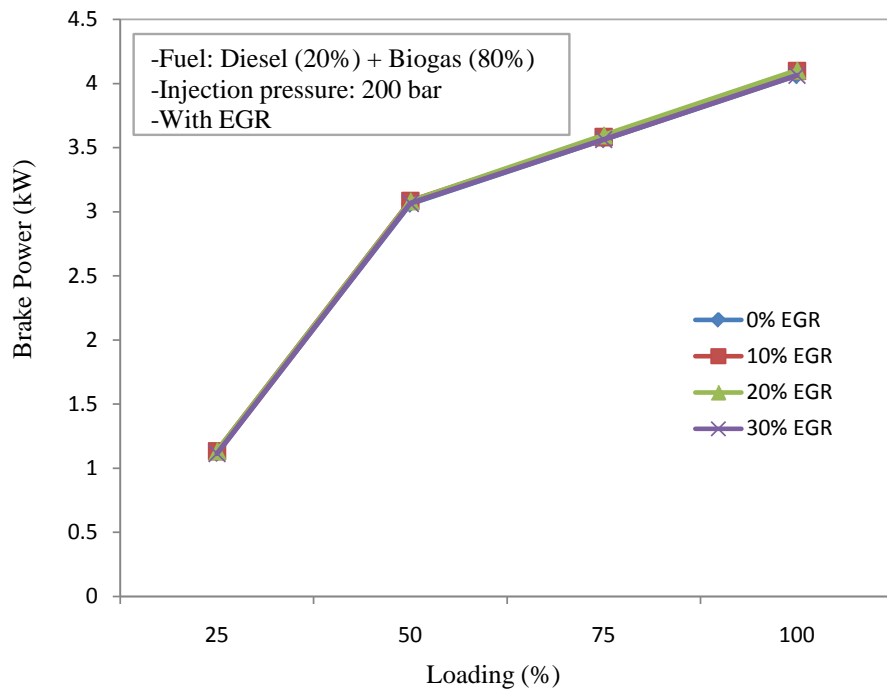


Figure 4.20: Variation of brake power with load for dual fuel operation with EGR

rise in combustion temperatures from quarter to half load as the engine approached steady state operation, as presented in Section 4.5.4. This rise in temperature results in a corresponding increase in combustion rate of the gaseous fuel [58]. This justifies the behaviour of the graph, since research has shown that dual fuel engines exhibit poor performance at low loads due to overall lean mixture and incomplete combustion because of small quantity of pilot fuel. The performance however improves rapidly towards high loads [58, 59].

#### 4.5.2 Brake Specific Fuel Consumption (BSFC)

Brake specific fuel consumption of the dual fuel mode was recorded for various EGR ratios. A comparison of BSFC at different loads and EGR ratios is presented in Fig. 4.21. It was observed that by increasing the load, the BSFC decreases. With loading,

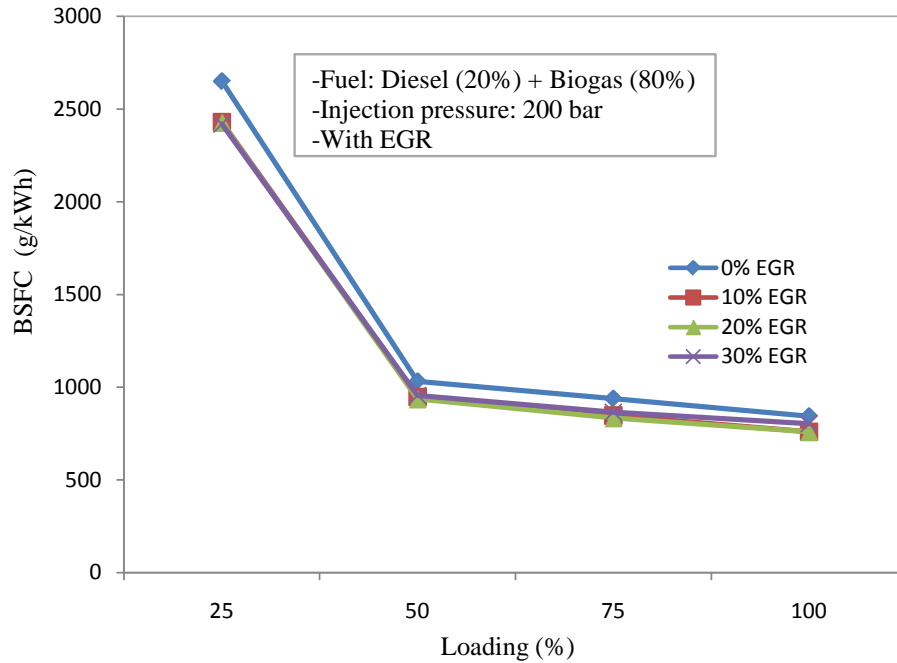


Figure 4.21: Variation of BSFC with load for dual fuel operation with EGR

the cylinder pressure and temperature rises due to increase in the amount of fuel consumed by the engine to overcome the load. The increase in temperature improves the combustion process resulting in a reduction in BSFC. The BSFC decreased with increasing percent EGR, with the maximum reduction being 9% at quarter load and the minimum percentage reduction being 6% at full load. It was noted that at part loads for load values below 50%, BSFC decreased drastically while on the other hand BSFC gradually reduced with the increase in load above 50%. This may be attributed to the rapid rise in combustion temperatures as presented in Section 4.5.4, which improves the combustion process proportionately. Similar results have been obtained from related work by other researchers, through experimental work [58] as well as through modeling [44].



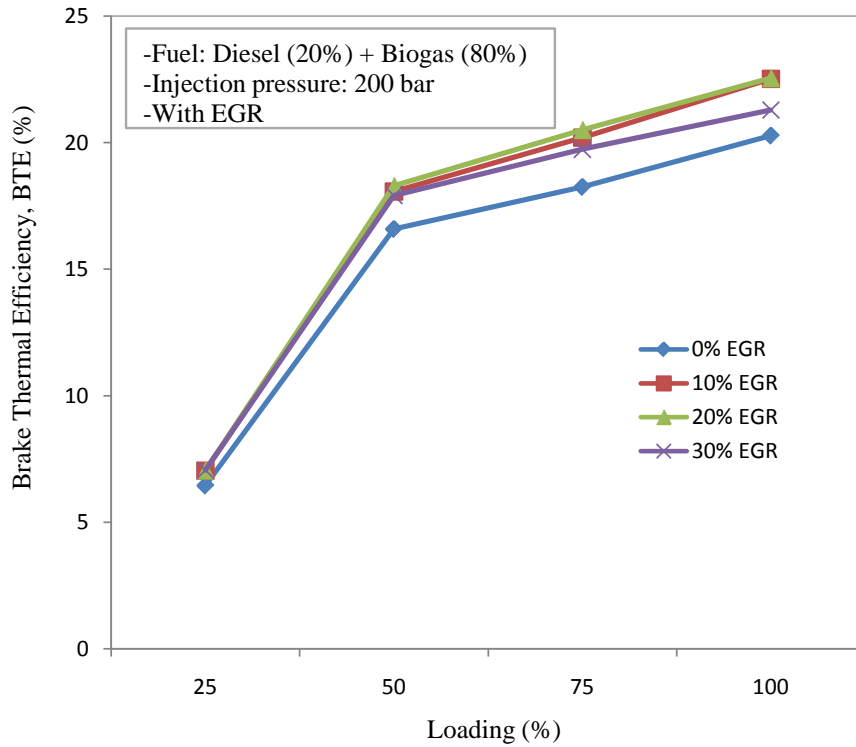


Figure 4.22: Variation of BTE with engine load for dual fuel operation with EGR

### 4.5.3 Brake Thermal Efficiency

From Fig. 4.22, showing variation of BTE with engine load, the brake thermal efficiency increased with engine load for all operating modes. As the EGR amount was increased from 0% to 30%, there was some increase in thermal efficiency at almost all loads. EGR ratio of 20% gave the best BTE at all loads, with the maximum percent difference being 9% at full load. The rise in BTE with EGR was attributed to re-burning of HC that enters the combustion chamber with the recirculation of exhaust gases [54]. It may also be attributed to the improved combustion of biogas as the inlet temperature increased when EGR was introduced, which enhanced the rate of combustion. It has been shown [60] that the effect of using EGR in a dual fuel engine has three effects: dilution effect, chemical effect and thermal effect. The chemical effect is associated with the dissociation of  $\text{CO}_2$  to form free radicals and has been shown to be of minor

effect. However, this effect may have caused the slight increase in thermal efficiency, especially at EGR ratio of up to 20%. The thermal efficiency decreased with any further increase of EGR ratio above 20%. For the case of EGR, the thermal efficiency was a minimum for 30% EGR ratio as shown in the figure and this may be due to the dilution effect of the EGR used, as more exhaust gases are present in the combustion chamber with reduced oxygen fraction [60]. Recirculation of too much exhaust gases also displaces much of the necessary air for combustion, leading to decrease in thermal efficiency. The remarkable rise in BTE from quarter to half load may be attributed to rapid increase in combustion temperatures with increasing pilot fuel quantities which in turn improves the combustion rate of biogas. It was concluded that EGR of 20% is the optimum ratio for dual fuel operation based on BTE.

#### 4.5.4 Exhaust Gas Temperature (EGT)

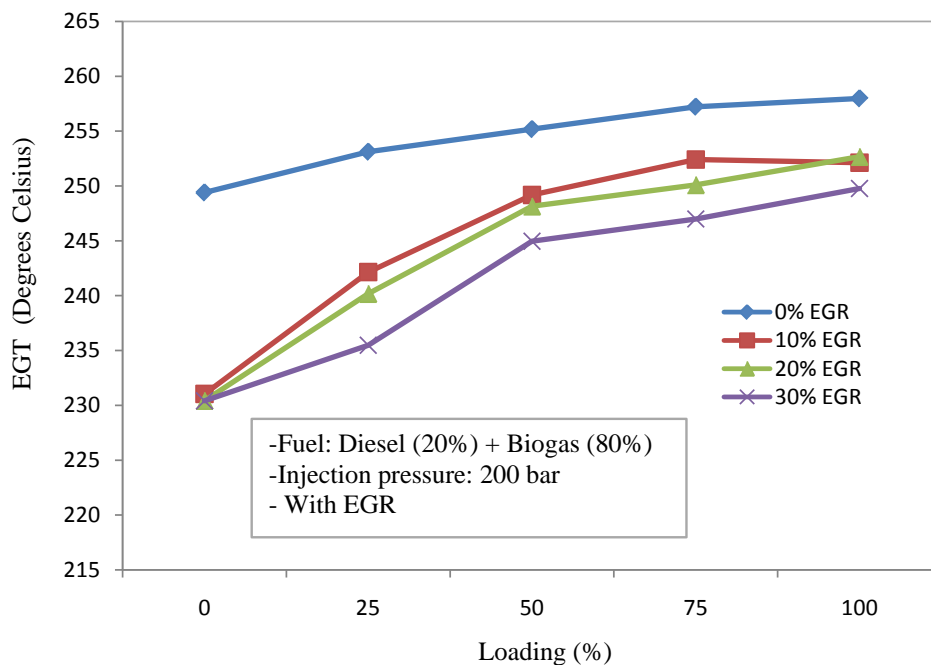


Figure 4.23: Variation of EGT with engine load for dual fuel operation with EGR

Exhaust gas temperature was measured to give an insight into the combustion characteristics of the engine since it is a fast and easier means of roughly investigating the behaviour of the combustion process. This was due to the fact that combustion characteristics of an engine is a relatively wide topic which would form another research altogether. Figure 4.23 shows the variation of the exhaust gas temperature with engine load for various conditions of EGR. The exhaust gas temperature was found to increase with engine load for all operating modes. This may be attributed to the increase of total energy input at high load following higher fuel consumption. It was also found that with increase in percentage of EGR, the exhaust gas temperatures reduced. This can be attributed to the oxygen deficient operation under EGR which results in lower combustion temperatures and furthermore, specific heat of exhaust gas is more than that of intake air which also contributes to the lower combustion temperatures [54]. The maximum reduction in EGT was 7%, at quarter load while the minimum recorded difference in the same was 2% at full load. The decrease in EGT with exhaust gas recirculation shows the efficacy in reducing  $\text{NO}_x$  emission during dual fuel operation. The rise in EGT, especially for EGR cases was however steeper at low loads up to 50% and this may be attributed to the increase in quantity of pilot fuel with increasing load.

#### **4.5.5 Emissions**

This section presents results on variation of emissions of CO, CO<sub>2</sub> and HC with engine load for dual fuel operation with exhaust gas recirculation.

##### **(a) Variation of carbon monoxide emission with load for dual fuel operation with EGR**

Generally, CO emission from the engine occurs due to partial oxidation of the fuel mixture. The rate of CO formation is a function of unburned fuel and mixture temperature

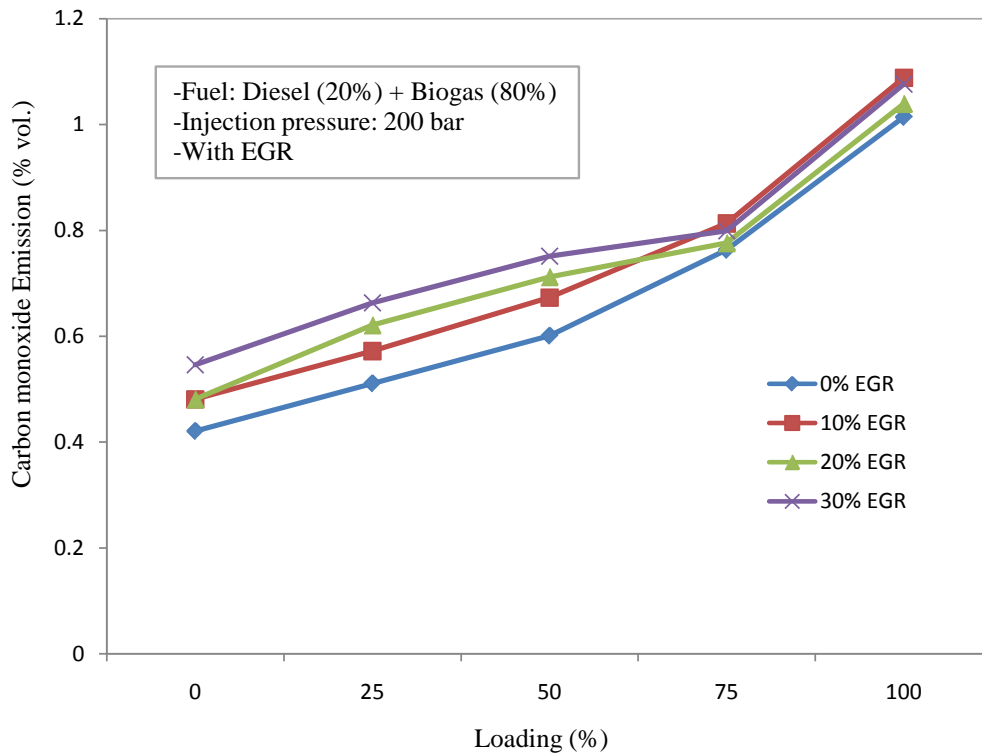


Figure 4.24: Variation of CO emission with load for dual fuel operation with EGR

during combustion, since both factors control the fuel decomposition and oxidation. The variation of CO emissions with percent EGR at various loads is shown in Fig. 4.24. Observation showed that with increase in percent EGR, CO emission increased; however, the increase in CO emission was marginal at higher engine loads above 75%. Higher CO emission at low loads was attributed to the low engine temperature and lean mixture at part loads. This makes the air fuel mixture to have incomplete combustion and few of the reactants escape into the exhaust as CO. At high engine loads beyond 75%, emissions of CO is highest for 10%EGR and lowest for 0%EGR, and the difference between emission levels for the various cases of EGR is minimal. This was attributed to the high thermal loading at high engine load which leads to improved combustion for all cases of EGR and hence marginal difference and overlap for various EGR rates. At low loads the CO emission was highest for EGR ratio of 30%.

### (b) Variation of Unburned hydrocarbon Emission with Load

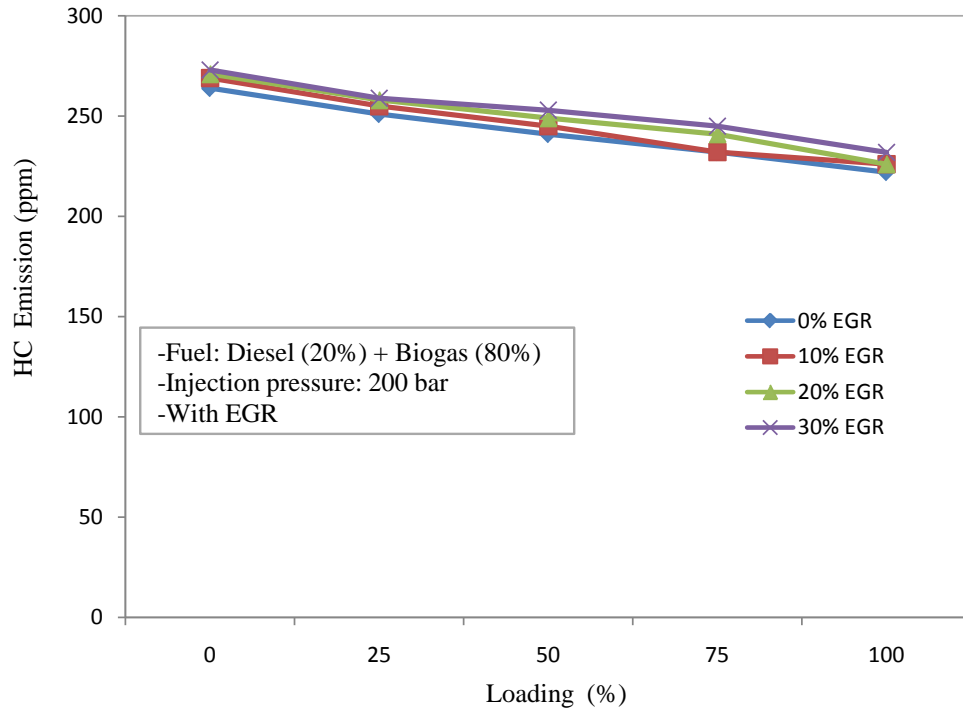


Figure 4.25: Variation of HC emission with load for dual fuel operation with EGR

HC emissions consist of fuel that is completely unburned or partially burned. HC emissions are a serious problem especially at light loads for dual fuel engines as revealed by the findings of other researchers, e.g [44, 58]. The comparison of HC emissions of various EGR rates in dual fuel mode is shown in Fig. 4.25. Observation showed that with more recirculated exhaust gases the HC emission increased, though slightly. The maximum percentage increase in HC emission was 5%, recorded at no load. More emission of HC with EGR was attributed to reduction in fresh air with increase in exhaust gas flow rate which resulted in incomplete combustion of the richer mixture. The trend of decreasing HC emissions from no load to full load compared to diesel fuel was attributed to increase in engine temperature with load, which in turn improved the combustion rate of the fuel.

### (c) Variation of Carbon dioxide Emission with Load

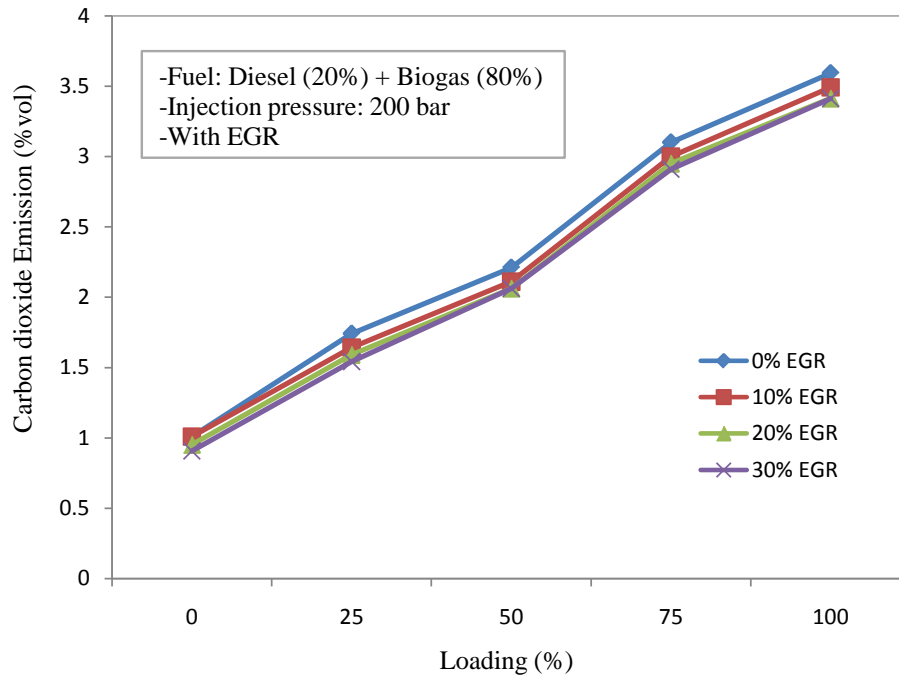


Figure 4.26: Variation of CO<sub>2</sub> emission with load for dual fuel operation with EGR

Figure 4.26 describes the variations of carbon dioxide emission with percent EGR for various loads. Emission of carbon dioxide was found to increase with engine load while the same decreased slightly with EGR from 10% to 30% EGR. CO<sub>2</sub> decreased by up to 6% following exhaust gas recirculation. Reduction in carbon dioxide emission with increase in EGR was attributed to substitution of some of the fresh air with exhaust gas leading to incomplete combustion of the fuel and decrease in CO<sub>2</sub> which is a product of fuel oxidation.

## CHAPTER FIVE

### 5.0 CONCLUSIONS AND RECOMMENDATIONS

#### 5.1 Conclusions

In this research, a single cylinder four stroke diesel engine was modified into a dual fuel engine that uses diesel and biogas fuels. The performance of the dual fuel engine in comparison to the diesel engine was evaluated by considering performance parameters of brake power, brake specific fuel consumption, brake thermal efficiency and exhaust gas temperature as well as emission characteristics of CO, HC and CO<sub>2</sub>. The study focused on investigating various effects of dual-fuel combustion of diesel and biogas on the performance and exhaust emission characteristics of a single cylinder four stroke DI diesel engine under various experimental conditions. The following conclusions were drawn from the analysis:

- A direct injection compression ignition engine was modified to run on biogas, with diesel as the pilot fuel. This led to the conclusion that DIC engines can be modified into dual fuel engines and be used in stationary applications such as power generation, hoisting in construction sites and as a prime mover for water pumps, flour mills among other applications. The modification of diesel engine into a dual fuel engine would involve introducing an air-fuel mixing chamber along the air intake system to provide an effective means of admitting the gaseous fuel into the combustion chamber and for homogenous mixing of air and the gaseous fuel. A modification has also to be made at the diesel injection pump to allow adjustment of the injection quantities of the pilot fuel as may be necessary.
- The maximum substitution of diesel with biogas was possible up to 80% and engine operation on biogas alone was not possible. This was due to the high

autoignition temperature of biogas which made it difficult to ignite without considerable amount of diesel. This led to the conclusion that utilization of biogas in DICI engine can help substitute use of diesel by up to 80% since it cannot fully replace it. This will help reduce dependence on petroleum fuels and save on finances compared to when diesel is relied on fully.

- The optimum ratio for exhaust gas recirculation in the dual fuel engine was 20% based on BSFC and BTE. When exhaust gas was recirculated up to an EGR ratio of about 20%, it improved both BSFC and BTE. BSFC decreased with EGR while BTE increased with the same by up to 11% . The decrease in BSFC with EGR was attributed to increase in intake charge temperature which enhanced the rate of combustion of the fuel. The increase in BTE with EGR was attributed to re-burning of HC that enters combustion chamber with the recirculation of exhaust gases coupled with the increase in intake charge temperature and increase in rate of combustion of the fuel.
- While EGR led to an increase in CO and HC emissions, it led to a decrease in CO<sub>2</sub> emissions for both the single fuel and dual fuel modes.
- The brake power and the brake thermal efficiency decreased with use of biogas due to the calorific value of biogas being lower compared to diesel. The lower heating value of biogas is at least 50% lower than for diesel.
- Both CO and HC emissions of the dual fuel engine were higher than for diesel operation by upto 2 and 12 times respectively. This was majorly attributed to displacement of the air necessary for combustion with biogas.

Biogas is a good fuel for dual fuel engines and can form a perfect supplement to the fossil fuels used in the country since it is renewable and affordable.



## 5.2 Recommendations

From this work and the discussions made, the following are the recommendations for future study:

- Biogas is a suitable renewable fuel for compression ignition (CI) engines in the dual fuel mode. However, the thermal efficiency is low and hydrocarbon emission levels are high. One of the reasons for this is the presence of CO<sub>2</sub> in biogas. It is therefore recommended that the CO<sub>2</sub> present in biogas should be removed by upgrading the gas in order to enhance the flammability limits and improve flame speed; to improve thermal efficiency and lower emissions. This was not done due to the limitations of funds and facilities available for this research.
- The other reason that leads to low thermal efficiency and increased emissions in dual fuel operation with biogas is the displacement of air needed for combustion, with the gaseous fuel. In order to help improve efficiency and reduce emissions, the engine should be modified to include a turbocharger which would enhance air intake and complete combustion of fuel. This could not be done due to limited research funds and scope of the research.
- Analysis of NO<sub>x</sub> emission was not carried out in this research due to lack of emission analyzer for NO<sub>x</sub>. It is therefore recommended that this be considered for future research, to find out the effect of EGR on NO<sub>x</sub> emission.

## REFERENCES

- [1] R. L. McCormick, C. J. Tennant, R. R. Hayes, S. Black, J. Ireland, T. McDaniel, A. Williams, M. Frailey, and C. A. Sharp, "Regulated emissions from biodiesel tested in heavy-duty engines meeting 2004 emission standards," Tech. Rep., SAE Technical Paper, 2005.
- [2] S. H. Yoon, S. H. Park, and C. S. Lee, "Experimental investigation on the fuel properties of biodiesel and its blends at various temperatures," *Energy & Fuels*, vol. 22, no. 1, pp. 652–656, 2007.
- [3] T. V. Mathew, "Fuel Consumption and Emission Studies," Tech. Rep., SAE Technical Paper, 2014.
- [4] R. Chandra, V. K. Vijay, P. M. V. Subbarao, and T. K. Khura, "Performance evaluation of a constant speed IC engine on CNG , methane enriched biogas and biogas," *Applied Energy*, vol. 88, no. 11, pp. 3969–3977, 2011.
- [5] T. Korakianitis, A. M. Namasivayam, and R. J. Crookes, "Hydrogen dual-fuelling of compression ignition engines with emulsified biodiesel as pilot fuel," *International Journal of Hydrogen Energy*, vol. 35, no. 24, pp. 13329–13344, 2010.
- [6] A K. Agrawal, S. K. Singh, S. Sinha, and M. K. Shukla, "Effect of EGR on the exhaust gas temperature and exhaust opacity in compression ignition engines," *Applied Energy*, vol. 88, no. 11, pp. 2900-2907, 2011.
- [7] S. A. Raja, D. S. Robinson, and C. L. R. Lee, "Biodiesel production from jatropha oil and its characterization," *Research Journal of Chemical Sciences*, vol. 1, no. 1, pp. 81–87, 2011.
- [8] N. H. S. Ray, M. K. Mohanty, and C. M. R., "A Study on Application of Biogas as fuel in Compression Ignition Engines," *International Journal of Innovations in Engineering and Technology*, vol. 3, no. 1, pp. 239–245, 2013.

- [9] P. M. Njeru and P. Njogu, "Conversion of Water Hyacinth Derived Biogas to Biomethane for Electricity Generation in Kenya: A Waste to Energy (WtE) Approach," in *Proceedings of 2014 International Conference on Sustainable Research and Innovation, Volume 5, 7th-9th May 2014*, vol. 5, pp. 79–81, 2014.
- [10] J. R. Wilson, O. Ajuonu, T. D. Center, M. P. Hill, M. H. Julien, F. F. Katarigira, P. Neuenschwander, S. W. Njoka, J. Ogwang, R. H. Reeder, and T. Van, "The decline of water hyacinth on Lake Victoria was due to biological control by *Neochetina* spp.," *Aquatic Botany*, vol. 87, pp. 90–93, 2007.
- [11] A. M. Mailu, "Preliminary Assessment of the Social , Economic and Environmental Impacts of Water Hyacinth in the Lake Victoria Basin and the Status of Control Major Threats to Lake Victoria," Tech. Rep., Kenya Agricultural Research Institute, 2001.
- [12] M. Theuri, "Water hyacinth: Can its aggressive invasion be controlled ?," Tech. Rep. April, UNEP Global Environmental Alert Service (GEAS), 2013.
- [13] K. G.M. and K. E.M., "Biogas Production," Tech. Rep. 10, Kenya Agricultural Research Institute, Nairobi-Kenya, 2003.
- [14] L. Wilson, "Promoting Biogas Systems in Kenya, A Feasibility Study," Tech. Rep. October, Biogas for Better Life-An African Initiative, 2007.
- [15] B. R. Prasath, E. Leelakrishnan, N. Lokesh, H. Suriyan, and E. G. Prakash, "Hydrogen Operated Internal Combustion Engines: A New Generation Fuel," *International Journal of Emerging Technology and Advanced Engineering*, vol. 2, no. 4, pp. 52–57, 2012.

- [16] N. Tippayawong, A. Promwungkwa, and P. Rerkkriangkrai, “Long-term operation of a small biogas/diesel dual-fuel engine for on-farm electricity generation,” *Biosystems engineering*, vol. 98, no. 1, pp. 26–32, 2007.
- [17] S. Hyun and C. Sik, “Experimental investigation on the combustion and exhaust emission characteristics of biogas biodiesel dual-fuel combustion in a CI engine,” *Fuel Processing Technology*, vol. 92, no. 5, pp. 992–1000, 2011.
- [18] S. Mihic, “Biogas Fuel for Internal Combustion Engines,” Tech. Rep., SAE Tech. Paper, 2004.
- [19] C. Garnier, A. Bilcan, O. Le Corre, and C. Rahmouni, “Characterisation of a syngas-diesel fuelled CI engine,” Tech. Rep., SAE Technical Paper, 2005.
- [20] L. P. Goswami, G. Patel, C. Khadia, P. K. Sen, and S. K. Bohidar, “A Review on Dual Fuel Engine using Diesel as Primary Fuel and Various Secondary Fuels,” *International Journal of Research in Advent Technology*, vol. 2, no. 11, pp. 74–80, 2014.
- [21] J. Stewart, A. Clarke, and R. Chen, “An experimental study of the dual-fuel performance of a small compression ignition diesel engine operating with three gaseous fuels,” *Proceedings of the Institution of Mechanical Engineers, Part D: Journal of Automobile Engineering*, vol. 221, pp. 943–956, 2007.
- [22] C. Christen and D. Brand, “Gas and Dual Fuel Engines as a Clean and Efficient Solution,” Tech. Rep., ABB Turbo Systems Ltd, Switzerland, 2013.
- [23] W. W. Pulkrabek, “Sec.4-4 Self-Ignition and Octane Number 143,” in *Engineering Fundamentals of the Internal Combustion Engine*, no. 143, ch. Four, pp. 143–149, Prentice Hall, 2001.

- [24] G. A. Karim, “Combustion in gas fueled compression ignition engines of the dual fuel type,” *Journal of engineering for gas turbines and power*, vol. 125, no. 3, pp. 827–836, 2003.
- [25] M. M. Roy, E. Tomita, N. Kawahara, Y. Harada, and A. Sakane, “An experimental investigation on engine performance and emissions of a supercharged Hydrogen-Diesel dual-fuel engine,” *International Journal of Hydrogen Energy*, vol. 35, no. 2, pp. 844–853, 2010.
- [26] I. D. Bedoya, S. Saxena, F. J. Cadavid, R. W. Dibble, and M. Wissink, “Experimental evaluation of strategies to increase the operating range of a biogas-fueled HCCI engine for power generation,” *Applied Energy*, vol. 97, pp. 618–629, 2012.
- [27] R. Chandra, V. K. Vijay, P. M. V. Subbarao, and T. K. Khura, “Performance evaluation of a constant speed IC engine on CNG, methane enriched biogas and biogas,” *Applied Energy*, vol. 88, no. 11, pp. 3969–3977, 2011.
- [28] K. von Mitzlaff, *A Handbook of Engine for Biogas; Theory, Modification, Econum, Operation*. Friedr. Vieweg and Sohn Verlagsgesellschaft, Germany, 1988.
- [29] S. Siripornakarachai and T. Sucharitakul, “Modification and tuning of diesel bus engine for biogas electricity production,” *Maejo International Journal of Science and Technology*, vol. 1, no. 2, pp. 194–207, 2007.
- [30] C. Rossetto, S. Nelson, M. D. Souza, R. F. Santo, J. D. Souza, and O. L. Klaus, “Performance of an Otto cycle engine using biogas as fuel,” *African Journal of Agricultural Reseach*, vol. 8, no. 45, pp. 5607–5610, 2013.
- [31] H. S. Sorathia and H. J. Yadav, “Energy analyses to a CE-Engine using Diesel and Bio-gas Dual Fuel -A Review Study,” *International Journal of Advanced Engineering Research and Studies*, vol. 1, no. 2, pp. 212–217, 2012.

- [32] N.H.Ray, P.R.Swain, and M.K.Mohanty, “An Investigation on Performance Characteristics of CI Engine using Biogas and Diesel in Dual Fuel Mode,” *International Journal of Science, Engineering and Technology Research (IJSETR)*, vol. 3, no. 6, pp. 1716–1723, 2014.
- [33] M. R. Murari, E. Tomita, N. Kawahara, and Y. Harada, “Comparison of performance and emissions of a supercharged dual-fuel engine fueled by hydrogen and hydrogen-containing gaseous fuels,” *International Journal of Hydrogen Energy*, vol. 36, no. 12, pp. 7339–7352, 2011.
- [34] G. Gopal, P. Srinivasa Rao, K. V. Gopalakrishnan, and B. S. Murthy, “Use of hydrogen in dual-fuel engines,” *International Journal of Hydrogen Energy*, vol. 7, no. 3, pp. 267–272, 1982.
- [35] G. H. Abd-Alla, “Using exhaust gas recirculation in internal combustion engines: a review,” *Energy Conversion and Management*, vol. 43, no. 8, pp. 1027–1042, 2002.
- [36] P. K. Bose and D. Maji, “An experimental investigation on engine performance and emissions of a single cylinder diesel engine using hydrogen as inducted fuel and diesel as injected fuel with exhaust gas recirculation,” *International journal of hydrogen energy*, vol. 34, no. 11, pp. 4847–4854, 2009.
- [37] A. Tsolakis, J. J. Hernandez, A. Megaritis, and M. Crampton, “Dual fuel diesel engine operation using H<sub>2</sub>. Effect on particulate emissions,” *Energy & Fuels*, vol. 19, no. 2, pp. 418–425, 2005.
- [38] B. B. Sahoo, N. Sahoo, and U. K. Saha, “Effect of H<sub>2</sub> : CO ratio in syngas on the performance of a dual fuel diesel engine operation,” *Applied Thermal Engineering*, vol. 30, pp. 1–8, 2011.

- [39] C. T. Spaeth, *Performance Characteristics of a Diesel Fuel Piloted Syngas Compression Ignition Engine*. PhD thesis, Queens University, 2012.
- [40] C. Sayin, K. Uslu, and M. Canakci, "Influence of injection timing on the exhaust emissions of a dual-fuel CI engine," *Renewable Energy*, vol. 33, pp. 1314–1323, 2008.
- [41] Z. Wen, J. Ignosh, and J. Arogo, "Fuel Ethanol," Tech. Rep., Virginia State University, Virginia, 2009.
- [42] D. Huang, H. Zhou, and L. Lin, "Biodiesel: an alternative to conventional fuel," *Energy Procedia*, vol. 16, pp. 1874–1885, 2012.
- [43] N. R. Kumar, Y. M. C. Sekhar, and S. Adinarayana, "Effects of Compression Ratio and EGR on Performance, Combustion and Emissions of Direct Injection Diesel Engine," *International Journal of Applied Science and Engineering*, vol. 11, no. 1, pp. 41–49, 2013.
- [44] A. Hosseinzadeh, R. K. Saray, and S. M. S. Mahmoudi, "Comparison of thermal, radical and chemical effects of EGR gases using availability analysis in dual-fuel engines at part loads," *Energy Conversion and Management*, vol. 51, no. 11, pp. 2321–2329, 2010.
- [45] C.C. Lien, J.L. Lin, and C.H. Ting, "Water Scrubbing for Removal of Hydrogen Sulfide in biogas from Hog Farms," *Journal of Agricultural Chemistry and Environment*, vol. 3, no. 1, pp. 1–6, 2014.
- [46] K. M. Agrawal, B. R. Barve, and S. S. Khan, "Biogas From Pressmud," *IOSR Journal of Mechanical and Civil Engineering (IOSR-JMCE)*, vol. 4, no. 45, pp. 37–41, 2010.

- [47] J. Strickland, A. Cummings, S. Joseph, J. J. Liccione, and Gary L. Foureman, "Toxicological Review of Hydrogen sulfide," Tech. Rep. 7783, U.S. Environmental Protection Agency Washington, DC, 2003.
- [48] L. Skirtic, *Hydrogen Sulfide , Oil and Gas , and People 's Health* . PhD thesis, University of California, Berkeley, 2006.
- [49] V. R. Gaikwad and P. K. Katti, "Design of Biogas Scrubbing , Compression & Storage System," *IOSR Journal of Electrical and Electronics Engineering*, vol. 1, no. 2, pp. 58–63, 2014.
- [50] M. S. Rathore and P. Ghodasara, "Prediction on Reduction of Emission of NO<sub>x</sub> in Diesel Engine using Bio-diesel Fuel and EGR (Exhaust Gas Recirculation) System," *International Journal of Mechanical Engineering*, vol. 1, no. 1, pp. 18–25, 2009.
- [51] Z. Salhab, "Effect of Exhaust Gas Recirculation on the Emission and Performance of Hydrogen Fueled Spark-ignition Engine," *Applied Energy* vol. 12, no. 2, pp. 1–6, 2012.
- [52] V. Manieniyan and S. Sivaprakasam, "Experimental Analysis of Exhaust Gas Recirculation on DI Diesel Engine Operating with Biodiesel," *International Journal of Engineering and Technology*, vol. 3, no. 2, pp. 129–135, 2013.
- [53] P. Saichaitanya, K. Simhadri, and G. Vamsidurgamohan, "Impact of Cold and Hot Exhaust Gas Recirculation on Diesel Engine," *International Journal of Engineering Research and Applications*, vol. 3, no. 5, pp. 430–434, 2013.
- [54] K. Venkateswarlu, B. Sree, and S. Chandra, Rama V. Venkata, "The Effect of Exhaust Gas Recirculation and Di-Tertiary Butyl Peroxide on Diesel-Biodiesel Blends for Performance and Emission Studies," *International Journal of Advanced Science and Technology*, vol. 54, no. 10, pp. 49–60, 2013.



- [55] D. K. Das, S. P. Dash, and M. K. Ghosal, "Performance Study of a Diesel Engine by using producer gas from Selected Agricultural Residues on Dual-Fuel Mode of Diesel-cum-Producer gas," *Sustainable Transport*, pp. 3541–3548, 2011.
- [56] P. R. Bevington and D. K. Robinson, *Data Reduction and Error Analysis for the Physical Sciences*. New York: Kent A. Peterson, Mc Graw Hill, third ed., 2003.
- [57] D. G. Cacuci, *Sensitivity and Uncertainty Analysis*. New York: Chapman and Hall/ CRC, 1 ed., 2003.
- [58] B. P. Pattanaik, C. Nayak, and B. K. Nanda, "Investigation on utilization of biogas & Karanja oil biodiesel in dual fuel mode in a single cylinder DI diesel engine," *International Journal of Energy and Environment*, vol. 4, no. 2, pp. 279–290, 2013.
- [59] S. K. Mahla, L. M. Das, and M. K. G. Babu, "Effect of EGR on Performance and Emission Characteristics of Natural Gas Fueled Diesel Engine," *Jordan Journal of Mechanical and Industrial Engineering*, vol. 4, no. 4, pp. 523–530, 2010.
- [60] M. Y. E. Selim, "Effect of exhaust gas recirculation on some combustion characteristics of dual fuel engine," *Energy Conversion and Management*, vol. 44, no. 1, pp. 707–721, 2003.

## APPENDIX A

### Diesel Engine Exhausts

There are two categories of diesel engine: (1) Open-chamber or direct-injection engines: Are preferred for heavy-duty applications because they offer the best fuel economy; (2) Divided chamber or indirect-injection engines: Have been preferred for light-duty applications because they are less sensitive to differences in fuels, have a wider range of speeds (and therefore greater power:weight ratio), run more quietly and emit fewer pollutants.

The major products of the complete combustion of diesel (petroleum-based fuels) in an internal combustion engine are carbon dioxide (13%) and water (13%), with nitrogen from air comprising most of the remaining exhaust (73%). A very small portion of the nitrogen is converted to nitrogen oxides and some nitrated hydrocarbons. Some excess oxygen may be emitted, depending on the operating conditions of the engine. Diesel engines are designed to operate with excess air (air:fuel ratio, 25-30:1, unlike gasoline engines which are designed to operate at a nearly stoichiometric ratio (air:fuel ratio, 14.6:1).

Incomplete combustion results in the emission of carbon monoxide, unburnt fuel and lubricating oil and of oxidation and nitration products of the fuel and lubricating oil. These incomplete combustion products comprise thousands of chemical components present in the gas and particulate phases. The concentration of a chemical species in engine exhaust is a function of several factors, including engine type, engine operating conditions, fuel and lubricating oil composition and emission control system.

## APPENDIX B

### Exhaust Gas Recirculation

#### B.1 Classification of EGR Systems

EGR systems have been classified on the basis of EGR temperature, configuration and pressure [6].

##### B.1.1 Classification based on temperature

- *Hot EGR*: Exhaust gas is recirculated without being cooled, resulting in increased intake charge temperature.
- *Fully cooled EGR*: Exhaust gas is fully cooled before mixing with fresh intake air using a water-cooled heat exchanger. In this case, the moisture present in the exhaust gas may condense and the resulting water droplets may cause undesirable effects inside the engine cylinder.
- *Partly cooled EGR*: To avoid water condensation, the temperature of the exhaust gas is kept just above its dew point temperature.

##### B.1.2 Classification based on configuration

- *Long route system (LR)*: In an LR system the pressure drop across the air intake and the stagnation pressure in the exhaust gas stream make the EGR possible. The exhaust gas velocity creates a small stagnation pressure, which in combination with low pressure after the intake air, gives rise to a pressure difference to accomplish EGR across the entire torque/speed envelope of the engine.

- *Short route system (SR)*: These systems differed mainly in the method used to set up a positive pressure difference across the EGR circuit. Another way of controlling the EGR-rate is to use variable nozzle turbine (VNT). Most of the VNT systems have single entrance, which reduce the efficiency of the system by exhaust pulse separation. Cooled EGR should be supplied effectively. Lundquist and others used a variable venturi, in which EGR-injector was allowed to move axially, thus varying the critical area.

### B.1.3 Classification based on pressure

Two different routes for EGR, namely low-pressure and high-pressure route systems may be used.

- *Low pressure route system*:The passage for EGR is provided from downstream of the turbine to the upstream side of the compressor. It is found that by using the low pressure route method, EGR is possible up to a high load region, with significant reduction in  $\text{NO}_x$ . However, some problems occur, which influence durability, prohibitory high compressor outlet temperature and intercooler clogging.
- *High pressure route system*:The EGR is passed from upstream of the turbine to downstream of the compressor. In the high pressure route EGR method, although EGR is possible in the high load regions, the excess air ratio decreases and fuel consumption increases remarkably.